POWER REACTOR TECHNOLOGY

A Quarterly Technical Progress Review

Prepared for U. S. ATOMIC ENERGY COMMISSION by GENERAL NUCLEAR ENGINEERING CORP.

December 1960

● VOLUME 4

● NUMBER 1

TECHNICAL PROGRESS REVIEWS

To meet the needs of industry for concise summaries of current atomic developments, the Atomic Energy Commission is publishing this series, Technical Progress Reviews. Issued quarterly, each of the reviews digests and evaluates the latest findings in a specific area of nuclear technology and science.

The four journals published in this series are:

Nuclear Safety, W. B. Cottrell, editor, R. A. Charpie, advisory editor, and associates, Oak Ridge National Laboratory

Power Reactor Technology, Walter H. Zinn and associates, General Nuclear Engineering Corporation

Reactor Core Materials (covering solid material developments), R. W. Dayton, E. M. Simons, and associates, Battelle Memorial Institute

Reactor Fuel Processing, Stephen Lawroski and associates, Chemical Engineering Division, Argonne National Laboratory

Each journal may be purchased ($2.00 per year for subscription and individual issues $0.55) from the Superintendent of Documents, U. S. Government Printing Office, Washington 25, D. C. See back cover for remittance instructions and foreign postage requirements.

Availability of Reports Cited in This Review

Unclassified AEC reports are available for inspection at AEC depository libraries and are sold by the Office of Technical Services, Department of Commerce, Washington 25, D. C. Some of the reports cited are not available owing to their preliminary nature; however, the information contained in them will eventually be made available in formal progress or topical reports.

Unclassified reports issued by other Government agencies or private organizations should be requested from the originator.

Unclassified British and Canadian reports may be inspected at AEC depository libraries. British reports are sold by the British Information Service, 45 Rockefeller Plaza, New York, N. Y.; Canadian reports (AECL series) are sold by the Scientific Document Distribution Office, Atomic Energy of Canada, Ltd., Chalk River, Ontario, Canada.

Classified U. S. and foreign reports identified in this journal as Classified may be purchased by properly cleared Access Permit Holders from the Office of Technical Information Extension, U. S. Atomic Energy Commission, P. O. Box 1001, Oak Ridge, Tenn. Such reports may be inspected at classified AEC depository libraries.

POWER REACTOR TECHNOLOGY

A REVIEW OF RECENT DEVELOPMENTS

Prepared for U. S. ATOMIC ENERGY COMMISSION
by GENERAL NUCLEAR ENGINEERING CORP.

● DEC. 1960

● VOLUME 4

● NUMBER 1

foreword

This quarterly review of reactor development has been prepared at the request of the Office of Technical Information of the U. S. Atomic Energy Commission. Its purpose is to assist interested organizations in the task of keeping abreast of new results in reactor technology for civilian application.

The report is a concise discussion of selected phases of research and development for which there have been significant advances or a heightened interest in the past few months. It is not meant to be a comprehensive abstract of all material published during the quarter, nor is it meant to be a treatise on any part of the subject. The intention is to cover the various areas of reactor development from the general viewpoint of the reactor designer rather than from the more detailed points of view of specialists in the individual areas. However, papers which are thought to be of particular significance or particular usefulness in specialized fields will be mentioned in short notes. In the overall plan of the report, it is intended that various subjects will be treated from time to time and will be brought up to date at that time.

Any interpretation of results which is given represents only the opinion of the editors of the report, who are General Nuclear Engineering Corporation personnel. Readers are urged to consult the original references in order to obtain all the background of the work reported and to obtain the interpretation of the results given by the original authors.

W. H. ZINN
General Nuclear Engineering Corporation

contents

Issued quarterly by the U. S. Atomic Energy Commission. Use of funds for printing this publication approved by the Director of the Bureau of the Budget on November 1, 1960.

Section 1 EVALUATIONS

Small Power Reactors

In early 1959, the U. S. Atomic Energy Commission initiated a study to assess the feasibility of low-level power generation through the use of certain types of small-sized nuclear reactors. Evaluation and state-of-the-art reports were prepared by the Commission and by several nuclear engineering companies, covering the pressurized-water, the boiling-water, and the organic-moderated reactor types. These reports, listed as references 1 to 6, were reviewed in the March 1960 issue of *Power Reactor Technology*, Vol. 3, No. 2, pages 6 to 12. After the studies, in November 1959, the Commission invited proposals for a small-sized pressurized-water reactor complex, to generate 235,000 lb of dry and saturated steam per hour at a pressure of 500 psig. The reactor complex, to be owned by the Commission, would produce steam for sale to a cooperative or publicly owned electric-power-generating organization, which would furnish fossil-fuel superheat and turbogenerating equipment to generate 22,000 kw(e) gross.* The specifications and conceptual design upon which the invitation to reactor suppliers was based are given in two published reports. These reports, the last in the small-reactor series, are listed as references 9 and 10.

Process Heat

Reference 11 contains the proceedings of a symposium on low-temperature nuclear process heat, which was conducted by the AEC in October 1959. The purposes of the meeting were to (1) present technical and economic information on low-temperature process-heat reactors and (2) ascertain from those present the extent of industry interest in participating in the development of such reactors. With regard to the second purpose, the answers to a questionnaire circulated at the meeting indicated a strong majority opinion that progress in nuclear-process-steam applications would be slow without substantial government aid. A plurality of those responding favored government aid in the form of payment of research and development costs and of sharing the reactor construction costs; this preference was particularly strong among the users of process heat.

The substance of much of the technical information on process heat has been covered in the June 1959 issue of *Power Reactor Technology*, Vol. 2, No. 3, pages 4 and 5, and the December 1959 issue, Vol. 3, No. 1, pages 1 to 5. However, a discussion of considerable interest is that by Robert W. Ritzmann, AEC Division of Reactor Development, on the factors entering the choice of materials and steam pressure for the Experimental Low-Temperature Process-Heat Reactor (ELPHR).* Briefly, the usefulness of relatively low temperatures for process-steam applications supports hopes of lowering reactor costs and fuel costs, through the use of carbon or low-alloy steel for the reactor pri-

* The invitation to municipal and cooperative utilities stipulated that the AEC would furnish the fossil-fuel superheater if necessary.[7] Proposals by the City of Jamestown, N. Y., and the Dairyland Power Cooperative of LaCrosse, Wis., are being considered by the Commission.[8]

* This reactor, a pressurized-water reactor, was scheduled to serve as the steam source for the experimental saline-water conversion plant being built at Point Loma, San Diego, Calif., by the Department of the Interior; however, the Point Loma site was questioned on safeguard grounds. A recently announced decision will permit the conversion-plant construction to proceed using a conventional heat source.

mary system and through the use of aluminum for the fuel jackets and core structure. The two materials are not entirely compatible with each other in the sense that the low-alloy steel requires a *p*H of the primary water on the alkaline side for best anticorrosion performance, whereas the aluminum alloys show the best corrosion resistance when the water is slightly acid. Since the anticipated use of the ELPHR (for the saline-water conversion plant) required secondary steam at only 5 psig, it was decided that both materials could be used, with neutral primary water, and that the reactor could be used as a long-term experiment to determine the maximum temperature at which the combination of materials would perform satisfactorily. Estimates by Argonne National Laboratory (ANL) indicated that secondary steam production at 15 psig could be reliably expected, that 65-psig steam was a reasonable expectation, and that considerable potential existed for the attainment of 180-psig steam through a research and development program. Consequently the reactor system was to be designed for a power output of 40 Mw(t) of secondary steam at 180 psig, but initial operation was planned at 30 Mw(t), with 15-psig secondary steam.

In connection with the use of aluminum alloys in water-cooled reactors, a paper[12] summarizing some British work on aqueous corrosion is of interest.

References

1. Task Force Evaluation Report: Small-Sized Nuclear Power Plant Program, USAEC Report TID-8508, June 1, 1959.
2. Generating Cooperatives and Municipalities: Statistical Survey, USAEC Report TID-8509, June 1, 1959.
3. General Nuclear Engineering Corp., A Brief Study of Boiling-Water Reactors in the 5- to 40-Mw(e) Range, USAEC Report TID-8510, Oct. 10, 1959.
4. Atomics International, Small-Sized Organic-Moderated Reactors [10 to 40 Mw(e)], USAEC Report TID-8511, Oct. 10, 1959.
5. Atomics International, 20,000-Kilowatt Organic-Moderated Power Plant, USAEC Report TID-8512, Oct. 10, 1959.
6. Alco Products, Inc., Survey of PWR Power Plants [10- to 30-Mw(e) Size], USAEC Report TID-8513, Oct. 10, 1959.
7. Roundup of Key Developments in Nucleonics, *Nucleonics*, 18(2): 18–19 (February 1960).
8. Reactor News, *Nucleonics*, 18(9): 25 (September 1960).
9. Gibbs & Hill, Inc., and Internuclear Company, Small-Size Pressurized-Water Reactor Specifications, USAEC Report TID-8525, Nov. 16, 1959.
10. Gibbs & Hill, Inc., and Internuclear Company, Small-Size Pressurized-Water Reactor Conceptual Design, USAEC Report TID-8526, Apr. 11, 1960.
11. Proceedings of the 1959 Symposium on Low-Temperature Nuclear Process Heat, USAEC Report TID-7580, January 1960.
12. E. C. W. Perryman, Aluminum Alloys for Water-Cooled Power Reactors, *J. Brit. Nuclear Energy Conf.*, 5(2): 97–109 (April 1960).

Section II

FUEL CYCLES

Isotope Separation

When enriched uranium serves predominantly as the fuel in a nuclear power industry, the characteristics of the isotope-separation process may have important effects, both on fuel costs and on the efficiency of fuel utilization. Snyder[1] summarizes some of the results of the theory of a diffusion cascade, shows how the major variables are related to the cost of enriched uranium, and discusses the AEC price schedule for enriched uranium in relation to these variables.

One of the functions which occurs frequently in the equations describing ideal cascades is the so-called "separative-work" function.[2] Although this function does not have the dimensions of work or energy, it is closely related to the amount of work that must be done to achieve a given separation by a given process. It is proportional to the total quantity of fluid which must be circulated to produce a unit mass of the desired product. Similarly, it is directly related to total pump capacity, pumping power consumed, barrier area required, and other parameters which are closely related to the expense involved in achieving a given separation by a unit approaching an ideal cascade. Separative work can be expressed[1] as a function of the concentrations of feed, waste, and product stream only, as indicated in Eq. 1.

$$\Delta_{pf} = P\left[\pi_p + \left(\frac{x_p - x_f}{x_f - x_w}\right)\pi_w - \left(\frac{x_p - x_w}{x_f - x_w}\right)\pi_f\right] \qquad (1)$$

where P = quantity of product, in pounds, produced without regard to time period

x_p, x_f, x_w = assays of product, feed, and waste, as weight fraction U^{235} contained in a mixture of U^{235} and U^{238}

$\pi = (2x - 1)[\ln x/(1 - x)]$

Several facts can be stated[1] by examining Eq. 1:

For an enriched product of assay x_p, the amounts of separative work and of feed required vary according to the tails assay. The lower the tails assay the less the requirements for feed and the greater the requirements for separative work per unit of the enriched product.

Uranium feed of any assay greater than the tails assay can be enriched in the cascade. Increasing the feed assay decreases the quantities of feed and separative work required for a particular enriched product.

For a particular feed assay and tails assay, the higher the product assay desired the greater the amounts of feed and separative work required per unit of uranium in the product.

The cost of the product can be written[1] as follows:

$$c_p P = c_f F_\Delta + c_\Delta \Delta_{pf} \qquad (2)$$

where c_p, c_f, c_Δ = unit costs of product, feed, and separative work

F = quantity of feed, in pounds, introduced without regard to time period

From a material balance,

$$F = P\left(\frac{x_p - x_w}{x_f - x_w}\right) \qquad (3)$$

Substituting Eqs. 1 and 3 into Eq. 2 yields:*

$$c_p = c_f\left(\frac{x_p - x_w}{x_f - x_w}\right) + c_\Delta\left[\pi_p + \left(\frac{x_p - x_f}{x_f - x_w}\right)\pi_w - \left(\frac{x_p - x_w}{x_f - x_w}\right)\pi_f\right]$$

This equation can be rewritten into what is referred to as a standard cost equation as follows:

$$c_p = c_\Delta\ [\pi_p - \pi_w + A(x_p - x_w)] \qquad (4)$$

where

$$A = \frac{\frac{c_f}{c_\Delta} - (\pi_f - \pi_w)}{(x_f - x_w)}$$

Inspection of Eq. 4 indicates that the unit cost of product varies with the tails assay for fixed values of x_p, x_f, c_f, and c_Δ. Setting the derivative of the unit cost of product with respect to tails assay equal to zero results in Fig. 1, wherein the tails assay for a minimum-cost product is plotted. As pointed out in reference 1, the tails assay for minimum product cost is independent of product assay but depends on the assay of feed and the ratio of the feed and separative-work costs.

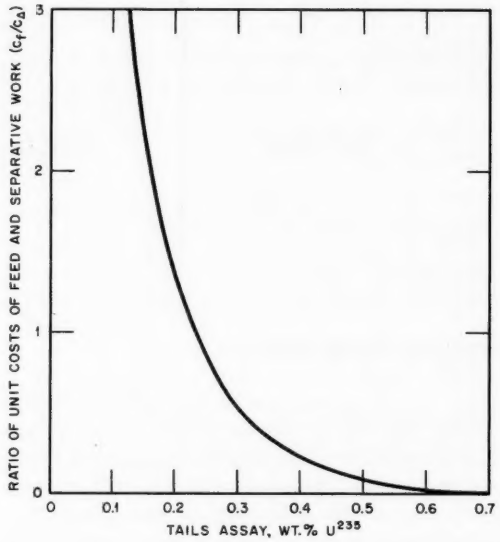

Figure 1—Tails assay for minimum unit cost of product.[1]

On Nov. 18, 1956, the AEC announced a schedule of charges for enriched uranium (reviewed in the December 1957 issue of *Power Reactor Technology*, Vol. 1, No. 1, pages 1 and 2; this schedule is consistent with a value of c = \$39.27 per kilogram of uranium, and c_Δ = \$37.29 per kilogram of separative work. From Fig. 1 this implies an optimum tails assay of 0.221 per cent, and the cost of enriched uranium can be back-calculated from Eq. 4 using this optimum value.

The effects of sidestream withdrawals or additions are also considered in reference 1. The cases considered are: constant separative work and constant tails assay; constant feed rate and tails assay; and constant rates of separative work and feed.

The burnup charge for the U^{235} consumed in a reactor can be calculated from ideal-cascade theory.[1] If x is the assay of U^{235} fed to the reactor and c is the charge for the uranium at the specified assay, then c/x is the cost per gram of contained U^{235} at the initial assay and is equal to the unit burnup charge if all the U^{235} is consumed. If very little of the U^{235} is consumed, the unit burnup charge is approximated by dc/dx, which can be obtained from the cost

*The relations of the equation may be illustrated by examination of the components of cost for fuel of a specific enrichment. The tabulation below shows this breakdown, computed for two different product enrichments, 2 per cent U^{235} and 90 per cent U^{235}, for a fuel enrichment of 0.7115 per cent U^{235} and a waste enrichment of 0.221 per cent U^{235}. The computed costs agree approximately with the AEC schedule.

	2% enrichment	90% enrichment
π_p	3.74	2
$\pi_w\left(\frac{x_p - x_f}{x_f - x_w}\right)$	(6.09)(2.63) = 16.02	(6.09)(182) = 1108
$-\pi_f\left(\frac{x_p - x_w}{x_f - x_w}\right)$	−(4.87)(3.63) = −17.68	−(4.87)(183) = −891
Δ_{pf}/P	2.08	219
$37.29(\Delta_{pf}/P)$	78	8,167
$39.27\left(\frac{x_p - x_w}{x_f - x_w}\right)$	(39.27)(3.63) = 143	7,186
Cost of product, \$/kg	221	15,353

equations presented previously. These approximations are valid only if no conversion has taken place and if the uranium is valued on the same schedule of charges before and after irradiation.

Reference 1 ends with a discussion of the blending of enriched uranium of different assays. The same amount of uranium would be fed to the ideal cascade to produce the blending ingredients as to produce the final product directly in the cascade. The separative work required to produce the blending ingredients, however, is greater than that required to produce the final product directly in the cascade, and this difference is equal to the separative work required to separate the final product back into the blending ingredients. Thus, if no other considerations apply, it is always cheaper to upgrade the enrichment of a particular batch of uranium by recycling it to the diffusion plant than by blending it with uranium of higher enrichment. However, if the fuel to be upgraded is in a chemical form other than UF_6 (the form used in the diffusion plant), then blending may lead to a net saving by eliminating the chemical conversion step (see the September 1958 issue of *Power Reactor Technology*, Vol. 1, No. 4, pages 20 and 21). Similarly, if natural uranium can be purchased in the open market at a price significantly below the $39.27 per kilogram on which the AEC price schedule is based, then it may be profitable to obtain slightly enriched fuel by blending more highly enriched material with natural uranium.

From the point of view of the long-term future of nuclear fuel supplies, some obvious but nevertheless significant conclusions can be drawn, as follows:

1. A significant fraction of U^{235} remains in the diffusion-plant tails. If the discharge enrichment is indeed 0.221 per cent, this amounts to 31 per cent of the U^{235} in the natural-uranium feed if the product is highly enriched uranium. Unless there is a real demand for the product, it is not clear that there are obvious reasons for operating at the "optimum" tail assay.

2. In any case, if the U^{235} content of the tailings must be considered as "lost," this loss represents a significant handicap to the basic fuel utilization by partially enriched reactors.

3. Since the cost of fuel (natural uranium) apparently accounts for about half the cost of enriched fuel, any future rises in the cost of natural uranium, because of the depletion of high-grade ore deposits, will be strongly reflected also in the costs of enriched fuels.

Maximum Conversion Ratios in Thermal Reactors

In the ultimate nuclear power economy, the basic nuclear fuel cost will depend upon the cost per pound of mining and extracting the natural nuclear fuel material and upon the average amount of energy extracted from each pound of natural fuel material mined. The reserves of uranium that can be mined at relatively low cost appear to be insufficient for a large-scale nuclear power industry unless the energy yield per pound of uranium mined is increased by a substantial factor above that currently obtained in nuclear fuel cycles. Such an increase in energy yield is doubly effective in extending the fuel supply, for it not only increases the amount of energy obtained from a given fuel reserve but it also effectively increases the reserve by making the use of the higher-cost uranium deposits economically practical. To increase the specific energy yield by a substantial factor appears to require that bred fissionable isotopes be recycled as reactor fuel and that relatively high average conversion ratios be attained throughout the power-reactor complex. These considerations have been reviewed in the June 1959 issue of *Power Reactor Technology*, Vol. 2, No. 3, pages 1 to 11, and the March 1960 issue, Vol. 3, No. 2, pages 21 to 29, and more recently further related discussions have appeared in the literature.[3,4]

Evidently, an important long-term question is how high the conversion ratio can be in the reactor types currently under vigorous development. Since fuel recycle appears to be needed for high fuel utilization, one desires to know, not simply the initial conversion ratio but the average conversion ratio over the fuel cycle. The important isotopes involved are not only the naturally available U^{235} but also the bred isotopes of the plutonium or U^{233} chains. Reliable estimates of maximum attainable conversion ratios in thermal reactors (especially in those of the solid-fuel types) have been very difficult because they require rather detailed considerations of the neutron energy spectrum in the thermal and near-thermal ranges and because they require similarly detailed knowledge of the heavy-isotope cross sections and

neutron yields over the same energy ranges. Although the information in these areas is still imperfect, it is adequate to justify estimates of maximum attainable conversion ratios. Two new estimates of this type are reported in references 5 and 6.

Reference 5 is a progress report which covers only the case of metallic uranium (U^{238} plus U^{235} at various enrichments) in H_2O. The results, however, illustrate the main features of H_2O-moderated systems in which U^{235} is the fissionable isotope, and probably define, very nearly, the upper limits of attainable conversion ratios.

For every neutron absorbed in U^{235}, an average number, η^{25}, of fission neutrons are produced. The net production of neutrons is $\eta^{25} - 1$, and, if there were no neutron losses, these neutrons could be absorbed in U^{238} to produce $\eta^{25} - 1$ atoms of Pu^{239} for every atom of U^{235} destroyed. A further effect enters, however, because fast neutrons in the reactor cause some fissions of U^{238}, and these fissions yield additional surplus neutrons whose production has not entailed the destruction of any U^{235}. These neutrons from U^{238} fission are taken into account, in reference 5, by an effective η for U^{235}, $(\eta^{25})_{eff}$, defined as the total number of neutrons produced by fissions in U^{235}, augmented by the net number $(\nu - 1)$ produced in U^{238}, per neutron absorbed in U^{235}. It may be expressed in terms of a U^{238} fission factor, ϵ:

$$(\eta^{25})_{eff} = \eta^{25}\epsilon$$

and

$$\epsilon = 1 + \frac{\bar{\nu}^{28} - 1}{\bar{\nu}^{25}}\,\delta^{28}$$

where δ^{28} is the ratio of the number of fissions in U^{238} to the number in U^{235} and $\bar{\nu}$ is the average number of neutrons produced per fission. The quantity $(\eta^{25})_{eff} - 1$ is equal to the maximum conversion ratio that could be attained if there were no neutron losses by leakage or by absorption in nonfuel materials.

The value of $(\eta^{25})_{eff}$ depends upon the uranium-to-H_2O ratio, the enrichment, and, to some extent, the fuel geometry. The latter effect was not investigated in the work reported,[5] which considered lattices composed of 0.600-in.-diameter rods; but only large changes in geometry are likely to be important.

The U^{238} fission factor ϵ is most sensitive to to the uranium-to-H_2O ratio because it is a fast-neutron effect, and for high ratios it makes an important contribution to the excess neutrons. On the other hand, the capture-to-fission ratio (α) for U^{235} is, on the average, higher in the low epithermal energy range than in the thermal range. Consequently η^{25} decreases as the ratio of absorption to moderation increases, i.e., whenever either the uranium-to-H_2O ratio or the enrichment is increased. Figure 2 shows the values of ϵ, η^{25}, and $(\eta^{25})_{eff}$ computed in reference 5 for 2 per cent enrichment, as functions of uranium-to-H_2O ratio. It is evident that the increase in ϵ, as uranium-to-H_2O is increased, more than compensates for the decrease in η^{25}. The very important net effect of enrichment is shown in Fig. 3, reproduced from reference 5.

Any parasitic neutron absorption, of course, wastes neutrons and lowers the actual conversion ratio below the maximum represented by $(\eta^{25})_{eff} - 1$).

Although the quantity $(\eta^{25})_{eff} - 1$ determines the maximum fraction of neutrons available for conversion, the actual conversion ratio in a given lattice is determined by the ratio of ab-

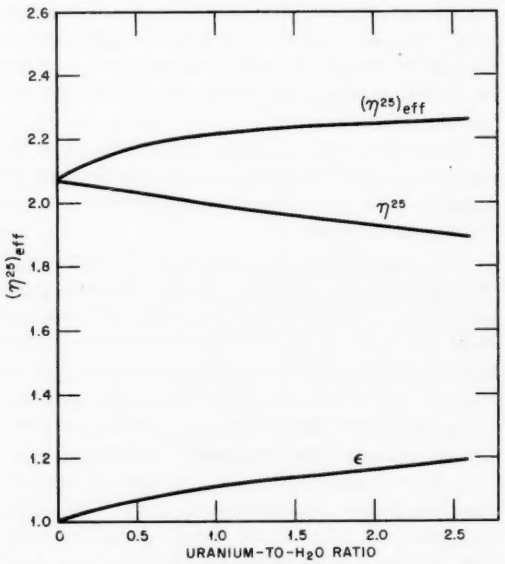

Figure 2—Variation of components of $(\eta^{25})_{eff}$ with uranium-to-water ratio.[5] (Values of components are computed for 2 per cent U^{235} enrichment.)

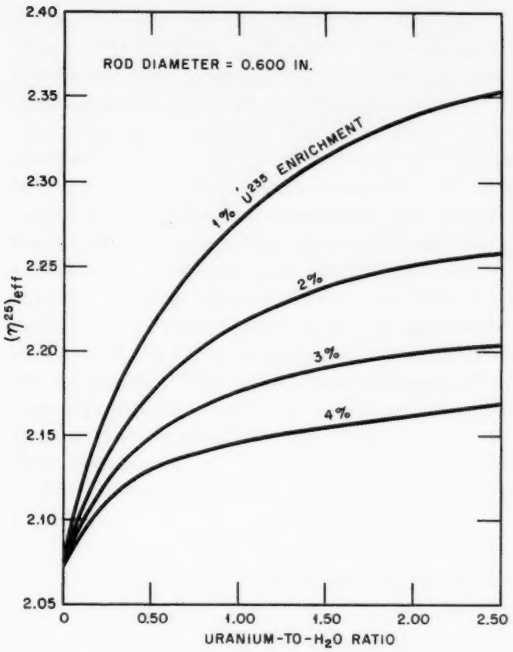

Figure 3—Effect of enrichment on $(\eta^{25})_{eff}$ in uranium metal–water lattices.[5]

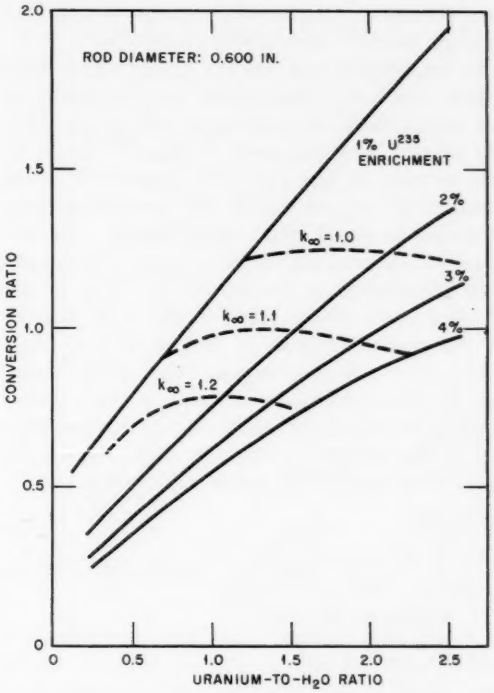

Figure 4—Conversion ratio for uranium metal–water lattices.[5] (The dashed curves of constant k_∞ have been added by the editors of *Power Reactor Technology* from other data in reference 5.)

sorption in U^{238} to absorption in U^{235}. Figure 4 gives the actual (computed) conversion ratios, for fuels of four different enrichments, as functions of uranium-to-H_2O ratio. The curves rise continuously with uranium-to-H_2O ratio. However, the requirement of criticality defines the combinations of enrichment and fuel-to-water ratio that can be used in a self-sustaining reactor. The dashed curves have been drawn in to show these combinations in terms of k_∞, the infinite multiplication factor. These curves take into account the neutron absorption by H_2O (disadvantage factor neglected) but do not consider other parasitic absorbers. It is evident that, if infinitely large reactors could be built containing only metallic uranium and H_2O ($k_\infty = 1.0$), quite high conversion ratios might be expected. Actual reactors will lose neutrons to leakage, to structural materials, to fission products, and perhaps to control elements, and the neutron economies of the best of them will probably lie somewhere in the region bounded by the curves $k_\infty = 1.1$ and $k_\infty = 1.2$. This range, of course, extends from rather unexciting conversion ratios of perhaps 0.75 to quite high ratios near 1.0. The case will be somewhat poorer for reactors using oxide fuels since the fractional U^{238} fission will be lower, and the parasitic neutron losses will probably be higher, at a given value of η^{25}.

Fundamentally, the important result of the study[5] is the conclusion that the value of $(\eta^{25})_{eff}$ may be as high as about 2.25 for metallic fuel over a range of enrichments and uranium-to-H_2O ratios consistent with the attainment of a usable reactivity level. Also worthy of note is the result (Fig. 4) that, for a given value of k_∞, the conversion ratio is not extremely sensitive to uranium-to-H_2O ratio.

Reference 6 extends the work of Chernick* and Chernick and Moore,[7] on the potential breeding ratios of thermal reactors fueled with U^{233}, to include the effects of higher isotopes

* Reviewed in the March 1960 issue of *Power Reactor Technology*, Vol. 3, No. 2, in connection with the October 1959 Conference on the Physics of Breeding.[8,9]

and fission products, and considers also the case of reactors fueled with plutonium.

In considering the effects of the higher isotopes, the fuel composition corresponding to the equilibrium recycle case, with no processing losses, was assumed. In the U^{233} cycle, no absorptions in isotopes higher than U^{236} were considered. In all cases the moderator was assumed to be at room temperature. The degree of moderation of the neutron spectrum was considered in terms of the ratio of the slowing-down power ($\xi\Sigma_s$) to the atom density of the initial fissionable isotope (N_{23} or N_{49}). The primary fertile isotope (Th^{232} or U^{238}) was not considered to be present in the chain-reacting system; the practical case corresponding to the calculation would be that in which the conversion would take place in a blanket.

Table II-1 summarizes the results* of the breeding-ratio estimates for the U^{233} cycle, with D_2O and H_2O moderators, and the effects of neutron capture by Pa^{233} and fission products. Beryllium and graphite are also considered as moderators in reference 6. In Table II-1 the breeding ratio (*B.R.*) refers to the number of neutrons available for conversion per fissionable atom destroyed, when the losses to the moderator are deducted, i.e., *B.R.* = (net neutron production by fission – neutron absorption in moderator)/(neutron absorption in all fissionable isotopes). The quantity *B.R.* is the change in breeding ratio caused by the effect in question. In the case of absorption by Pa^{233} the effect, for a given neutron energy spectrum, is proportional to the thermal-neutron flux, or, if the Pa^{233} is mixed with U^{233}, to the specific power, P/M, in megawatts per kilogram of fissionable isotope. The loss to the nonsaturating fission products is proportional to the average fractional burnup, B, of the fuel in the equilibrium reactor.

Table II-1 CALCULATED BREEDING CHARACTERISTICS FOR U^{233} CYCLE[6]

Moderating ratio ($\xi\Sigma_s/N_{23}$)	1000	2000	5000	10,000
Breeding ratio with D_2O moderator for:				
Pure U^{233}	1.212	1.240	1.259	1.262
U^{233} plus higher isotopes	1.151	1.198	1.228	1.234
Breeding ratio with H_2O moderator for:				
Pure U^{233}	1.199	1.200	1.139	1.007
U^{233} plus higher isotopes	1.141	1.162	1.113	1.000
$\Delta B.R.$ by Pa^{233} absorption for:				
Resonance integral = 900 b	$-0.108\ P/M$	$-0.061\ P/M$	$-0.030\ P/M$	$-0.021\ P/M$
Resonance integral = 1200 b	$-0.146\ P/M$	$-0.079\ P/M$	$-0.033\ P/M$	$-0.024\ P/M$
$\Delta B.R.$ by absorption in saturating fission products for:				
$P/M = 1$	−0.045			−0.053
$P/M = 10$	−0.060			−0.063
$\Delta B.R.$ by absorption in nonsaturating fission products	$-0.26\ B$			$-0.08\ B$

The presence of the higher isotopes in the U^{233} case causes an appreciable reduction in the breeding ratio, although the ratio remains above unity for D_2O, H_2O, beryllium, and graphite moderators when the only neutron losses are to absorption in the moderator. Resonance absorption was found to be important in the cases of absorption by Pa^{233} (the intermediate product, with 27-day half life, between Th^{233} and U^{233}) and the long-lived fission products; the losses in breeding ratio due to these absorptions were consequently affected strongly by the degree of moderation.

In addition to the effects listed in Table II-1, Levine[6] points out that there is a contribution to the breeding ratio from fast-neutron fission of U^{234}. He estimates that this contribution

* Tables II-1 and II-2 are adapted from data given[6] in *Nuclear Science and Engineering*.

Table II-2 CALCULATED BREEDING CHARACTERISTICS FOR Pu^{239} CYCLE[6]

Moderating ratio ($\xi\Sigma_s/N_{49}$)	2000	5000	10,000
Breeding ratio with D_2O moderator for Pu^{239} plus higher isotopes:			
$\alpha_{41}^{res} = 0.6$	0.77	0.82+	0.82–
$\alpha_{41}^{res} = 0.2$	0.85–	0.85+	0.84
Breeding ratio with H_2O moderator for pure Pu^{239}	0.77	0.79+	0.79+
Breeding ratio with H_2O moderator for Pu^{239} plus higher isotopes:			
$\alpha_{41}^{res} = 0.6$	0.76	0.80	0.78
$\alpha_{41}^{res} = 0.2$	0.85	0.81	0.78
$\Delta B.R.$ by absorption in saturating fission products for:			
$P/M = 1$	−0.044		−0.048
$P/M = 10$	−0.057		−0.061
$\Delta B.R.$ by absorption in nonsaturating fission products	−0.132 B		−0.046 B
$\Delta B.R.$ due to fast fission in Pu^{240} when H_2O is the moderator	0.021		0.008

may amount to 0.024 for H_2O moderator at $\xi\Sigma_s/N_{23} = 1000$. The contribution will be less for other moderators and for higher moderating ratios.

In the case of the Pu^{239} cycle, the breeding-ratio estimates are less certain owing to uncertainties in the values of η for Pu^{239} and Pu^{241} and to the greater sensitivity of η_{49} to the details of the thermal-neutron spectrum. The results of the calculations for this cycle are summarized in Table II-2 for extreme values of α_{41} in the resonance energy region.

From these studies it would appear that the characteristics of the U^{233} cycle are favorable for the attainment of a significant breeding gain in a fluid-fuel reactor designed to minimize losses by neutron absorption in structural materials, fission products, and Pa^{233}. The elucidation of the question of whether a positive breeding gain can be achieved is, of course, the main objective of reference 6. As to the question of how high the average conversion ratio can be in reactors of the types currently going into commercial use, it appears that, although the principles involved are well understood, a comprehensive answer, even within the limits imposed by existing uncertainties in physical constants, will require a rather large amount of detailed analysis.

The proceedings of a British symposium on fuel cycles are contained in reference 10. The cycles considered are mainly once-through cycles for the graphite-moderated gas-cooled reactors, but within this limited area the coverage is rather comprehensive, including practical, as well as theoretical, considerations.

References

1. A. J. Snyder, Methods of Calculating U^{235} Outputs and Charges by Use of the Ideal Cascade Theory, USAEC Report TID-8522, February 1960.
2. M. Benedict and T. H. Pigford, *Nuclear Chemical Engineering*, pp. 396–399, McGraw-Hill Book Company, Inc., New York, 1957.
3. J. F. Kaufmann and E. D. Jordan, Breeding Potential of Thermal Reactors, *Nuclear Sci. and Eng.*, 8(1): 85 (July 1960).
4. W. H. Zinn and J. R. Dietrich, Nuclear Fuel Resources and Reactor Fuel Costs, *World Power Conference*, Vol. IV B/9, June 1960.
5. Combustion Engineering, Inc., Nuclear Division, Study of Slightly Enriched Uranium-Water Lattices with High Conversion Ratio, Quarterly Progress Report for August 1 to October 31, 1959, USAEC Report NYO-2702, May 1960.
6. M. M. Levine, Breeding Ratio in U^{233} and Pu^{239} Fueled Reactors, *Nuclear Sci. and Eng.*, 7(6): 545–551 (June 1960).
7. J. Chernick and S. O. Moore, Breeding Potential of Thermal Reactors, *Nuclear Sci. and Eng.*, 6(6): 537 (December 1959).
8. J. Chernick, Breeding Potential of Near Thermal Reactors, in Proceedings of the Conference on

the Physics of Breeding, October 19–21, 1959, USAEC Report ANL-6122, pp. 285–295, Argonne National Laboratory, Aug. 1, 1960.

9. M. M. Levine, The Effect of Higher Isotope Production on Breeding, in Proceedings of the Conference on the Physics of Breeding, October 19–21, 1959, USAEC Report ANL-6122, pp. 296–305, Argonne National Laboratory, Aug. 1, 1960.
10. Symposium on Nuclear Fuel Cycles, *J. Brit. Nuclear Energy Conf.*, 4(3) (July 1959).

Section III

REACTOR PHYSICS

Flux Hardening Effects

The effects of "hardening" of the thermal-neutron spectrum within the fuel of a heterogeneous reactor are treated analytically in references 1 and 2. The neutron spectrum is assumed Maxwellian in the moderator; the $1/E$ tail that should be appended to the Maxwellian flux distribution was omitted in both analyses in order to simplify the problem.

Reference 1 treats explicitly the case of a fuel rod surrounded by moderator in cylindrical geometry and makes use of the diffusion-theory approximation. The neutrons are treated as a single group of Maxwellian distribution with the same temperature everywhere in the moderator. This implies that the neutrons leaving the fuel assume at once the Maxwellian spectrum of neutrons far from the fuel. Within the fuel, the neutrons are treated as a continuum of independent groups, each group having a spatial distribution within the fuel given by $I_0(K_f r)$. Here r is the distance from the center of fuel rod, and K_f is the reciprocal of fuel diffusion length, which is energy-dependent. At the fuel-moderator interface, the boundary conditions used are: (1) continuity of inward current for each energy group and (2) continuity of the integral over energy of the outward current. The diffusion-theory solution leads directly to an expression for thermal utilization which includes a self-shielding factor η containing all the effects of flux hardening. In the case of the usual one-group representation of the thermal neutrons (of a single energy $E = 4T/\pi$ in a $1/v$ absorbing medium), the self-shielding factor η reduces to the usual expression

$$\eta_0 = \frac{(\overline{K}_f a)\, I_0(\overline{K}_f a)}{2 I_1(\overline{K}_f a)}$$

where a is the fuel-rod radius and $\overline{K}_f = K_f(4T/\pi)$. Another form of η (designated by η_1) is given for comparison and is that employed by Plass in a calculation (on spheres) reviewed by Weinberg and Wigner.[3]

The results of calculations are presented for two representative cases of metallic uranium rods (natural and 3.5 per cent enrichment) in graphite. In both cases the effect of flux hardening, as indicated by the self-shielding factor η derived in reference 1, is to reduce the thermal utilization by about 0.6 per cent. Use of the η_1 correction employed by Plass results in only about a 0.16 per cent reduction. Since the η_1 correction is based on the assumption that neutrons diffuse with no moderation, in either the fuel or the moderator, from a Maxwellian source in the moderator, it is expected that the actual result is between the two results based on η and η_1.

Reference 2 presents a generalized study of the hardening effects induced through various thicknesses of a $1/v$ type absorbing slab. Both the normal incidence and the isotropic incidence of a Maxwellian spectrum on one side of the slab are considered. Transmission curves are calculated, as measured by the reaction rate of a $1/v$ detector or by the following important non-$1/v$ reaction rates: fission of Pu^{241}, fission and absorption of U^{235} and Pu^{239}, and absorption or activation in cadmium, indium, samarium, gadolinium, and lutetium.

The detailed but rather straightforward calculations were performed on a digital computer, and the results comprised a set of some 1400 numbers which are analyzed in reference 2 to reduce them to some systematic effect. The results include: (1) the reaction rate in the detector, (2) the flux depression factor, which is the fraction of neutron density remaining after passage through the absorbing slab, and (3) the

form of the spectrum after passage. In addition, these results yield, for the hardened neutron spectra, the effective cross sections of the detector reaction rates studied.

The results were first examined with the usual view of treating the hardening effect as equivalent to an increase in the neutron temperature. It is concluded that the raised temperature approximation is a very poor one. The final analysis adopted was to express the quantity $(\hat{\sigma}_H/\hat{\sigma}_M) - 1$ as a double polynomial in T and t by least-squares fitting to a nine-coefficient formula. Here $\hat{\sigma}_M$ and $\hat{\sigma}_H$ are the effective cross sections for a Maxwellian and a hardened spectrum, respectively; T is the temperature of the Maxwellian spectrum incident on the absorbing slab; and t is the flux depression factor previously defined. The nine coefficients are listed for each reaction for both normal and isotropic beam incidence. In order to illustrate the hardening effects obtained, some typical curves relating $\hat{\sigma}_H/\hat{\sigma}_M$ to t are presented for the several reactions studied. A table is presented relating t to the absorber thickness parameter K, which is a generalized parameter including thickness and the 2200 m/sec absorption cross section of the $1/v$ absorbing slab. However, in view of the approximations involved, as, for example, the neglect of scattering effects in the absorber and the use of a specific absorber geometry, it is expected that better estimates of $\hat{\sigma}_H$ can be obtained from the flux depression factor. The flux depression factor could be obtained from measurements or from a refined and reliable theory rather than for the specific geometry (without scattering) used in the analysis in reference 2. This procedure would imply that the relation between hardening effects and flux depression factor is more nearly preserved, irrespective of the geometrical factors and of whether or not scattering processes are considered.

An example is given in reference 2 illustrating the application of the results to the case of a two-sided fuel element in the reactor. A natural-uranium element, in which a small amount of plutonium has been formed, is treated, and a plot is obtained of the variation of the fission cross section of the Pu^{239} through the thickness of fuel. The fission cross section at the center of the slab turns out to be 2.9 per cent above the value for the unperturbed Maxwellian. Factors of this magnitude can be quite important in the calculation of burnup limits due to reactivity loss in fuel.

Resonance Absorption and Doppler Temperature Coefficient

Experimental and analytical determinations of the Doppler temperature coefficients for the effective resonance integrals of U^{238} and Th^{232} are covered in references 4 to 7. The variations of the coefficients with fuel temperature and surface-to-mass ratio are also covered. Reference 4 reports measurements made with the DIMPLE pile oscillator on bars of U^{238} and Th^{232}, of various diameters, at various temperatures up to 270°C; the Doppler coefficient values indicated by the measurements are compared with the available data. The relative contributions to the Doppler coefficient of the volume and surface effects were obtained by activation measurements, as described in reference 5, and were shown to be in reasonably good agreement with theoretical considerations. Monte Carlo calculations for the U^{238} Doppler coefficient are described in reference 6 and are shown to give reasonably good agreement with the results of reactivity measurements. Discrepancies in the U^{238} Doppler coefficient as obtained from activation measurements and from reactivity measurements still exist; the activation experiments generally give results about half those obtained from the reactivity measurements. Theoretical considerations suggest a $1/\sqrt{T}$ dependency of the U^{238} Doppler coefficient with temperature. This variation is indicated by the experimental data of reference 7 and also by the Monte Carlo results in reference 6. The important details of the Doppler coefficient determinations described in references 4 to 7, inclusive, are summarized below.

The samples studied[4] with the DIMPLE pile oscillator varied in diameter from 0.230 to 0.976 in. in the case of uranium and from 0.230 to 0.612 in. in that of thorium. The bars were enclosed in an aluminum furnace and were heated electrically, steps being taken to keep the moderator from becoming heated when hot bars were oscillated. After suitable corrections were applied for empty furnace effects, for moderating effects of the bars and thermal-flux depressions in the bars, and for slight variations in the daily aluminum substandard measurements, the quantity observed in the measurements was $d\Sigma_{\text{eff}}/dt$. The effective cross section Σ_{eff} is given by the Westcott formulation[8] as

$$\Sigma_{\text{eff}} = \Sigma_M + r\sqrt{\frac{4T}{\pi T_0}}\,\Sigma_r$$

where Σ_r = resonance integral above $1/v$
Σ_M = Maxwellian cross section
r = epithermal index defined by Westcott[8]
T = neutron temperature
t = temperature of the bar
$T_0 = 293°\text{K}$

The value of $r\sqrt{T/T_0}$ was determined in the middle of the empty furnace by irradiation of thin gold foils, bare and cadmium covered. The quantity $d\Sigma_M/dt$ is shown to be negligible in the measurements, and therefore the Doppler coefficient may be inferred as

$$\frac{1}{r\Sigma_r}\sqrt{\frac{\pi T_0}{4T}}\frac{d\Sigma_{\text{eff}}}{dt}$$

where Σ_r must be obtained from the various published formulas. The formula of Hellstrand[9] was used for the uranium bars; the information for thorium is rather scarce and at variance and hence required an averaging of the Σ_r values given by the various available formulas and measurements.

A graph of inferred Doppler coefficient versus surface-to-mass ratio for uranium-metal bars shows a tendency to increasing Doppler coefficient with increasing surface-to-mass ratio. The experimental accuracy did not permit this to be done for thorium. The accuracy of the experiments and the limited temperature range investigated did not permit determination of the temperature dependency of the Doppler coefficient. Reasonably good agreement was obtained with the Doppler coefficients for uranium metal, as measured by reactivity methods by Davis[10,11] and by Adyasevich et al.,[12] and with the activation measurements of Egiazarov.[13] There appears, however, to be a marked discrepancy between the results obtained by reactivity methods and the Doppler coefficients determined by Rodeback[14] and Pearce,[5] which were obtained by activation experiments under cadmium. Within the experimental errors, the results for thorium are in reasonably good agreement with three values quoted by other workers,[5,14,15] which include two by the activation technique.

Reference 5 describes activation experiments to study the radial dependence of the Doppler effect in uniformly heated 1-in.-diameter bars of uranium and thorium. A theory is developed which satisfactorily describes the fractional changes in reaction rate, with bar temperature, near the surfaces of the samples.

In the experiments two identical samples of uranium (or thorium) metal were irradiated simultaneously under cadmium in GLEEP with a constant temperature difference maintained between the samples. The samples were in similar furnaces and contained foils similarly exposed. The irradiations were made at the center of GLEEP in a square empty channel wherein the flux gradient was essentially zero. In addition, the samples and furnaces were mounted parallel to the channel axis, 5 cm either side of the axis, and were rotated about this axis during the irradiation. These steps ensured that the hot and the cold samples received the same irradiation.

The sample consisted of two cylindrical pieces (made up as two cylindrical halves of a bar). The activation in the main body of the cylinder was measured by a single foil (depleted uranium or thorium) pressed in between the two halves, and the region close to the surface was measured by a stack of foils placed on the flat end. The 22.12-min beta decay of Th^{233} and the 23.5-min beta decay of U^{239} were measured. Brass masks sufficiently thick to stop the beta particles and having several different apertures were used to obtain some radial resolution of the volume activation. The activations of the foils stacked on the flat end were used to derive the radial dependence near the surface. For this purpose, a special irradiation using a foil on the curved surface was made to normalize the surface activation obtained with the foils stacked on the flat end. Corrections were made for fission-product activity (~1.6 per cent, independent of fuel temperature), and extreme care was taken to minimize systematic errors.

Epicadmium-activation data points are plotted as a function of penetration into the uranium (or thorium) bar at ambient temperature. Also plotted as a function of radius is the percentage increase in the epicadmium activation per atom caused by heating the bar, or $100\Delta I_+/I_+$, where I_+ is the effective resonance integral per atom including the $1/v$ epicadmium contribution and ΔI_+ is the change due to heating. The Doppler effect consists of a volume effect which is constant, within the experimental error, through the rod, and a superimposed surface effect which penetrates less than 0.5 mm in uranium and ex-

tends to a depth of approximately 2 mm for thorium.

The Doppler coefficients averaged through the bar with the $1/v$ contribution included were obtained as $(0.90 \pm 0.17) \times 10^{-4}/°C$ for uranium and $(2.71 \pm 0.15) \times 10^{-4}/°C$ for thorium. For uranium, Rodeback[14] obtained the value $(0.8 \pm 0.2) \times 10^{-4}/°C$ using an activation method. As previously discussed, values obtained by reactivity measurements are higher by a factor of approximately 2. For thorium, Rodeback[14] obtained the value $(2.0 \pm 0.3) \times 10^{-4}/°C$ by activation experiments, and Davis[15] obtained the value $(2.3 \pm 0.2) \times 10^{-4}/°C$ by reactivity measurements; here the agreement is reasonably good. With the $1/v$ contribution subtracted out, the Doppler coefficients obtained in reference 5 are determined as $1.0 \times 10^{-4}/°C$ for uranium and $3.8 \times 10^{-4}/°C$ for thorium. Because of the uncertainty in the value of the effective resonance integral for thorium and the relatively large $1/v$ contribution, the value determined for thorium may be in appreciable error.

A theory is developed in reference 5 for the surface term on the basis of which predictions of the radial variation of the Doppler coefficient near the rod surface are made. The agreement between theory and experiment is quite satisfactory. A prediction is also made for the volume effect, based on the temperature dependence of the effective resonance integral derived by Dresner,[16] which is also in reasonably good agreement with the experimental results. A brief discussion of the theory developed in reference 5 is given below.

Reference 5 distinguishes three types of Doppler effect, depending on the neutron spectrum. That designated as type 2, of main interest in the report, considers only those neutrons which have not had a potential scattering event in the lump. Neutrons are considered to impinge on a lump with a single resonance; the manner in which the neutron spectrum within the lump is depleted is calculated as a function of the penetration parameter $p = Z/\lambda_0$ and of the Doppler width parameter $t = (\Delta/\Gamma)^2$. Here Z is the distance into the lump, λ_0 is the mean free path at the resonance energy, $\Delta = 2(E_0 kT/A)^{1/2}$ is the "Doppler width," and Γ is the total width of the resonance. The lump is assumed to be at a constant temperature, and the potential scattering is taken to be zero. An attempt is made to include the effect of resonance scattering and the broadening of this scattering in the neutron-spectrum depletion calculations. For this, two models are adopted: one based on a one-collision process, the other on a many-collision process. Each of the resolved resonances of U^{238} and Th^{232} is assigned to one or the other of these two models by considerations involving their capture and scattering widths and the probability of a scattered neutron being degraded out of the resonance. These considerations are included in the formulation by appropriate modification of λ_0 for each resonance according to the model assignment. The effect of resonance scattering is to introduce extra attenuation of the incoming beam but does not change the main features of the type 2 effect.

From considerations of the spectrum depletion obtained with penetration distance into the lump, self-shielding factors are determined by numerical integration, and they are plotted versus p for various values of t for a single resonance. The effective absorption integral, $I'(p,t)$, for one resonance is given by the product of I_∞/π and the self-shielding factor, where I_∞ is the infinite dilution resonance integral and the factor $1/\pi$ is included for normalization. Curves are given, for a single resonance, of $I'(2t)/I'(t)$ versus p for various values of t. A curve for a given t value gives, as a function of the penetration parameter p, the ratio of the activation within the resonance at Kelvin temperature $2T$ to the activation at temperature T. The curves exhibit the characteristic peaks seen in the experiments; the peaks occur close to, but inside, the surface of the samples.

In making the predictions based on the theory developed in the report,[5] the total activation was taken to be the sum of the contributions from the resolved resonances plus the epicadmium $1/v$ contribution. The incident flux was assumed isotropic, and the calculation was done for a slab geometry with the resonances being assigned to either a one-collision or a many-collision model. The agreement with the experimental peak is satisfactory in view of the simplifications in the model and the uncertainty in the resonance parameters.

In the type 3 Doppler effect, the slowing-down spectrum in a homogeneous medium with potential scattering is considered. This effect predominates at the center of the 1-in.-diameter fuel rods. The experimental values are consistent with Dresner's theoretical predictions[16] on the type 3 effect.

Reference 6 describes the machine programs written for a Monte Carlo study of resonance absorption in reactor lattices. The reference includes the results of calculations of the effective resonance integrals for the Calder Hall lattice at three different temperatures (300, 900, and 1500°K). They show that the Doppler coefficient averaged over each temperature range, 300 to 900°K and 900 to 1500°K, is not constant with temperature. The variation obtained suggests a temperature dependence of the coefficient even greater than the $1/\sqrt{T}$ relation that has been proposed by various investigators.

Measurements of the fuel temperature coefficient of reactivity have been reported[7] for a seven-rod cluster of 1.8 wt.% enriched uranium dioxide with air coolant. The investigation is in support of the design of the gas-cooled graphite-moderated reactor (EGCR). The PCTR technique for measurement of the temperature coefficient of k_∞ is described in reference 17. Each fuel rod of the seven-rod cluster in the central test lattice contained its own internal heat source. The heat source was provided by mounting the hollow UO_2 pellets (ID = 0.323 in., OD = 0.705 in.), which made up each fuel rod, on an electrically insulating rod and installing Nichrome heating wires in the insulating rod. The mounted pellets were placed in a 304 stainless-steel tube and were plugged with a thermal-electrical insulator at each end. Perforated disks of thermal-electrical insulation supported the rods at each end and governed the rod spacing. The seven-rod cluster was assembled inside a lined graphite sleeve, the lining being a $\frac{5}{16}$-in.-thick layer of lampblack insulation confined in place by a 0.003-in.-thick aluminum cylinder secured to the sleeve. The lampblack minimized the heat leakage from the fuel. Iron-constantan thermocouples were used in the test section to determine the temperature variation in the fuel cluster and to determine an average fuel temperature. Temperatures were also measured in the graphite immediately adjacent to the lampblack insulation layer, and 1 in. radially outward from the surface of the graphite sleeve, indicating the surrounding moderator temperature.

Heating of the test section resulted in a decrease in reactivity of the PCTR, as determined by gradual withdrawal of a calibrated control rod to maintain criticality. After appropriate corrections, the change in PCTR reactivity was plotted versus change in fuel temperature; the fuel temperature range covered in the experiments is 50 to 500°C. The change in average temperature of the graphite sleeve, which is an indication of the heat loss to the graphite moderator, was also plotted as a function of fuel temperature. Two heating cycles (42 and 65 min), which differed only in the time needed to reach the maximum fuel temperature, were run. The two sets of data display nearly the same negative slope of PCTR reactivity versus fuel temperature, although differences begin to appear at about 320°C and increase with further increase in temperature. Because of the shorter heating time and, consequently, a lower probability of moderator heating, the 42-min run was used in the analysis of the experiment. From a multiple least-squares analysis of the data and an experimentally determined normalizing factor for the test lattice, the change in resonance escape probability with fuel temperature was determined. On the basis of a measured room-temperature value of resonance escape probability ($p_0 = 0.824 \pm 0.006$), the change in the effective resonance integral with temperature was found to be

$$\frac{1}{\Sigma}\frac{d\Sigma}{dT} = (1.00 \pm 0.11)[(1.87 \pm 0.05) \times 10^{-4} - (1.74 \pm 0.25) \times 10^{-7} T\ (°C) + (4.58 \pm 0.68) \times 10^{-11} T^2\ (°C)]$$

Data taken during a 122-min heating cycle with the lampblack insulation removed yielded results that differ from those quoted by as much as 20 per cent. The large difference is attributed to moderator heating quite far out into the surrounding graphite.

Extrapolation of the temperature-dependent equation much beyond the 500°C limit of the experimental data is not expected to yield accurate results. Two expressions that may give more realistic values, depending on the extrapolation, are

$$\frac{1}{\Sigma}\frac{d\Sigma}{dT} = 2.49 \times 10^{-4} \exp[-1.02 \times 10^{-3} T\ (°K)]$$

or

$$\frac{1}{\Sigma}\frac{d\Sigma}{dT} = 2.90 \times 10^{-3} T^{-0.480}\ (°K)$$

The latter form of the equation is indicated by theoretical considerations.

Reference 18 describes experiments performed to measure the ratio of surface-to-volume activation by resonance neutrons in a uranium-metal rod. The uranium oxide coated aluminum foils that were used had an equivalent uranium-metal thickness of 0.06 mil. The uranium was depleted to 5 ppm U^{235}. Two foils were attached to the fuel-rod surface, and two more foils were placed inside the fuel rod. This was accomplished by drilling a hole through the fuel rod along a diameter and then stacking uranium-metal foils through the hole, the uranium oxide coated foils being positioned 0.010 in. on either side of the center line.

The 74-kev gamma activity from the decay of U^{239} was counted. Determination of the amount of uranium on the aluminum foils was accomplished by alpha counting and by the irradiated activities normalized using these values. Corrections were applied both for the U^{238} fission-product activity in the presence of the 74-kev gamma activity and to eliminate the 103-kev gamma activity due to the decay of the excited states of Pu^{239}. Irradiations were repeated with the inside and surface foils interchanged. Three sets of four foils were used, thus giving six independent determinations which were averaged.

Measurements were made to extend the spatial distribution of resonance neutron captures (originally reported in reference 19) to the surface. For this specific case, the surface-to-volume activation ratio was obtained as 8.9. Reference 20 gives results of measurements of lattice interaction effects on U^{238} resonance capture for three fuel rods (uranium metal, high-density UO_2, and low-density UO_2) and for three different lattice spacings (an isolated rod, and water-to-uranium ratios of 2.4 and 1). The change in the surface-to-volume activation ratio due to lattice interaction effects is the same for the three different rod densities. Furthermore, the measured change agrees well with that indicated by the Dancoff integral which gives the change in surface capture of "black neutrons" with lattice spacing. It is hence concluded that, under the range of conditions investigated, lattice interaction effects at rod center are small enough to be masked by the experimental uncertainty.

Thermal-Neutron Diffusion Parameters

Measurements on the diffusion length of thermal neutrons in water at temperatures up to 296°C are reported in references 21 to 23; also given in reference 22 are the results of measurements in Dowtherm A from 20 to 180°C. An Sb^{124}-Be source emitting predominantly 25-kev neutrons was used in the measurements reported in references 21 and 23. The source neutrons slow down to thermal energies with a characteristic relaxation length in room-temperature water of 1.58 cm, whereas the thermal-diffusion length is 2.8 cm. Since both increase inversely with water density, the thermalization length remains shorter than the diffusion length at the higher temperatures. Hence, at large distances from the source (relative to the relaxation lengths), the neutron-attenuation process is essentially characterized by the thermal-diffusion length. Foil measurements made in water within a pressure vessel were used to obtain a semilog plot of the product of foil distance and foil activity versus foil distance. The negative slope of the straight line fitting the data points (least squares) gives the thermal-diffusion length. Corrections to the foil data were applied for internormalization based on foil weight and for the effect of one foil on the activity of the next in line. The possible effect of the epithermal source on the thermal-flux distribution at the distances from the source used in the foil measurements was considered; it was concluded that the source correction, which would decrease slightly the values obtained, is probably less than the quoted error.

In reference 21 it is shown that the data may be represented by either of two fairly simple approximations for the variation of the transport cross section of water with neutron energy. The one approximation is to take the variation as proportional to $1/v$; the other approximation is that due to Radkowsky.[24] Reference 23 also compares the measured diffusion lengths with those obtained by the Radkowsky prescription.

The thermal-neutron diffusion parameters in water and Dowtherm A, as measured using the pulsed-source technique, are given in reference 22 over the temperature range 22 to 80°C for water and 20 to 180°C for Dowtherm A. From the results, it is concluded that the thermaliza-

tion properties of Dowtherm A are a little better than those of water.

In reference 25 the elastic scattering of slow neutrons from the water molecule is calculated by considering the molecule as a rigid asymmetric rotator, following the method of Goryunov.[26] The partial scattering from each rotational state is calculated separately, since the incident neutron energy considered is of the same order of magnitude as the rotational level separation.

It is shown that, in taking the thermal average at $T = 300°K$, the contribution to the elastic scattering from rotational states with quantum number $j \geq 4$ is not negligible, as has been supposed by Goryunov. This is true also for the total scattering, which was calculated for just one incident neutron energy: 0.0006 ev. The reasons for choosing such a low value were: (1) with so little neutron energy, there is hardly any absorption of energy by the molecule; transitions from a given initial state to all higher energy states are excluded except for one or two exceptional cases where the levels are closer than 0.0006 ev; hence the number of final states is decreased to a large extent due to conservation of energy; (2) some computational simplifications are possible; and (3) this is the lowest energy for which the experimental value (260 barns) of the scattering cross section is available. A systematic calculation of nearly 250 partial cross sections was made, and the final results after thermal averaging are presented in tabular form. The calculational results indicate a total scattering cross section of about 290 barns at $T = 300°K$ for the 0.0006-ev neutron energy. It is conjectured that the discrepancy between calculated and experimental values is due to the neglect of zero-point vibrations of the nuclei around their position of equilibrium. It has been found that the cross section for scattering from a rigid-static (nonrotating) H_2O molecule is reduced by 7 per cent when, instead of considering the molecule as rigid, one allows for the zero-point vibrations of the nuclei.

Power Distributions in H_2O-Moderated Lattices

Reference 27 reports several detailed measurements of neutron-flux distribution in lattices used for the Yankee critical experiments and compares their results with those calculated by several different techniques. Flux peaking and power peaking were measured at a water slot which bisected a cylindrical core along a diametral plane, and power density distributions were measured along selected radii of another cylindrical assembly containing, alternatively, cruciform control rods or cruciform rod followers. The best of the calculation methods gave good agreement with experiment except near the control rods, where the discrepancy was attributed to underestimation of the epithermal neutron absorption by the rods.

The calculational scheme that gave the best agreement with experiment consisted of a two-group or four-group diffusion-theory calculation, in one dimension (WANDA) or two dimensions (PDQ) as necessary to handle the geometry of the experiment, with the constants for the fast groups determined by an infinite-medium multigroup code (MUFT) and the thermal constants determined by Wigner-Wilkins averages in infinite media (SOFOCATE code). It was stated that the four-group calculations gave power distributions that varied by a negligible amount from those that resulted from the two-group calculations. The general features of the preferred calculational scheme were the same as those used by Goldsmith and Ryan[28] in fitting the results of activation-distribution measurements in highly enriched H_2O-moderated assemblies (reviewed in the December 1959 issue of *Power Reactor Technology*, Vol. 3, No. 1, pages 16 and 17). The further success of the method in the slightly enriched (2.7 per cent) UO_2-H_2O lattice of the Yankee critical experiment is quite encouraging.

Background Neutron Source

In a new reactor without an artificial neutron source, the significant contributions to the background neutron source are spontaneous fission, (α,n) reactions in light nuclei, and nuclear interactions of the cosmic radiation. The background strength has been computed[29] for a number of different reactors, and the results are summarized in Table III-1, which is taken from reference 29.

The reference states that the background source strength has recently been measured in a critical assembly fueled with highly enriched uranium in Zircaloy-2. The measurement was in good agreement with calculation; however, the addition of boron did not increase the back-

Table III-1 CALCULATED BACKGROUND NEUTRON-SOURCE STRENGTHS[29]

Fuel material	Spontaneous fission-neutron yield per gram of U per second	(α,n) neutron yield per gram of U per second	Neutrons from cosmic radiation			Total neutron yield per gram of U per second	Experiment or reactor type
			Grams core material per gram of U	Condensed material above core center, g/cm^2	Neutron yield per gram of U per second		
Natural U metal	1.6×10^{-2}		1	200	2.4×10^{-4}	1.6×10^{-2}	Hanson's sphere*
Natural U metal	1.6×10^{-2}		9	1000	2×10^{-5}	1.6×10^{-2}	X-10 graphite-moderated reactor
Natural $U-O_2$	1.6×10^{-2}	2.4×10^{-4}	10	1000	2×10^{-5}	1.6×10^{-2}	Littler's graphite-moderated reactor†
Enriched U metal	1.5×10^{-3}		1	200	2.4×10^{-4}	1.7×10^{-3}	Godiva sphere
Enriched U–Al	1.5×10^{-3}	3.5×10^{-1}	20	200	5×10^{-4}	3.5×10^{-1}	Water-moderated critical facility
Enriched $U-O_2$	1.5×10^{-3}	3×10^{-2}	20	200	5×10^{-4}	3.2×10^{-2}	Water-moderated critical facility
Enriched U–Zr	1.5×10^{-3}	5×10^{-4}	20	200	5×10^{-4}	2.5×10^{-3}	Water-moderated critical facility
				500	1×10^{-4}	2.1×10^{-3}	Water-moderated power facility
Enriched U–Zr with added natural B (500 ppm)	1.5×10^{-3}	3.2×10^{-2}	20	200	5×10^{-4}	3.4×10^{-2}	Water-moderated critical facility
				500	1×10^{-4}	3.4×10^{-2}	Water-moderated power facility

*O. Hanson, Capture and Inelastic Scattering in Spheres of Various Metals, USAEC Report LA-276, 1945.

†J. Littler, A Determination of the Rate of Emission of Spontaneous Fission Neutrons by Natural Uranium, *Proc. Phys. Soc. (London)*, 65A: 203 (1952).

ground as much as calculated. It was postulated that there might be segregation of uranium-rich and boron-rich lumps in the microstructure of the fuel elements.

Recent Measurements

Average Number of Neutrons Produced per Fission for U^{238}

Measurements of ν (average number of neutrons produced per fission), for spontaneous fission and for fission induced by neutrons of the U^{235} fission spectrum, in U^{238}, are reported in reference 30. The value for fission-spectrum-induced fission was measured by two methods: the scattering method and the coincidence method. The former gave a value of $\nu = 2.87 \pm 0.35$, whereas the latter, more precise, technique gave $\nu = 2.93 \pm 0.075$, based on a value of 2.47 ± 0.03 for the value of ν for thermal-neutron fission of U^{235}. The value for spontaneous fission of U^{238}, measured also by the coincidence method relative to the thermal ν of U^{235}, was $\nu(U^{238}, \text{spontaneous}) = 2.10 \pm 0.08$.

The reference[30] discusses the relation of the measurements to previous measurements and suggests that the current best value of $\nu(U^{238})$ for fission which is induced by fission-spectrum neutrons is 2.86 ± 0.05 if $\nu(U^{235}, \text{thermal})$ is accepted as 2.47 ± 0.03. It is stated that the 2.86 value is in good agreement with Leachman's equation[31]

$$\nu(E) = \nu(0) + aE$$

with $\nu(0) = 2.40$, $a = 0.14\ (\text{Mev})^{-1}$, and E (effective, for U^{235} fission spectrum) = 3.1 Mev.

A recent discussion of ν for fast-neutron fission of other isotopes is contained in reference 32.

Specific Alpha Activity of Plutonium

Russian measurements of the specific alpha activities of Pu^{239} and Pu^{240} show[33] that 1 μg of Pu^{239} gives 136,200 ± 200 alpha decays per minute, corresponding to a half life of 24,390 ± 30 years, and that 1 μg of Pu^{240} gives 500,000 ± 4000 alpha decays per minute, corresponding to a half life of 6620 ± 50 years.

Absorption of Th^{233}

Reference 34 describes measurements of the thermal-absorption cross section and the resonance absorption integral for the isotope Th^{233}, which has a 23-min half life. Determinations of the resonance absorption integrals of Th^{233} and Co^{59} were incidental to the Th^{233} measurement, and these results are reported also.

Resonance Integrals

Resonance absorption integrals for a number of elements and isotopes (38 in all), measured in the Harwell D_2O reactor, DIMPLE, are reported in reference 35. The measurements were made with the pile oscillator. The samples were oscillated first in a highly thermalized spectrum and then in a hardened spectrum, the different spectra being obtained by variation of the fuel loading of the reactor. The effect of a sample on the reactivity of the reactor in either the thermalized or the hardened spectrum is determined by its effective absorption cross section in that spectrum. The resonance integral can be derived from the difference between the effective cross sections in the two spectra if the relative intensities of the epithermal- and thermal-neutron components of the hardened spectra are determined by measurements on an absorber of known resonance integral. Gold was used as this standard resonance absorber. Its resonance integral (above $1/v$) was taken as 1513 ± 60 barns, the value given in the earlier work of Macklin and Pomerance.[36]

Graphite Absorption Cross Section

The neutron absorption cross section of graphite varies according to its impurity content. A program has been under way to intercompare graphite absorption cross sections between laboratories in the United States, the United Kingdom, and France. Reference 37 describes measurements at Hanford on several graphite samples from the three countries and compares the Hanford results with those obtained in France and the United Kingdom.

At Hanford the cross section for one graphite sample was determined in the PCTR by reactivity comparison against copper, which was in turn calibrated against gold. The measured graphite sample—σ_a (2200 m/sec) = 3.80 ± 0.04 mb—was then used as a standard for measurement of the other samples in the Hanford Test Reactor (HTR). The results are given in Table III-2* for six different lots of graphite and for

*Table III-2 is reprinted here by permission from *Nuclear Science and Engineering*.[37]

Table III-2 COMPARISON OF HANFORD, HARWELL, AND ZOÉ GRAPHITE ABSORPTION CROSS-SECTION MEASUREMENTS[37]

(Values Given Are in Millibarns)

Lot	Hanford	Harwell	Zoé
I (American)	3.51 ± 0.06	3.63 ± 0.30†	
II (American)	3.65 ± 0.06	3.75 ± 0.30	
III (American)	3.54 ± 0.06*		3.65 ± 0.15*
IV (British)	3.67 ± 0.06	3.76 ± 0.30	
V (British)	3.93 ± 0.06	4.12 ± 0.30	
VI (French)	3.53 ± 0.06*		3.80 ± 0.15*

*The French values for Lot VI were obtained by measuring in Zoé pieces cut from the ends of the bars before sending them to Hanford. The cross-section values quoted are relative to boron. As a general rule, extremities of bars are somewhat less pure than the central part [private communication from H. Hering, Saclay]. Dr. Hering states that in the mean this difference amounts to 0.05 mb for the French bars. However, this would probably provide no explanation for the differences in the French and American scales as deduced from the measurements in this table. A better cross check on the French graphite will be obtained by sending three bars back to France for measurements in Zoé. The individual measurements on the test bars are as shown in the tabulation:

	Lot III			Lot VI			
Graphite bar number	1657B 8B	994B 15B	1503B 60B	5485	5501	5506	5516
French values	3.71	3.63	3.60	3.76	3.79	3.83	3.84
American values	3.59	3.54	3.48	3.50	3.52	3.56	3.55

Note: It should be pointed out that one extremity of bar 8B was very impure [private communication from H. Hering, Saclay]. The quoted error of ±0.15 mb for the French measurements includes all systematic errors and corresponds to the probable error.

†The British absolute cross-section scale is based upon a series of diffusion-length experiments performed at Harwell on graphite blocks intercompared in GLEEP. Their values are consistent with a transport mean free path of 2.53 cm at a density of 1.65 g/cm^3. The uncertainty of 0.30 mb is their estimated experimental error and is the result of the uncertainty in the diffusion-length measurements.

individual bars in two of the lots. The French measurements are pile-oscillator measurements, and the British measurements are danger coefficient measurements performed in GLEEP in a manner very similar to the HTR tests. All measurements have been corrected, at the laboratories where these measurements were made, for nitrogen absorbed in the graphite pores.

Slowing-Down Measurements

A measurement of the age from fission to indium resonance in H_2O, the result of which was previously discussed (reviewed in the September 1959 issue of *Power Reactor Technology*, Vol. 2, No. 4, pages 30 to 33) in relation to theoretical results,[38] has recently been reported in detail.[39] The measured age is $\tau = 27.3 \pm 0.9$ cm^2, where the quoted error is meant to indicate a bound on the error rather than a probable error.

Measurements of the age to indium resonance in H_2O, of neutrons from the fission of U^{233}, are reported in reference 40. The weighted average of three measurements on U^{233} was 27.6 ± 0.6 cm^2, whereas two measurements on U^{235}, by identical procedures, gave a weighted average of 29.1 ± 0.8 cm^2. Since corrections for some of the sources of systematic errors were not made, the reference claims only relative significance for the results: the conclusion is that the age of U^{233} neutrons in water appears to be less than that of U^{235} neutrons by 5 ± 3 per cent. It is stated that this result is in agreement with the theoretical results in reference 41.

Table III-3 COMPARISON OF EXPERIMENTAL DATA FOR VARIOUS ORGANIC LIQUIDS AND WATER*[43]

Moderator	Neutron age in pure moderator (τ), cm^2	Relative number of hydrogen nuclei/cm^3	Relative number of moderator nuclei/cm^3	Density, g/cm^3
Water	31.4	1.00	1.000	1.00
Isoamyl alcohol, $(CH_3)_2CHCH_2CH_2OH$	25.5 ± 2	0.996	0.999	0.813
Cyclohexanone, $C_6H_{10}O$	33.5 ± 2.7	0.871	0.988	0.947
Benzyl alcohol, $C_6H_5CH_2OH_2$	36 ± 2.9	0.694	0.915	1.043
Toluene, $C_6H_5CH_3$	41 ± 3.2	0.678	0.848	0.866
Formic acid (87%), HCO_2H	49.5 ± 2.6†	0.533	0.81	1.19
Mixture of organic compounds	52.5 ± 4.2	~0.55	~0.75	

*Of the lattice volume, 84 per cent was occupied by the moderator, six per cent by uranium, five per cent by steel, and five per cent by air spaces.

†Direct measurement to indium resonance energy by L. A. Gerasevaia and V. V. Vavilov.

Age measurements of Na-Be neutrons in water and kerosene are reported in reference 42. The measurements were made primarily to investigate certain aspects of the discrepancy between experiment and theory for the age of fission neutrons in H_2O. The use of a nearly monoenergetic neutron source removes the uncertainties connected with the broad and somewhat uncertain fission spectrum, whereas the measurement in kerosene circumvents the uncertainties, due to the rapidly varying oxygen cross section, which enter into the H_2O case. The results of the measurements were found to be in good agreement with calculated ages for both H_2O and kerosene. The calculations for H_2O have been made by the combination Monte Carlo–moments method (by Coveyou) and for kerosene by the moments method (by Goldstein). The results for the age to indium resonance were:

	Measured	Calculated
H_2O	13.88 ± 0.22	13.90 ± 0.14
Kerosene	13.84 ± 0.21	13.94 ± (0.08)

The errors quoted are standard deviations. In the calculation for kerosene the quoted standard deviation takes into account only the uncertainty in the carbon-to-hydrogen ratio of the moderator.

Reference 43 describes critical experiments in a small assembly moderated by various organic liquids. Values of the ages (to thermal) for the various liquids were derived from measurements of the buckling and the change in reactivity with moderator level. The results are given in Table III-3.* The quoted ages for the organics were obtained by normalization to the age for H_2O, which was taken to be 31.4 cm^2.

Critical and Exponential Experiments

In the September 1960 issue of *Power Reactor Technology*, Vol. 3, No. 4, a brief tabular summary was given of critical and exponential experiments reported since the compilation in *Reactor Physics Constants*.[44] In the future, new exponential and critical work will be cited in *Power Reactor Technology* as this work is published. Usually it is impractical to do more than indicate the scope of each investigation since the results are seldom useful unless they are reported in detail.

The Yankee critical experimental measurements of critical size, buckling, reflector savings, migration area, disadvantage factor, resonance escape probability, and temperature coefficient (volume ratios of 2.2, 2.9, and 3.9 to 1 for water to uranium metal) are described in references 45 and 46. The fuel elements are composed of 2.7 per cent enriched UO_2 pellets clad in stainless steel. Using the experimental data in reference 45, a calculation system[47] was

*Table III-3 is reprinted here by permission from *Journal of Nuclear Energy: Part A, Reactor Science*.[43]

deduced from theory and experiment for predicting the shutdown available in the control rods for the final design of the first Yankee core. The general purpose of the calculations was to obtain an experimental value for the empirical fast-neutron absorption cross section to be used in the one- and two-dimensional analysis. The experimental information of most interest consisted of measurements of the negative axial buckling in a region containing a bank of control rods, and measurements by boron substitution of the worths of individual rods, banks inserted to various depths, and groups of rods. The fuel used for the control-rod experiments was 3.4 per cent enriched UO_2. The basic multiplying characteristics of the BR-3 fuel elements[46,48] were also measured for water-to-uranium metal volume ratios of 2.9 and 3.9 to 1. These measurements consisted of critical size, buckling, reflector savings, resonance escape probability, fast effect, and disadvantage factor. The BR-3 fuel elements are composed of 4.4 per cent enriched UO_2 pellets clad in stainless steel.

As an extension of the Yankee and the BR-3 critical experiments, a series of two-region critical experiments[48] was performed at the Westinghouse Reactor Evaluation Center. The primary purpose of these experiments was to measure the spatial distribution of neutron flux and power production in reactor cores of simple geometric shape containing two regions of different fuel enrichments, in order that a comparison could be made with analytically derived distributions for the same cores. The two-region measurements consisted of determinations of critical water heights, radial flux plots using gold foils and depleted uranium foils, and radial power plots obtained by measuring fission-product activity in the fuel itself. The cores used were right-circular cylinders of Yankee CRX (2.7 per cent enriched) fuel surrounded by annuli of BR-3 (4.4 per cent enriched) fuel. Two sets of the Yankee CRX core plates, those of 0.435- and 0.470-in. pitch (giving volume ratios of 2.9 and 3.9 to 1 for water to uranium metal), were used.

The results of the loose lattice experimental work performed under the Multi-Region Lattice Program conducted at the Westinghouse Reactor Evaluation Center are described in reference 49. The purpose of the experiments was to obtain critical mass information in the range of moderating ratios close to the optimum and to verify the physics computational methods now used for fuel-storage calculations. The experimental measurements consisted of critical size, buckling, reflector savings, and microscopic parameter measurements. These measurements were made in cores containing 2.73 per cent enriched Yankee fuel (UO_2–stainless steel clad fuel rods) with lattice pitches of 0.573, 0.615, and 0.665 in. (giving volume ratios of 7.03 : 1, 8.51 : 1, and 10.38 : 1 for water to uranium metal. The microscopic parameter measurements were made only in the cores with the two smallest lattice pitches. The buckling, reflector savings, and microscopic parameters were measured in cores containing two control-rod followers. The critical sizes were determined for each lattice pitch for the cases of both two and four control-rod followers; the clean critical size was then obtained by extrapolation.

Critical experiments[50] for the Consolidated Edison Thorium Reactor (CETR) have provided data on thorium oxide–uranium oxide fuel, in stainless-steel cladding, moderated with light water. These data are for cores with metal-to-water volume ratios near 1 (the region of interest in pressurized-water-reactor design). Experiments at ANL have provided data on similar fuel in aluminum cladding moderated with heavy water. These data are for the low metal-to-water volume ratios that accompany heavy-water moderation. The Thorium Uranium Physics Experimental program (TUPE) conducted by the Babcock and Wilcox Company is intended to complement these data by providing information on lattices with ratios between the CETR and ANL values, a region which is of interest for boiling-water-reactor design. TUPE cores contain thorium oxide–uranium oxide pins clad with aluminum and have metal-to-water volume ratios ranging from 0.3 to 1.0 and for N_{02}/N_{25} = 25/1 and 15/1. A series of "clean core" measurements was done on five lattices, including flux mappings, critical mass determinations, cadmium ratio measurements for U^{235} and thorium, and flux depression measurements. These data were then analyzed to obtain material buckling, the ratio of infinite-medium thermal multiplication to infinite-medium resonance multiplication, the thermal-disadvantage factors for moderator and for cladding, the thorium resonance escape probability, and the U^{235} resonance escape probability. Leakage experiments, including partial water-height experiments and

lattice poisoning experiments, were performed on two cores. Leakage experiments were performed on two additional cores without lattice poisoning. The leakage experiments consisted of determination of the water-height coefficient of reactivity as a function of water height and boric acid concentration in the moderator. These data were analyzed to determine migration area and infinite-medium multiplication constant. The experimental results were checked against several of the available calculational models.

A program of critical approach and exponential measurements[51] of 3.063 per cent enriched uranium rods in light water is being conducted at Hanford Atomic Products Operation. Critical masses, buckling, and some extrapolation lengths have been measured for four rod diameters (0.300, 0.600, 0.925, and 0.175 in.) with various lattice spacings. The latest measurements were with rods 0.175 in. in diameter by 23.5 in. in length, encased in 0.025-in.-wall Lucite tubes for insertion into hexagonal lattice frameworks. All lattices were moderated and completely reflected with light water. In addition, critical-approach type measurements[52] were made with assemblies having circular, elliptic, and rectangular cross sections, to try to evaluate some of the perturbation effects that are usually present when making heterogeneous critical mass measurements. Using the 0.175-in. rods arranged in a triangular lattice with a water-to-uranium (total) volume ratio of 8.0, the investigations were: (1) to determine the effect of the irregular outer boundary on the measured critical mass, (2) to obtain information on the effect of geometry on the extrapolation distance, (3) to examine the feasibility of determining more accurately the effective radius of the extrapolated critical cylinder by introducing a shape deformation which is then successively decreased to zero, and (4) to compare the theoretical buckling formulations with experiments.

Measurements[53] of the lattice parameters, including the infinite multiplication factor, thermal utilization, resonance escape probability, and fast effect, have been performed in the PCTR at Hanford in support of the Experimental Gas-Cooled Reactor (EGCR) program. The EGCR fuel element is a seven-rod cluster of 1.8 per cent enriched UO_2 clad in stainless steel. The lattice spacing is 8 in. Detailed flux traverses were required for this lattice because there is a strong axial flux dependence caused principally by the stainless-steel end caps and spiders which break the continuity of the UO_2 columns by displacing some of the UO_2 pellets at each end of the cell. Since one of the problems[54] encountered in the design of the EGCR has been the possibility of bowing in the outer six rods of the seven-rod cluster, two detailed flux traverses (radial and axial) were made on the EGCR lattice in the PCTR to obtain data needed to solve this problem.

References 55 to 60 describe the criticality measurements made by the Dow Chemical Company, on plutonium-Plexiglas and plutonium-graphite assemblies, and on enriched uranium metal in $UO_2(NO_3)_2$ solutions. Neutron multiplication measurements[55,56] were made on cylindrical disk assemblies constructed of alternate layers of Plexiglas and plutonium-metal sheet. Both bare and tamped assemblies were investigated. The hydrogen-to-plutonium atomic ratios were varied from 0 to 90 for the tamped arrays and from 0 to 94 for the untamped arrays. Neutron multiplication measurements[57,58] were also made on a similar assembly of graphite and plutonium-metal sheet, on cylindrical assemblies[59] of enriched metal disks immersed in water and in concentrated solutions of enriched $UO_2(NO_3)_2$, and on two identical finite metal slab assemblies[60] separated and reflected by Plexiglas. The thickness of the plutonium sheet was varied in order to study the effects of inhomogeneity.

Experiments[43] to study the properties of organic compounds as moderators were carried out in the U.S.S.R. with a small liquid-moderated critical assembly. The fuel elements containing highly enriched uranium were arranged in a triangular lattice. The critical masses, the rate of increase of reactivity with rising level of the moderator above the critical level, and the Laplacian λt^2 for the distribution of thermal neutrons were experimentally determined.

Criticality and neutron activation distribution measurements[61] were initiated at Bettis Atomic Power Laboratory, in the High-Temperature Test Facility (HTTF), on a highly enriched uranium–zirconium slab core. The temperature defect and the temperature coefficient were measured near operating power-reactor temperatures, and the thermal-neutron activation measurements are being obtained not only in the core and adjacent reflector regions but also at a relatively large distance into the water re-

flector. The data will be compared with calculational results to check the applicability of current nuclear design models and to predict control requirements, power distributions, and depletion rates. The slab is 6 in. wide and 30 in. high and of length varied to make it "clean" critical at various temperatures. It is constructed of 9.5 wt.% uranium–zirconium alloy plates clad with zirconium and positioned in grooved zirconium boxes which are clamped together to form a relatively uniform composition. The average metal-to-water ratio of the assembly is 1.2.

References

1. E. U. Vaughan, Flux Hardening in Fuel Rods, USAEC Report NAA-SR-4780, Atomics International, Mar. 15, 1960.
2. C. H. Westcott, Effective Fission and Capture Cross-Sections for Hardened Maxwellian Neutron Spectra, *J. Nuclear Energy: Pt. A, Reactor Sci.*, 12(3): 113–121 (June 1960).
3. A. M. Weinberg and E. P. Wigner, *The Physical Theory of Neutron Chain Reactors*, University of Chicago Press, 1958.
4. V. G. Small, An Experimental Determination of the Increase with Temperature of the Resonance Absorption in Uranium and Thorium, British Report AERE-R/R-2774, April 1959.
5. R. M. Pearce, Radial Dependence of the Doppler Effect in Bars of Uranium and Thorium, *J. Nuclear Energy: Pt. A, Reactor Sci.*, 11(2/4): 136–149 (February 1960).
6. K. W. Morton, A Monte Carlo Study of the Resonance Absorption and Its Temperature Variation in a Square Uranium-Graphite Lattice, British Report AERE-R-2929, July 1959.
7. F. C. Engesser and T. J. Oakes, The Fuel-Temperature Coefficient for Seven-Rod Clusters of Uranium Oxide with Air Coolant, in Nuclear Physics Research Quarterly Report for October–December 1959, USAEC Report HW-63576, pp. 36–54, Hanford Atomic Products Operation, Jan. 20, 1960.
8. C. H. Westcott, Effective Cross-Section Values for Well-Moderated Thermal Reactor Spectra, Canadian Report CRRP-787 (AECL-670), Aug. 1, 1958.
9. E. Hellstrand, Measurements of the Effective Resonance Integral in Uranium Metal and Oxide in Different Geometries, *J. Appl. Phys.*, 28(12): 1493–1502 (1957).
10. M. V. Davis, Resonance Capture of Neutrons by Uranium Cylinders, USAEC Report HW-37766, Hanford Atomic Products Operation, Aug. 18, 1955.
11. M. V. Davis, Resonance Absorption of Neutrons by Uranium Cylinders, *J. Appl. Phys.*, 28(2): 250 (1957).
12. B. P. Ad'yasevich et al., Measurement of Temperature Effects in Uranium-Graphite Systems, *Conf. Acad. Sci. U.S.S.R. Peaceful Uses At. Energy, Moscow, 1955, Session Div. Phys. Math. Sci.*, pp. 109–121 (1956) (English translation).
13. M. B. Egiazarov et al., Measuring the Resonance Absorption of Neutrons in a Uranium-Graphite Lattice, *Conf. Acad. Sci. U.S.S.R. Peaceful Uses At. Energy, Moscow, 1955, Session Div. Phys. Sci.*, pp. 59–67 (1956) (English translation).
14. G. W. Rodeback, Temperature Coefficients of Uranium and Thorium Resonance Integrals, USAEC Report NAA-SR-1641, Atomics International, Sept. 1, 1956.
15. M. V. Davis, Resonance Absorption of Neutrons by Thorium Cylinders, *J. Appl. Phys.*, 28(2): 714 (1957).
16. L. Dresner, Resonance Absorption of Neutrons in Nuclear Reactors (thesis), USAEC Report ORNL-2659, Oak Ridge National Laboratory, Mar. 10, 1959.
17. R. E. Heineman, Measurement of Fuel-Temperature Coefficients of k_∞ with the PCTR, in Nuclear Physics Quarterly Report for April–June 1958, USAEC Report HW-56919, pp. 42–45, Hanford Atomic Products Operation, July 21, 1958.
18. G. G. Smith and D. Klein, Surface-to-Volume Activation by Resonance Neutrons in a Uranium Metal Rod, USAEC Report WAPD-BT-17, pp. 48–50, Westinghouse Electric Corp., Bettis Atomic Power Laboratory, May 17, 1960.
19. D. Klein et al., Spatial Distribution of U^{238} Resonance Neutron Capture in Uranium Metal Rods, *Nuclear Sci. and Eng.*, 3(6): 698 (June 1958).
20. J. Hardy et al., Resonance Capture, in Reactor Physics and Mathematics Technical Progress Report for the Period March 1 to June 1, 1960, USAEC Report WAPD-MRJ-10, pp. 3–5, Westinghouse Electric Corp., Bettis Atomic Power Laboratory, June 1960.
21. K. S. Rockey and W. Skolnik, Measurements on the Diffusion Length of Thermal Neutrons in Water from 25 to 296°C, *Nuclear Sci. and Eng.*, 8(1): 62–65 (July 1960).
22. M. Kuchle, Measurements of the Temperature Dependence of Thermal Neutron Diffusion Parameters in Water and Dowtherm A (Letters to the Editors), *Nuclear Sci. and Eng.*, 8(1): 88 (July 1960).
23. M. Reier and J. DeJuren, Diffusion Length Measurements, *Nuclear Sci. and Eng.*, 8(1): 10 (July 1960).
24. A. Radkowsky, Temperature Dependence of Thermal Transport Mean Free Path, in Physics Division Quarterly Report for April–June 1950, USAEC Report ANL-4476, pp. 89–100, Argonne National Laboratory, July 5, 1950.

25. P. G. Khubchandani and A. Rahman, Scattering of Slow Neutrons by the Water Molecule, *J. Nuclear Energy: Pt. A, Reactor Sci.*, 11(2/4): 89–94 (February 1960).
26. A. F. Goryunov, Scattering of Slow Neutrons by Water Molecules, *J. Nuclear Energy*, 4: 109–114 (1957).
27. R. A. Dannels and W. J. Eich, Neutron Flux Peaking and Power Shapes: A Comparison of Theory and Experiment, USAEC Report YAEC-151, Westinghouse Electric Corp., Bettis Atomic Power Laboratory, October 1959.
28. M. Goldsmith and T. M. Ryan, Thermal Activation Shapes in a Water-Moderated Critical Assembly, *Nuclear Sci. and Eng.*, 5(5): 299 (May 1959).
29. D. R. Harris, Background Neutron Source in New Reactors, in Reactor Physics and Mathematics Technical Progress Report for the Period March 1 to June 1, 1960, USAEC Report WAPD-MRJ-10, p. 77, Westinghouse Electric Corp., Bettis Atomic Power Laboratory, June 1960.
30. Rudolph Sher and Jean Leroy, The Value of ν for Fission Spectrum Induced and Spontaneous Fission of U^{238}, *J. Nuclear Energy: Pt. A, Reactor Sci.*, 12(3): 101 (June 1960).
31. R. B. Leachman, The Fission Process: Mechanisms and Data, *Proceedings of the Second United Nations International Conference on the Peaceful Uses of Atomic Energy, Geneva, 1958*, Vol. 15, p. 229, United Nations, New York, 1958.
32. James Terrell, The Status of Measurements of $\bar{\nu}$ and $\sigma(n,\gamma)$ for Fast Neutrons, in Proceedings of the Conference on the Physics of Breeding, October 19–21, 1959, USAEC Report ANL-6122, pp. 33–50, Argonne National Laboratory, Aug. 1, 1960.
33. Ia. P. Dokuchaev, The Specific α-Activity of Pu^{239} and Pu^{240}, *J. Nuclear Energy: Pt. A. Reactor Sci.*, 11(2/4): 195 (February 1960).
34. E. J. Johnston et al., The Thermal-Neutron-Absorption Cross Section of Th^{233} and the Resonance Integrals of Th^{232}, Th^{233}, and Co^{59}, *J. Nuclear Energy: Pt. A, Reactor Sci.*, 11(2/4): 95 (February 1960).
35. R. B. Tattersall et al., Pile Oscillator Measurements of Resonance Absorption Integrals, *J. Nuclear Energy: Pt. A, Reactor Sci.*, 12(1/2): 32 (May 1960).
36. R. L. Macklin and H. S. Pomerance, Resonance Capture Integrals, *Proceedings of the Second United Nations International Conference on the Peaceful Uses of Atomic Energy, Geneva, 1958*, Vol. 5, p. 96, United Nations, New York, 1958.
37. P. F. Nichols, Absorption Cross Section of Graphite, *Nuclear Sci. and Eng.*, 7(5): 395 (May 1960).
38. W. C. Redman, Considerations of Neutron Age in Light Water: Review of Experiments, *Trans. Am. Nuclear Soc.*, 2(1) (June 1959).
39. D. B. Lombard and C. H. Blanchard, Fission-to-Indium Age in Water, *Nuclear Sci. and Eng.*, 7(5): 448 (May 1960).
40. W. G. Pettus, Age of U^{233} Fission Neutrons in Water, *Nuclear Sci. and Eng.*, 8(2): 171 (August 1960).
41. Martin Faber and P. F. Zweifel, The Age of U^{233} Fission Neutrons in Water, *Nuclear Sci. and Eng.*, 6(1): 81 (July 1959).
42. D. Graham Foster, Jr., Age of Na-Be Neutrons in Water and Kerosene, *Nuclear Sci. and Eng.*, 8(2): 148 (August 1960).
43. B. G. Dubovskii and M. N. Lantsov, Organic Compounds as Moderators in Nuclear Reactors, *J. Nuclear Energy: Pt. A, Reactor Sci.*, 12(3): 122 (June 1960).
44. Argonne National Laboratory, Reactor Physics Constants, USAEC Report ANL-5800, July 1, 1958.
45. P. W. Davison et al., Yankee Critical Experiments: Measurements on Lattices of Stainless-Steel-Clad Slightly Enriched Uranium Dioxide Fuel Rods in Light Water, USAEC Report YAEC-94, Westinghouse Electric Corp., Bettis Atomic Power Laboratory, Apr. 1, 1959.
46. V. E. Grob et al., Measurements of Parameters Leading to p_{28}, f, and ϵ in a Water-Moderated 4.4% Enriched UO_2 Lattice, *Nuclear Sci. and Eng.*, 7(6): 514 (June 1960).
47. W. H. Arnold, Jr., Physics Calculations for Control Rods in the First Yankee Core, USAEC Report YAEC-62, Westinghouse Electric Corp., Bettis Atomic Power Laboratory, September 1959.
48. P. W. Davison et al., Two-Region Critical Experiments with Water-Moderated Slightly Enriched UO_2 Lattices, USAEC Report YAEC-142, Westinghouse Electric Corp., Bettis Atomic Power Laboratory, Nov. 30, 1959.
49. V. E. Grob et al., Results of Critical Experiments in Loose Lattices of UO_2 Rods in H_2O, USAEC Report WCAP-1412, Westinghouse Reactor Evaluation Center, Mar. 30, 1960.
50. N. L. Snidow et al., Thorium–Uranium Physics Experiments, Final Report, USAEC Report BAW-1191, Babcock & Wilcox Co., May 1960.
51. R. C. Lloyd et al., Criticality Measurements of Heterogeneous 3.1 Per Cent Enriched Uranium and Water Systems, in Nuclear Physics Research Quarterly Report for October–December 1959, USAEC Report HW-63576, pp. 65–69, Hanford Atomic Products Operation, Jan. 20, 1960.
52. W. A. Reardon and R. C. Lloyd, Shape Perturbations in Critical Experiments, in Nuclear Physics Research Quarterly Report for October–December 1959, USAEC Report HW-63576, pp. 70–76, Hanford Atomic Products Operation, Jan. 20, 1960.
53. P. F. Nichols, Lattice Parameters for the Experimental Gas-Cooled Reactor, in Nuclear Physics Research Quarterly Report for October–December 1959, USAEC Report HW-63576, pp. 55–60, Hanford Atomic Products Operation, Jan. 20, 1960.
54. P. F. Nichols, EGCR Lattice Radial and Angular Power Distribution, in Nuclear Physics Research

Quarterly Report for October–December 1959, USAEC Report HW-63576, pp. 61–64, Hanford Atomic Products Operation, Jan. 20, 1960.

55. C. L. Schuske et al., Plutonium Plexiglas Assemblies, USAEC Report RFP-178, Dow Chemical Co., Jan. 20, 1960.
56. G. H. Bidinger et al., Plutonium Plexiglas Assemblies, Part II, USAEC Report RFP-190, Dow Chemical Co., Apr. 8, 1960.
57. A. Goodwin, Jr., and C. L. Schuske, Plutonium Graphite Assemblies, USAEC Report RFP-123, Dow Chemical Co., Sept. 29, 1958.
58. A. Goodwin, Jr., and C. L. Schuske, Plutonium Graphite Assemblies, Part II, USAEC Report RFP-158, Dow Chemical Co., Aug. 10, 1959.
59. A. Goodwin, Jr., et al., Criticality Studies of Enriched Uranium Metal in $UO_2(NO_3)_2$ Solutions, USAEC Report RFP-182, Dow Chemical Co., July 28, 1960.
60. C. L. Schuske et al., Interaction of Two Metal Slabs of Plutonium in Plexiglas, USAEC Report RFP-174, Dow Chemical Co., Dec. 28, 1959.
61. L. O. Herwig and W. F. Vogelsang, Highly Enriched Clean Critical Slab Assembly, in Reactor Physics and Mathematics Technical Progress Report for the Period March 1 to June 1, 1960, USAEC Report WAPD-MRJ-10, p. 11, Westinghouse Electric Corp., Bettis Atomic Power Laboratory, June 1960.

Section IV

HEAT TRANSFER AND FLUID FLOW

Liquid Cooling

The concept of departure from nucleate boiling (DNB) was discussed in the September 1960 issue of *Power Reactor Technology*, Vol. 3, No. 4, page 27, wherein a theoretical study was reported. Reference 1 reports on an experimental study of boiling heat transfer from a horizontal tube to a saturated liquid at atmospheric pressure in the nucleate, transition, and film boiling regions. The results are of interest to power-reactor technology in that they give insight into basic mechanisms involved in boiling heat transfer.

The apparatus used was designed to transfer heat through the walls of a horizontal pipe to a boiling fluid: the source of heat was a high-pressure hot-water loop, and both water and Freon 11 (Refrigerant 11) were employed as boiling liquids. Two series of runs were accomplished. The first series was planned to gain operating experience and to check the effect of surface variables on the boiling curve. The tube materials that were used and the liquid that was boiled are as follows:

Liquid boiled	Tube material (5/8 in. OD, 1/2 in. ID)
Refrigerant 11	304 stainless steel
Refrigerant 11	ETP copper
Refrigerant 11	Teflon-coated 304 stainless steel
Refrigerant 11	Ceramic-coated 304 stainless steel
Water	ETP copper

The second series of runs was performed to extend experimental data and utilized the following combinations:

Liquid boiled	Tube material (3/4 in. OD, 1/2 in. ID)
Refrigerant 11	SB161 nickel
Refrigerant 11	Chrome-plated ETP copper
Refrigerant 11	Ceramic-coated SB161 nickel
Water	Chrome-plated ETP copper
Water	Ceramic-coated ETP copper

Figure 5 is an example of the data obtained for the boiling of Refrigerant 11 on three different surfaces. The effect of the wall material, as well as the relative invariance of the peak heat flux, is evident. Figure 6 presents data for Refrigerant 11 boiling on stainless steel, and the numbers shown adjacent to the

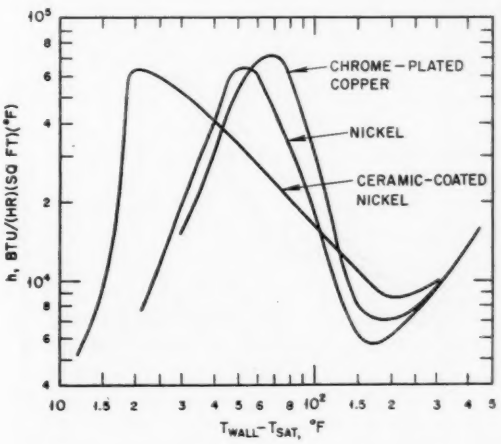

Figure 5— Heat transfer[1] to Refrigerant 11.

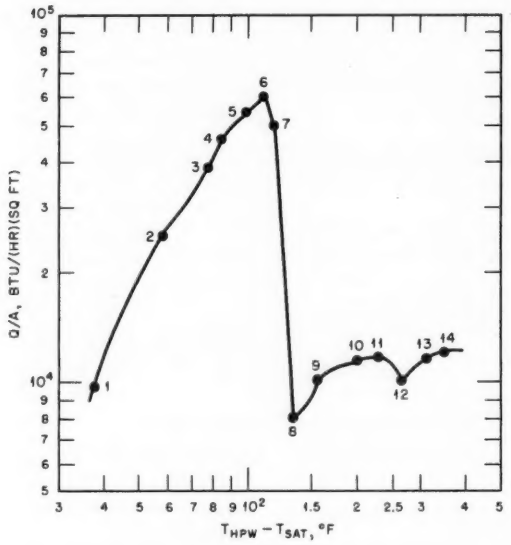

Figure 6—Heat transfer to Refrigerant 11 from stainless-steel tube.[1] (The subscript HPW = high-pressure water.)

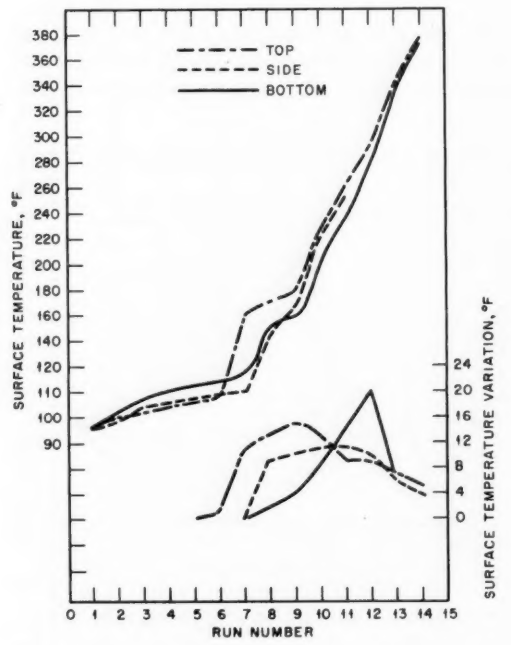

Figure 7—Wall temperature of stainless-steel tube.[1]

data points represent various runs, numbered 1 to 14. In an attempt to gain additional insight on DNB, three thermocouples were welded to the top, to the side, and to the bottom of an experimental stainless-steel pipe. Figure 7 illustrates the surface temperature and surface-temperature variation for those runs corresponding to the data points in Fig. 6. In runs 1 to 6, where nucleate boiling was the dominant effect, the surface temperatures were approximately constant, as can be seen in Fig. 7. With the onset of DNB, however, surface-temperature fluctuations become evident. These irregularities are present until run 14, where stable film boiling was evident. Photographic data are also presented in reference 1.

The conclusions, as summarized[1] in the reference, are:

1. $(Q/A)_{max}$ for these conditions is almost a constant and is unaffected by a shift of $(\Delta T)_{max}^{[*]}$ of as much as 40°.
2. $(\Delta T)_{max}$ is strongly dependent on surface conditions.
3. Data in the transition region is highly unstable, depending on surface conditions and on wetting properties of the liquid.
4. The inception of transition boiling is marked by violent motions of a two-phase mixture which alternately approaches and is driven from the heated surface. Thus a vapor film is gradually produced as the surface temperature rises, and stable film boiling is established only when the surface temperature becomes relatively constant.
5. The liquid does touch the surface during transition boiling.
6. There is no unique minimum point.[†]
7. The minimum point[†] does not necessarily mark the dividing line between transition and film boiling.
8. The criterion for stable film boiling should be the absence of fluctuations in the surface temperature.

Reference 2 is a study of "boiling songs" (the sustained sounds that are sometimes generated in connection with heat transfer at high heat-flux levels) and associated mechanical vibrations. It is based on observations made at different laboratories doing boiling heat-transfer experimentation and on a review of

* The ΔT at which Q/A is maximum.

† The point referred to is the minimum in the curve of Q/A vs. ΔT. It was found to be not unique in the sense that, for example, it varies with surface condition and may vary for different runs on the same apparatus.

recent literature. The conclusions are as follows:

1. Under certain conditions of local boiling, which includes a boilinglike mechanism at supercritical pressures, intense sounds (boiling songs) and mechanical vibrations can be generated.
2. The occurrence of these intense sounds and mechanical vibrations is intimately related to the operating conditions in the heated portion of the loop.
3. The boiling songs and associated vibrations are accompanied by large-amplitude pressure and flow fluctuations, although such fluctuations may occur without the generation of sounds or vibrations.
4. When these unusual phenomena occur in a system, the condition is reproducible and reversible.
5. These unusual phenomena exhibit a threshold condition, generally occurring at about 70–80% of the burnout heat flux.
6. In the case of intense sound generation, increasing the heat flux, while maintaining a constant inlet subcooling and flow rate, results in an increased intensity which maximizes and then decays as burnout is approached.
7. The intensity of the associated vibrations may show the same pattern as the sound generation phenomena, or may persist until the burnout condition.
8. During vibration, and probably during sound generation, the heated surface exhibits a periodicity in bubble formation; that is, all bubbles are synchronized and grow and collapse simultaneously.
9. The occurrence of boiling songs and associated vibrations appears to be confined to local (subcooled) boiling systems. There has not been a recorded occurrence of these phenomena in bulk boiling (net vapor generation) systems.
10. The unusual phenomena result from pressure waves and/or flow fluctuations which induce variable heat transfer in the system. The variability in the heat-transfer rate and energy dissipation of the pressure wave results in the intense sounds and vibrations.

It is noted in the reference that no instance of the occurrence of boiling songs has been recorded in rectangular channel geometries; it is postulated that this may be due to the damping provided by the heavy housings used with rectangular channels.

Gas Cooling

The quarterly progress reports of various groups designing gas-cooled reactors continue to yield useful heat-transfer data. Much of the work is concerned with the practical problems involved in cooling bundles of fuel elements installed in close-fitting coolant channels. Reference 3 reports work to investigate the effect of a fuel-rod spacer installed at the center of a seven-rod fuel cluster of the Experimental Gas-Cooled Reactor (EGCR) type. Correlation curves for the heat transfer upstream and downstream of the spacer have been derived from the experimental data. Data were also obtained on the circumferential surface-temperature distributions and mean heat-transfer coefficients for two of the tubes in a seven-rod cluster using a resistance-heated test loop. Preliminary results of a study of heat transfer in septafoil geometry (seven-rod cluster) by means of mass-removal measurements were reported.[3] The apparatus consisted of a cluster of seven rods designed to mock up the actual fuel-element dimensions, spacer configuration, etc. One of the rods in the cluster was coated with naphthalene. By locating this coated rod successively in each of the rod positions, it was possible to study mass removal at almost any position in the cluster by passing air through the cluster and then measuring the amount of sublimation. Preliminary analyses which compare the mass-transfer data with heat-transfer data show promise.

The air-flow test of a 19-rod cluster is reported in reference 4. The fuel element tested consisted of 19 closely spaced rods arranged on a triangular pitch to form a hexagonal bundle. Spiral wire spacers were used on the center rod and on the 12 peripheral rods.

Rod parameter	Model A
No. of rods	19
Rod pitch	Triangular
Shroud shape	Hexagonal
Rod diameter, in.	0.625
Type of spacing	Spiral wire
Spiral pitch, in.	12.5
Rod-to-rod spacing, in.	0.125
Rod-to-wall spacing, in.	0.125
Flow area, sq in.	4.450
Wetted perimeter, in.	54.5
Hydraulic diameter, in.	0.327
Test length, in.	53.5

The experimentally determined correlation is shown in Fig. 8. It can be noted that the data fall quite close to the accepted correlations for flow in smooth tubes.

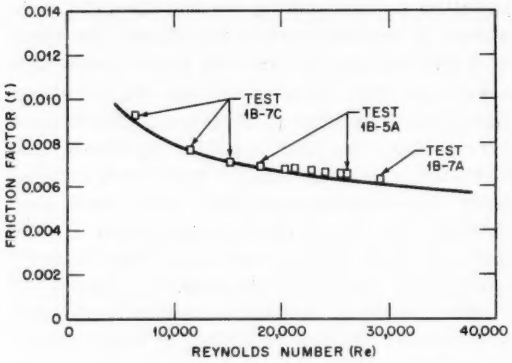

Figure 8 — Friction factor for 19-rod bundle with spiral wire spacers.[4]

Hot-Channel Factors

A recently declassified AERE technical note on statistical methods for the estimation of the maximum fuel-element temperature in a power reactor has become available.[5] Briefly, the paper discusses the question of how one ascertains that a given set of cladding temperature measurements taken within a power reactor represents the hot channel.

If n wall temperatures, T_{wall}, are measured, the average wall temperature, $\overline{T}$, and the variation, v, can be computed as follows:

$$\overline{T} = \frac{1}{n}\sum_{n} T_{\text{wall}}(i) \qquad (1)$$

$$v^2 = \frac{1}{n}\sum_{n}\left[T_{\text{wall}}(i) - \overline{T}\right]^2 \qquad (2)$$

In order to estimate the probability that some temperature in the reactor will exceed the measured average ($\overline{T}$) by as much as some amount ΔT, one must take into account not only the possible deviations of all the temperatures from the true average, but also the probable amount by which $\overline{T}$ deviates from the true average, and the probable amount by which the variation, v, differs from the "true" standard deviation, σ, which would result from a very large number of observations.

If p is the probability that the maximum temperature in any particular channel exceeds some temperature, T_p, then the relation between T_p and p may be written*

$$T_p = \overline{T} + f(p,n)v \qquad (3)$$

The reference provides a short table of $f(p,n)$, which is reproduced here as Table IV-1.† It is stated that a larger table can be obtained from the author.

Table IV-1 VALUES OF $f(p,n)$[5]

n	$p = 10^{-3}$	$p = 10^{-4}$	$p = 10^{-5}$
10	5.28	7.55	10.4
20	3.90	5.02	6.18
30	3.59	4.50	5.39
40	3.45	4.28	5.06
50	3.38	4.16	4.88
60	3.32	4.08	4.77
80	3.26	3.96	4.63
100	3.22	3.92	4.52
Limit	3.09	3.72	4.24

If the total number of fuel channels is N, then the probability, $P(N,p)$, that any one of N elements has a surface temperature greater than T_p is

$$P(N,p) = 1 - e^{-pN} \qquad (4)$$

If N were 4000, the following probabilities would obtain:

p	$P(N,p)$
10^{-3}	0.982
10^{-4}	0.33
10^{-5}	0.04

In the above discussion, only random errors normally distributed have been considered. In some cases, however, systematic errors in temperature measurement may be present, and the reference presents a method for the inclusion of these systematic variations.

* An equation of the same form was used in the analysis of hot-spot factors previously reviewed in the June 1960 issue of *Power Reactor Technology*, Vol. 3, No. 3, pages 7 and 8.

† Table IV-1 is reprinted here by permission from British Report IGR-TN/R-760.

Another technique used in the statistical analysis of hot-spot temperatures is presented in reference 3. The technique consisted of expanding the expression for fuel-rod surface temperature into a Taylor series about the mean value of each of the variables. It was found that the linear terms suffice to represent the temperature change due to an incremental change in any one of the independent variables, and the problem became one of adding 10 frequency functions since the following 10 independent variables were chosen:

Variable	Uncertainty
Gas temperatures at inlet to core	±40°F
Macroscopic fission cross section of fuel	±2%
Radial peak-to-average flux ratio	±1%
Axial peak-to-average flux ratio	±2%
Cross-sectional area of fuel pellets	±1.5%
Graphite-sleeve inside diameter	±0.2%
Stainless-steel-tubing outside diameter	±0.8%
Nominal heat-transfer coefficient	±10%
Observed gas outlet temperature	±25°F
Thermocouple error	±25°F

The basic fuel-element geometry is a cluster of seven rods; the graphite sleeve surrounds the cluster of fuel rods and the spacers and defines the outer coolant-flow boundary. Each of the 10 frequency functions represented one of the linear terms in the Taylor series expansion and, for simplicity and conservatism, each was considered rectangular with extremes as shown above.

The addition of ten square frequency functions is an arduous task, but fortunately it was found that only five rectangular distributions, each having extremes differing by not more than a factor of 2 or 3, sufficed to yield a frequency function that closely approached Gaussian form. The other five factors could only enhance this congruity, and so it was decided to consider that the result of adding all ten distributions would yield a normal distribution with a variance (square of the standard deviation) equal to the sum of the individual variances. (The variance of a rectangular frequency function is one-third the square of the difference between its extreme and mean.)

Thus, for the values quoted above, the standard deviation of the surface temperature was found to be 35.6°F. Therefore the probability that the hottest spot on the fuel-element surface will be at a temperature above the indicated value is the following:

Temp., °F	Probability of being above this temperature
Nominal	0.50
Nominal + 20	0.29
Nominal + 40	0.13
Nominal + 60	0.046
Nominal + 80	0.012
Nominal + 100	0.0025
Nominal + 120	0.00038

The previous two paragraphs are quoted from reference 3.

An experiment to determine hot-channel factors for the 19-rod, Model A, elements described above is reported in reference 4. The hot-channel factor is described as follows:

$$f = \frac{\text{measured surface temperature} - \text{inlet temperature}}{\text{calculated surface temperature} - \text{inlet temperature}}$$

The f factor thus includes both the coolant temperature rise and the film drop. Three tests were made: a uniformly heated bundle coated with temperature-sensitive paints, a uniformly heated bundle with thermocouples, and a bundle with radially varying heat generation, with thermocouples. The results are shown in Table IV-2, and an explanation of the geometry is given in Fig. 9.

A necessity in computing dimensional hot-channel factors from fuel-element dimensions

Table IV-2 HOT-CHANNEL FACTOR AS A FUNCTION OF RADIAL POSITION[4]

Location*	Conditions†					Relative power
	1	2	3*a*	3*b*	3*c*	
Center rod *A*	1.29	1.21	0.92	1.05	1.19	1.00
Middle rod *B*	1.32	‡	‡	‡	‡	1.14
Outer rod *C*:						
Inner surface	1.04	1.02	1.14	1.06	1.06	
Outer surface	1.14	0.93	1.03	0.96	0.89	
Outer rod *D*:						
Inner surface	1.08	1.08	1.10	1.08	1.14	1.42

*See Fig. 9.

†Conditions: 1, values as determined from temperature-sensitive paint with uniform heat flux. 2, values as determined from thermocouple measurements with uniform heat flux. 3, radial power distribution set by physics calculations (temperature measured with thermocouples): *a*, calculated temperature based on average conditions; *b*, calculated temperature based on average coolant temperature and local film temperature drop; *c*, calculated temperature based on no-mixing coolant temperature and local film temperature drop.

‡No measurement.

is to have an accurate method for securing these dimensions from fuel elements. A somewhat unusual eddy-current gauge for measuring channel dimensions has recently been described.[6] It is based on the fact that, when an

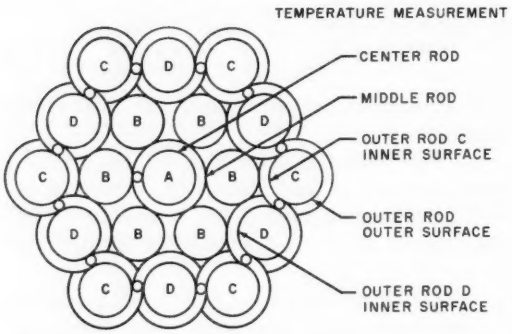

Figure 9—Nineteen-rod fuel bundle with spiral wire spacers.[4]

eddy-current probe coil is moved away from or closer to a conducting body, a change in the impedance of the coil is experienced. Reference 6 describes such a device and its application in measuring channel spacing of zirconium-clad uranium-bearing fuel plates. The cross-sectional view of the probe is shown in Fig. 10;

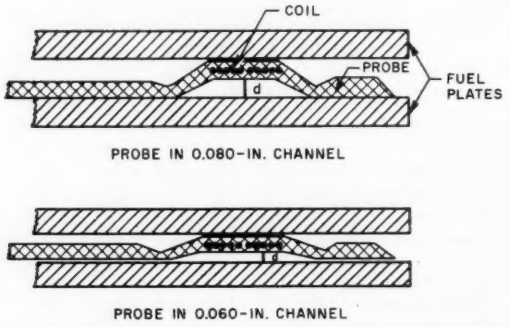

Figure 10—Eddy-current gauge for coolant-channel thickness.[6]

the probe material was nylon. The reference presents the circuit diagram for the electronic equipment auxiliary to the probe. After calibration, the eddy-current device was used to measure the channels of a production fuel element. The conclusions are quoted[6] below:

During the measurement of actual channels, the over-all performance of the equipment was noted. The equipment was easy to operate and required no special skills of the operator. A complete standardization of the gage could be done in less than one minute, and a "spot" check could be done in only a few seconds. However, it was found that frequent standardization was unnecessary.

The results of this investigation indicate that the eddy-current channel spacing gage is suitable for production testing of water-channel spacing. Under typical operating conditions, even with probes of widely differing characteristics, the gage exhibits a linear response and has a precision of 0.00027 in. for channels spaced from 0.060 to 0.080 in.

Since the measurements of one channel are continuously displayed on a strip chart recording in 10 sec, the method provides more information and is faster than conventional mechanical methods.

Short Notes

An IBM-704 program for the thermal analysis of a pressurized-water reactor during steady-state operation has recently been published.[7] The program, titled STDY-3, performs a complete steady-state parallel-channel thermal analysis of a rectangular water-channel core with plate type fuel elements. Enthalpy and temperature rise for the average channel are calculated, and two-phase pressure-drop calculations are performed. Hot-channel pressure drop, flow, enthalpy, temperature, and steam quality are also computed.

STDY-3 is a one-dimensional code, in that conditions are varied in the "z" (length) direction only. MITE-02 is a program for steady-state flow distribution within a single vertical rectangular channel but allows for two-dimensional treatment (variations across the thickness of the water channel are not allowed).[8] The model is a single vertical channel subdivided into a number of control volumes. The conservation of mass, momentum, and energy and the equations of state are written in finite difference form, and each control volume is treated on a macroscopic basis. The two-dimensional solutions allow for study of the effects of transverse flux gradients; one major assumption is made in the solution to the equations, namely, that transverse pressure gradients are negligible. The validity of this assumption has been checked experimentally.

References

1. B. J. Stock, Observations on Transition Boiling Heat-Transfer Phenomena, USAEC Report ANL-6175, Argonne National Laboratory, June 1960.
2. G. K. Firstenberg and J. H. Hutton, Boiling Songs and Associated Mechanical Vibrations, USAEC Report NDA-2131-12, Nuclear Development Corp. of America, June 30, 1960.
3. Oak Ridge National Laboratory, Gas-Cooled Reactor Project Quarterly Progress Report for the Period Ending June 30, 1960, USAEC Report ORNL-2964, Aug. 22, 1960.
4. General Atomic and Electric Boat Divisions, General Dynamics Corp., Maritime Gas-Cooled Reactor Program. Quarterly Progress Report for the Period Ending September 30, 1959, USAEC Report GA-1183, 1960.
5. A. Hitchcock, Statistical Methods for the Estimation of Maximum Fuel-Element Temperature, British Report IGR-TN/R-760, January 1958.
6. A. C. Lind, An Eddy Current Gage for Measuring Channel Spacing, in Reactor Technology Report No. 13, Engineering, USAEC Report KAPL-2000-10, p. E-48, Knolls Atomic Power Laboratory, June 1960.
7. R. S. Pyle, STDY-3, A Program for the Thermal Analysis of a Pressurized-Water Nuclear Reactor During Steady-State Operation, USAEC Report WAPD-TM-213, Westinghouse Electric Corp., Bettis Atomic Power Laboratory, June 1960.
8. R. I. Miller, Steady-State Two-Dimensional Flow of Water with Boiling in Nonuniformly Heated Rectangular Ducts, in Bettis Technical Review. Reactor Technology, USAEC Report WAPD-BT-18, p. 91, Westinghouse Electric Corp., Bettis Atomic Power Laboratory, April 1960.

Section V

REACTOR DYNAMICS

Stability of Boiling-Water Reactors

It is well known that the limits of stability must be considered in determining the maximum power level at which a boiling-water reactor can be operated. In reactors designed for power production, the stability limit is usually higher than the limit set by other considerations such as the central temperature of the fuel elements. The stability-limited power density has been found to be higher at high operating pressure than at low pressure. This difference may be attributed partly to the increase of steam density with pressure, which makes possible a higher power density for a given steam-to-water ratio in the reactor core at high pressure. It appears also, however, that the stability limit on steam-to-water ratio increases with operating pressure. At pressures near atmospheric, the BORAX and SPERT reactors became unstable when the reactivity compensated by steam amounted to something like 2 per cent k_{eff}, whereas the Experimental Boiling-Water Reactor (EBWR) and the Vallecitos Boiling-Water Reactor (VBWR), operating in the 600- to 1000-psi range, have operated stably with more than twice this amount of reactivity compensated by steam. Although this gain in stability with pressure is not necessarily surprising, it must be understood quantitatively before a thorough u n d e r s t a n d i n g of boiling-water-reactor stability can be claimed. A number of theoretical studies employing transfer-function techniques have been made, but these studies have been directed toward the analysis of the behavior of the higher pressure reactors, and the dynamic models used in deriving the transfer functions have not been tested in the lower pressure ranges.

A different approach has been used by Fleck, who has set up, in a one-dimensional model, the dynamic equations governing the flow of water and the flow and production of steam in a natural-circulation reactor; has coupled these equations to the reactor kinetics equations; and has obtained numerical solutions by machine computation. He has directed the analysis toward low-pressure reactors of the BORAX-I and SPERT-I types. An earlier study[1,2] has been reviewed in the December 1959 issue of *Power Reactor Technology*, Vol. 3, No. 1, pages 52 and 53. In that analysis the pressure was not treated as one of the dynamic variables. A later paper[3] by Fleck includes the effects of pressure variations. This work is of particular interest because the difference in compressibility of steam, between high and low operating pressures, is one of the explanations that has been invoked to explain the difference in stability limits with pressure.

Fleck considers the case in which the reactor tank is open to the atmosphere and there is no variation of pressure in the steam space above the reactor. Two pressure effects remain and are accounted for: (1) the dynamic effects within the core, involving the acceleration of the water, and the changing friction pressure drops due to varying water velocities; (2) the changes in the average hydrostatic pressure within the boiling volume of the core due to changes in the position of the boiling boundary.

Numerical calculations were made for the behavior of the SPERT-IA core at atmospheric pressure under the condition of ramp addition of reactivity. Three specific cases are reported:

1. Reactivity addition at a rate of 0.5 per cent per second with no head of water above the core (no upper reflector) and with the core water initially at saturation temperature.

2. Reactivity addition at a rate of 0.5 per cent per second with a 2-ft head of water above the core and with the core water initially at saturation temperature (at atmospheric pressure; the water was slightly subcooled at the core pressure because of the hydrostatic head).

3. Reactivity addition of 0.25 per cent per second with a 2-ft head of water above the core and an initial subcooling of 20°C.

For case 1 the calculation indicated an eventual instability, but only after a reactivity addition of 8.5 per cent. It was determined that this unstable oscillation represented a feedback instability involving the kinetics of the neutron chain reaction as well as the dynamics of the water-steam system. In cases 2 and 3, no coupled instability of this type was observed, but a purely hydraulic instability occurred in both cases: after the addition of 1.8 per cent reactivity in case 2 and after the addition of about 2 per cent reactivity in case 3.

The inclusion of the pressure as a dynamic variable apparently has not changed the main conclusion that was reached in the earlier study, namely, that hydraulic instability, rather than a coupled oscillation including the neutron kinetics, appears to be the major factor affecting the low-pressure stability limit of the boiling-water reactor.

EBR-I Mark III Core

After the Mark II core of the Experimental Breeder Reactor I (EBR-I) was damaged by a power excursion during a series of dynamics experiments, the Mark III core was built to a new design which minimized the bowing tendency of fuel rods under transverse temperature gradients. The behavior of the reactor with the Mark II core was discussed briefly in the December 1957 issue of *Power Reactor Technology*, Vol. 1, No. 1, pages 12 to 14. The design of the Mark III core has been described in reference 5. Subsequent operation showed that the reactor with the Mark III core is quite stable. A recent Argonne report[6] describes a very detailed analysis of the dynamic behavior of the reactor with the Mark III core and relates the analysis to the observed operating characteristics of the reactor.

The work reported in reference 6 employed an electronic analog of the reactor, which took into account the heat flow in the core and the expansions of the core and blanket components under the influence of changing temperatures. Agreement with the observed behavior of the reactor was good. Among the conclusions reached were the following:

> The feedback of EBR-I, Mark III is such that this reactor has dynamic characteristics which cause it to be stable well beyond its operating range. The large negative feedback is considered to be due to the condition that the spaced fuel rods cause the core to expand as a solid cylinder.
>
> . . . . . .
>
> EBR-I, Mark III is a nonlinear system[*] and accordingly should be represented by a nonlinear model. Linear analysis using the root locus method indicates a greater margin of safety than does the nonlinear model.
>
> . . . . . .
>
> A prompt positive coefficient capable of producing instability can exist and not be detected at normal operating conditions by qualitative inspection of response data. However, it can always be detected by a careful analysis of the operating data and of the effect of possible errors in the measurement of these data.
>
> Mathematical models of nuclear reactors and an electronic analog computer provide a safe and rapid means of investigating the dynamic characteristics of reactors prior to operation and are of great assistance in the attempt to reconcile the discrepancies between measured results and theoretical predictions.
>
> It is possible to construct an analog model of a reactor from analysis that has sufficient dynamic similarity to predict the performance of the reactor to the extent that there will be no unfortunate surprises when the reactor goes into operation.

Perhaps the most striking result of the study is the demonstration of the smallness of the mechanical distortions that, in small, high-leakage, fast reactors, will suffice to give observable effects on the dynamic response of reactor power.

---

*The nonlinearity is attributed to frictional restraint on the axial expansion of fuel rods. The rods are separated by full-length spacers, and bundles of the rods with their spacers are clamped tightly within subassembly cans. Thus the axial expansion of any given rod is partially restrained by friction against adjacent spacers and, ultimately, against the wall of the subassembly can. This restriction leads to a nonlinear relation between rod length and reactor power and gives a hysteresis effect if the reactor power is alternately raised and lowered.

References

1. J. A. Fleck, Jr., The Dynamic Behaviour of Boiling Water Reactors, University of California Radiation Laboratory, Livermore, May 1959.
2. J. A. Fleck, Jr., The Dynamic Behaviour of Boiling-Water Reactors, *J. Nuclear Energy: Pt. A, Reactor Sci.*, 11(2/4): 114 (February 1960).
3. J. A. Fleck, Jr., The Influence of Pressure Effects on Boiling-Water Reactor Dynamic Behavior, *Trans. Am. Nuclear Soc.*, 3(1): Paper 4–8 (June 1960).
4. J. A. Fleck, Jr., The Influence of Pressure on Boiling-Water Reactor Dynamic Behavior at Atmospheric Pressure, USAEC Report UCRL-5938-T, University of California Lawrence Radiation Laboratory, Livermore, July 1960.
5. F. W. Thalgott et al., Stability Studies on EBR-I, *Proceedings of the Second United Nations International Conference on the Peaceful Uses of Atomic Energy, Geneva, 1958*, Vol. 12, pp. 242–266, United Nations, New York, 1958.
6. J. C. Carter et al., The Internal Feedback of EBR-I, Mark III, USAEC Report ANL-6124, Argonne National Laboratory, February 1960.

Section VI

REACTOR HAZARDS: METAL-WATER REACTIONS

In the analysis of the hazards of water-cooled reactors, accidents that lead to the melting of the reactor fuel or the fuel cladding, either because of excessive power production or because of coolant loss, are often postulated. If the molten material can react chemically with the coolant water, the question of whether such a reaction might add significantly to the destructive energy release of the accident then arises. The answer to the question may have an important effect on the design of the containment structure.

The final report in a series[1–9] by the Atomic Power Equipment Department of the General Electric Company, covering an AEC-sponsored study of metal-water reactions, has been issued. The reports may be divided into three groups. References 1 to 4 treat the analysis of reactivity excursions in water-moderated reactors, to determine under what excursion conditions melting of fuel or fuel jackets may occur. Reference 8 considers the possible effects of a Zircaloy-water reaction during a loss-of-coolant accident, and references 5 to 7 and 9 cover studies of the details of the possible chemical reactions.

Reactivity Excursion

In the first group of reports,[1–4] a method is developed for calculating (by an analog computer) the time variation of reactor power and fuel temperature after the sudden introduction of excess reactivity, and until the reactor terminates the power excursion by water expulsion or some other means. The main assumptions are:

1. The spatial power distribution in the core is taken into account approximately by assuming that all the power is produced uniformly in a central volume of the core, the magnitude of the central, active volume being given by

$$\text{Active volume} = \frac{\text{total core volume}}{(F_R)(F_A)}$$

where F_R and F_A are the radial and axial hot-spot factors, respectively.

2. The only contributions to pressure change are those arising from inertial forces as the water is accelerated. The density and the elastic modulus of the water are assumed to be constant.

3. The processes considered as contributing to removal of the excess reactivity (reactor shutdown) are the formation of steam in the core by heat conduction from the fuel, the formation of radiolytic gases, the heating of the water by absorbed radiation, and the fuel temperature coefficient of reactivity due to Doppler broadening of the U^{238} resonances. Of these, the radiolytic gas production was found to be insignificant for short-period excursions, and it was subsequently neglected.

4. Steam is formed by film boiling at the fuel-element surface. The heat transfer to the water is given at all times by

$$q = \frac{T_S - T_0}{R_T}$$

where T_s is the surface temperature, T_0 is the initial water temperature (heating of the bulk liquid water by heat transfer from the fuel element is neglected), and R_T is the thermal resistance to the flow of heat from the fuel surface to the coolant, assumed to be constant. A time delay of 5 msec was assumed to occur before the beginning of steam formation after the fuel-element surface had reached the saturation temperature of the water.

The application of the method to the BORAX-I and SPERT-I reactors gave reasonably good agreement with the experimentally determined values of the total energy release during reactivity excursions of given periods. The shapes of the power-time curves showed poorer agreement with experiment, probably because of an inadequacy in the treatment of the steam expansion after the peak of the power curve.

The calculation method was used to investigate[2] the effects of various reactivity transients on typical H_2O-moderated reactors of three different types: one employing aluminum-clad, uranium-aluminum fuel plates; one employing zirconium-clad plates of zirconium-uranium alloy; and one employing rod type fuel elements of UO_2 jacketed in zirconium. The plate type elements were 60 mils thick, consisting of 20 mils of fuel alloy with 20 mils of cladding on each side; the rod elements contained UO_2 of 0.40 in. diameter, with a 25-mil jacket thickness. All three reactors were initially at a temperature of 212°F and at atmospheric pressure.

The calculations indicated that, for the reactor having uranium-aluminum fuel plates, no melting occurred during an excursion period of 4.9 msec, whereas melting was complete if the period was reduced to 3.3 msec. For the reactor having zirconium-uranium fuel plates, the corresponding periods were 12.2 and 8.6 msec. In these reactors the only important shutdown mechanism was steam formation. In the UO_2 reactor, steam formation was relatively unimportant. The effect of Doppler broadening was the major shutdown mechanism, although gamma heating of the water was also important. In this reactor a period of 4.34 msec did not result in fuel melting or jacket melting. The temperature distribution within the element at this period is shown in Fig. 11. The jacket temperature is actually relatively low. Obviously, in this case the maximum temperature reached is strongly dependent on the magnitude of the Doppler coefficient of reactivity. The coefficient used for the calculation was -1.67×10^{-5}/°F, corresponding to an average temperature coefficient of the resonance integral $(1/\sigma)(d\sigma/dT)$ of 6.7×10^{-5}/°F, and a low-temperature resonance escape probability of 0.80.

Since the reactor period of 4.34 msec represents an applied excess reactivity of about 2.2 per cent, it appears unlikely that a sufficiently severe accident would occur to cause fuel jacket melting in a UO_2-fueled reactor under the conditions analyzed. However, other initial conditions must be considered before the possibility of melting can be dismissed.[2] In particular, in a reactor of this type, a reactivity excursion occurring during full-power operation might be considerably more serious, since the hottest fuel elements would normally be operating with center temperatures well above 3000°F, and any reactivity reduction due to the Doppler coefficient would have to result from an additional temperature increment above this value.

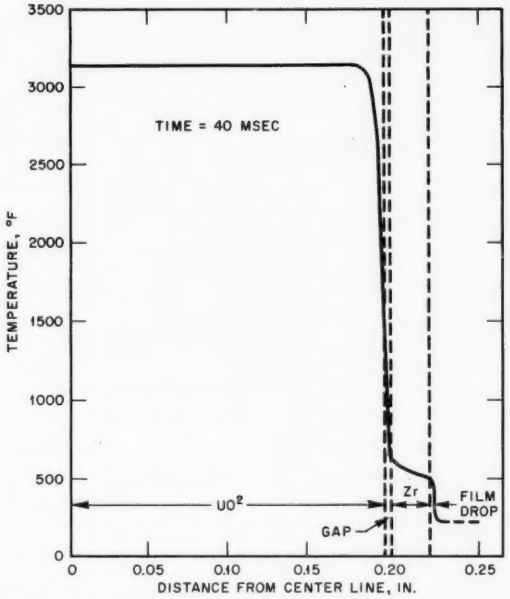

Figure 11—Temperature versus distance from the fuel-element center for a representative time after a nuclear excursion period of 4.34 msec (for a cylindrical zirconium-clad UO_2 fuel element).[2]

Loss-of-Coolant Accident

Reference 8 treats a severe loss-of-coolant accident in a UO_2-fueled reactor having the same characteristics as the UO_2-fueled reactor mentioned above. In the postulated accident the reactor has been operating at full power up to the time of a sudden large break in the primary system which drains the water to a level below the bottom of the core in 10 sec. After any given segment of fuel element is uncovered, it is

cooled by natural convection of steam, with ultimate heat loss to the walls of the reactor vessel. The initial operating power of the reactor is 500 Mw(t), corresponding to an average specific power of about 17 Mw per ton of uranium. The initial water temperature (before the break in the system) is 540°F, and the final pressure in the system (from $t = 10$ sec onward) is 25 psia. The radial power distribution is taken into account approximately by dividing the core into two radial zones of equal volume, with different uniform power densities in each: three-fourths of the total power is assumed to be generated in the central zone and one-fourth in the outer zone. The rate of chemical reaction between zirconium and steam is taken as the time derivative of the following equation, which is based on isothermal reaction-rate data:

$$v = 336.5\, t^{1/2} \exp -\left(\frac{34{,}000}{2RT}\right)$$

where v = volume (STP) of hydrogen evolved, ml/cm^2
t = time, sec
R = gas constant = 1.987 cal/(mole)(°K)
T = temperature of Zircaloy, °K

In applying the equation, the temperature, T, was taken as the average temperature (axially) in the appropriate core zone.

The analysis treats the temperature history of the fuel and cladding, and the amount of zirconium cladding consumed by the zirconium-steam reaction, up to the time that melting of the cladding occurs. The treatment of the molten material is deferred for further investigation.

The results show that, until the Zircaloy temperature reaches 2000°F, the contribution of the heat of chemical reaction to the temperature rise is small; thereafter its effect increases rapidly. This temperature is reached by the cladding at the mid-point of fuel elements in the central zone after about 700 sec. The mid-point cladding reaches the melting temperature after about 970 sec. By the time of melting, each fuel element in the central zone of the reactor has lost, at its mid-point, 5.5 mils of Zircaloy, or 20 per cent of its cladding, by oxidation. The chemical reaction in the colder outer zone of the reactor at the same time is insignificant.

Reaction Rates

References 5 to 7 and 9 consider the rates of metal-water reactions, possible methods of obtaining further experimental information on the kinetics of the reactions, and the current status of the over-all problem of predicting what (if any) possible sequences of events could lead to important releases of chemical energy in water-cooled nuclear reactors and what the magnitude of such releases might be. The answers to the latter problem are not now available, and the difficulty of the problem does not encourage the expectation that complete answers will soon be obtained. The important aspects of the problem, as outlined in reference 7, are summarized as follows:

1. It seems clear that no rapid chemical reactions are to be expected unless the metal in question reaches the molten state. Melting is necessary for a reaction under nuclear reactor conditions because it is the only reasonable process by which the metal can become sufficiently finely divided to offer a large surface to contact the water or steam. Melting is also favorable to a reaction because it can lead to the production of fresh metallic surfaces, free, at least momentarily, of oxide. Thus the first step in investigating the possibility of a reaction must be to determine the possibility, and the probable extent, of melting. Once the conditions of the hypothetical accident have been defined, reasonable estimates of the extent of melting (by nuclear heat) can be made by methods such as those treated in references 1 to 4 and 8.

2. Once the condition of melting has been established, the question is how much surface the molten metal actually does present to the water or steam. If the molten metal is thought of as existing in droplets, dispersed in the water, one needs to know the effective size of these droplets. This question is thought to be probably the most difficult in the whole problem. Possible mechanisms of dispersal are agitation and turbulence produced by the rapid formation of steam and the release of gaseous fission products by ruptured fuel elements. However, an adequate theoretical analysis of these effects seems improbable, and meaningful experiments are hard to devise.

3. The chemical reaction at the surfaces of the droplets will proceed at a rate determined

by, among other things, the surface temperature of the droplet. Thus a heat-transfer problem exists in determining this surface temperature as a function of time, as heat is added by the chemical reaction and is lost to the surrounding steam and water. Although this problem has not been solved, it would appear to be amenable to solution, provided, of course, that the relation between surface temperature and reaction rate is known.

4. Finally, it is necessary to establish this relation between surface temperature and reaction rate. Since the melting points of all metals of concern in reactors are far above the critical temperature of water, the chemical reaction of interest will always be a metal-steam reaction, although the layer of steam that separates the metal from liquid water may, in some cases, be quite thin. Reference 6 reviews experimental and theoretical information on metal-gas reactions and points out that there are two rate factors of fundamental importance: the rate at which water molecules collide with the reacting surface and, after the reaction has proceeded far enough to form an oxide coating on the surface, the rate at which the water (or the metal) can penetrate this surface barrier. The first of these factors, if controlling, should give a reaction rate that is constant in time (a linear increase in reaction product with time), whereas the second factor should yield a reaction rate which, for constant conditions, decreases with time as more and more oxide is added to the barrier layer. The reference[7] reviews the various rate laws that have been used to fit experimental data and suggests that, at the present stage of knowledge, the information useful for reactor-accident analysis can be encompassed by a law of the form

$$\Delta W = K_1 t / [1 + K_1 t^{1/2} / K_2 f(r_0, \Delta W)]$$

where ΔW = weight gain of metal sample per unit initial area, g/cm^2
t = time, sec
K_1, K_2 = constants for the system, functions of temperature and pressure
$f(r_0, \Delta W)$ = geometric term, depending on the initial radius, r_0, of the reacting material and the extent of reaction, ΔW ($f = 1$ for plane geometry)

For fast nuclear transient cases, K_1 will be the quantity of primary importance. An upper limit for K_1, derived from simple kinetic theory, is

$$K_1 \leq 16p / \sqrt{2\pi R M_{H_2O} T}$$

where p = pressure of the water vapor, dynes/cm^2
M_{H_2O} = molecular weight of H_2O
T = absolute temperature, °K
R = gas constant = 8.314×10^7 ergs/(mole)(deg)

Reference 7 concludes that the understanding of the chemical kinetics of the problem is reasonably good but that further experimental data are needed. Reference 9 is an investigation of methods for gathering further data for troublesome metals, such as zirconium, which are difficult because they react vigorously with the known crucible materials.

ANL Experiments

An experimental program on metal-water reactions is under way at ANL.[10–12] The laboratory techniques include both the electrical melting of metal wires in water and the contacting of a molten-metal surface by a pulse of water vapor admitted by quick-acting valves. In addition, preliminary results of uranium-water experiments in the TREAT reactor have been published.[11,12]

The TREAT reactor is designed to produce large excursions of nuclear power and has irradiation tubes in which samples, in suitable containers, can be subjected to large short-duration bursts of neutrons. The design of the reactor has been described in references 13 to 15. Additional physics data on the reactor are contained in references 16 and 17.

The tests reported were made on small cylindrical samples of uranium metal, 0.5 in. long by 0.2 in. in diameter, enriched to 20 per cent U^{235}. Some of the samples were of pure uranium, whereas others were of uranium–5 per cent zirconium–1.5 per cent molybdenum. For most of the tests, the samples were immersed in about 35 cm^3 of distilled water, in a stainless-steel autoclave which was installed in a TREAT irradiation thimble. The space above the water surface was filled with helium at 20 psia. In one case, however, only enough water was contained in the autoclave to saturate the helium

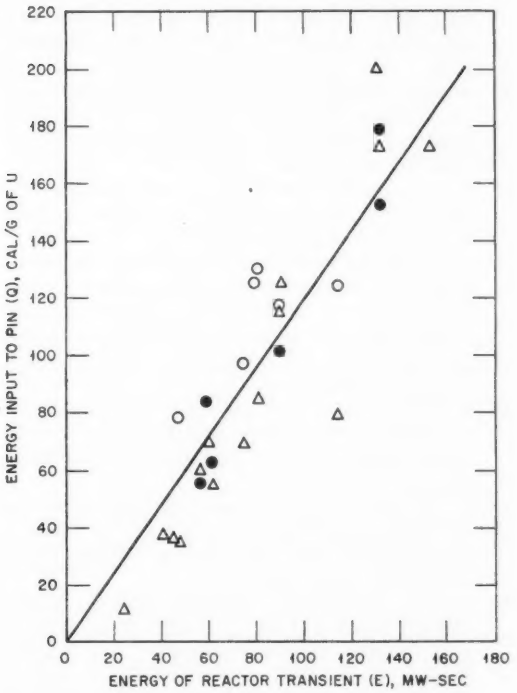

Figure 12—Correlation between pin energy and reactor energy.[12] Δ, gold foil. ●, Mo^{99}. ○, Ba^{140}.

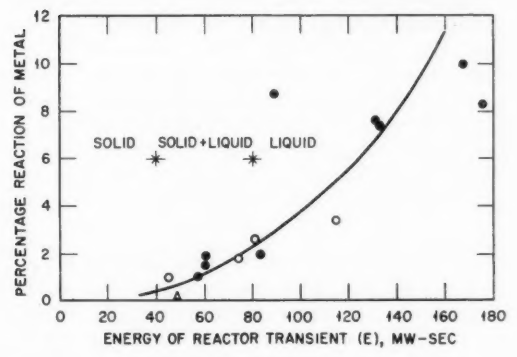

Figure 13—Metal-water experiments in TREAT.[12] ○, unclad uranium–liquid water. ●, uranium clad with Zircaloy-2–liquid water. Δ, unclad uranium–water vapor.

atmosphere. Transient pressure measurements were made in the autoclave, and temperature measurements were made in the water and in the uranium sample. In some cases the uranium sample was bare. Alternatively, the sample was covered by a Zircaloy-2 cladding in which a hole had been punctured at the bottom end; the hole diameter was 3 mils in some cases and 15 mils in others.

The energy of the nuclear transient was varied over a range which, at the low end, produced only partial melting of the uranium sample and, at the high end, produced complete melting and further heating of the liquid metal. In those cases which produced melting of the clad uranium without melting of the jacket, from 0.3 to 14 per cent of the molten metal sprayed out into the water in finely divided form through the hole that had been punctured in the jacket. The results of the tests are plotted, against energy of the transient, in Figs. 12 and 13. Figure 12 gives the relation between the fission-energy input to the sample (as measured by gold foils and by fission-product determinations on Mo^{99} and on Ba^{140}) and the total energy of the reactor transient. Figure 13 gives the percentage of sample reacted. Although the different sample types have been included in the same curves, the scatter of the data for a given type appears to be as great as the variation between types. Peak pressures as high as 660 psi were recorded in the autoclave. The pressure curves in all cases were smooth, with no indications of a shock or of pulses having durations significantly shorter than the reactor power pulses.

Reference 18 treats the calculation of metal-water reactions, under conditions such as those in the TREAT experiments, by means of analog computer. The theoretical model consists of the metal sample surrounded by a layer of UO_2 produced by the chemical reaction, with the metal losing heat to the surrounding water through the UO_2 layer. Logarithmic and parabolic rate laws for the chemical reaction are considered. The report contains a short appendix in which the calculations are compared with some of the early TREAT results.

References

1. E. Janssen et al., Metal-Water Reactions: I. A Method for Analyzing a Nuclear Excursion in a Water Cooled and Moderated Reactor, USAEC Report GEAP-3073, General Electric Co., Atomic Power Equipment Dept., Oct. 15, 1958.
2. J. I. Owens, Metal-Water Reactions: II. An Evaluation of Nuclear Excursions in Light Water Reactors, USAEC Report GEAP-3178, General Electric Co., Atomic Power Equipment Dept., June 15, 1959.
3. K. M. Horst, Metal-Water Reactions: III. Fuel-

Element Stresses During a Nuclear Accident, USAEC Report GEAP-3191, General Electric Co., Atomic Power Equipment Dept., July 24, 1959.
4. K. Hikido, Metal-Water Reactions: IV. An Evaluation of Heat Transfer Conditions During Severe Nuclear Excursions in Water-Cooled Reactors, USAEC Report GEAP-3204, General Electric Co., Atomic Power Equipment Dept., Sept. 15, 1959.
5. S. C. Furman, Metal-Water Reactions: V. The Kinetics of Metal-Water Reactions—Low Pressure Studies, USAEC Report GEAP-3208, General Electric Co., Vallecitos Atomic Laboratory, July 31, 1959.
6. L. F. Epstein, Metal-Water Reactions: VI. Analytical Formulations for the Reaction Rate, USAEC Report GEAP-3272, General Electric Co., Vallecitos Atomic Laboratory, Sept. 30, 1959.
7. L. F. Epstein, Metal-Water Reactions: VIII. Reactor Safety Aspects of Metal-Water Reactions, USAEC Report GEAP-3335, General Electric Co., Vallecitos Atomic Laboratory, Jan. 31, 1960.
8. R. W. Lockhart et al., Metal-Water Reactions: VIII. Preliminary Considerations of the Effects of a Zircaloy-Water Reaction During a Loss of Coolant Accident in a Nuclear Reactor, USAEC Report GEAP-3279, General Electric Co., Atomic Power Equipment Dept., Sept. 30, 1959.
9. S. C. Furman and P. A. McManus, Metal-Water Reactions: IX. The Kinetics of Metal-Water Reactions. Feasibility Study of Some New Techniques, USAEC Report GEAP-3338, General Electric Co., Vallecitos Atomic Laboratory, Jan. 31, 1960.
10. Argonne National Laboratory, Chemical Engineering Division Summary Report for April, May, and June 1959, USAEC Report ANL-6029, September 1959.
11. Argonne National Laboratory, Chemical Engineering Division Summary Report for October, November, and December 1959, USAEC Report ANL-6101, February 1960.
12. Argonne National Laboratory, Chemical Engineering Division Summary Report for January, February, and March 1960, USAEC Report ANL-6145.
13. G. A. Freund et al., TREAT, A Pulsed Graphite-Moderated Reactor for Kinetic Experiments, *Proceedings of the Second United Nations International Conference on the Peaceful Uses of Atomic Energy, Geneva, 1958*, Vol. 10, p. 461, United Nations, New York, 1958.
14. D. R. MacFarlane et al., Hazards Summary Report on the Transient Reactor Test Facility (TREAT), USAEC Report ANL-5923, Argonne National Laboratory, October 1958.
15. G. A. Freund et al., Design Summary Report on the Transient Reactor Test Facility TREAT, USAEC Report ANL-6034, Argonne National Laboratory, February 1960.
16. Haig P. Iskenderian, Physics Analyses of the TREAT Reactor Design, USAEC Report ANL-6025, Argonne National Laboratory, August 1959.
17. Haig P. Iskenderian, Post Criticality Studies on the TREAT Reactor, USAEC Report ANL-6115, Argonne National Laboratory, February 1960.
18. R. C. Liimatainen et al., Analog Computer Study of Metal-Water Reactions Initiated by Nuclear Reactor Transients, USAEC Report ANL-6129, Argonne National Laboratory, May 1960.

Section VII

RADIATION PROTECTION REGULATIONS

Changes have recently been made in the AEC regulations for radiation protection. The quantitative aspects of these changes are summarized in the following quotations from an AEC press release of Sept. 7, 1960.

The Atomic Energy Commission has revised its regulations for the protection of employees in atomic energy industries and the general public against hazards arising out of the possession or use of AEC-licensed radioactive materials.

The revisions are embodied in amendments to Title 10, Chapter 1, Part 20, of the *Code of Federal Regulations* entitled "Standards for Protection Against Radiation." The amendments become effective on January 1, 1960.

. . . . . .

On May 13, 1960, the President approved recommendations [*] on exposure made to him by the Federal Radiation Council for the guidance of agencies in the executive branch of the government. The numerical values contained in the guides recommended by the Council are substantially the same as the corresponding values contained in the current basic recommendations of the National Committee on Radiation Protection and Measurements and as those incorporated in Part 20 by these amendments.

. . . . . .

The principal effect of the amendments will be to limit the lifetime accumulated dose of radiation workers to approximately one-third the limits permitted under the regulation as it now stands. The amendments will limit the total external radiation exposure that any worker may accumulate beyond the age of 18 to an average of five rems per year and to not more than three rems in any one quarter. Present limits for radiation workers are 0.3 rem per week, (or approximately 15 rems a year) without further restrictions as to accumulated dose.

. . . . . .

Radiation limits as set in the regulations are not to be regarded as absolute limits below which no hazard from radiation exists and above which an individual automatically receives a dangerous dose of radiation. The limits may be compared to speed limits, which are established to promote traffic safety.

. . . . . .

In establishing the limits now incorporated in the amendments to Part 20 of the Commission's regulations, the National Committee on Radiation Protection and Measurements pointed out that the lowering of the limits should not be interpreted as indicating that exposures at levels currently permitted by the regulations have caused damage. NCRP said changes, rather, were based on a desire to bring radiation standards into accord with new trends of scientific opinion and to reflect awareness of the probability of a large future increase in radiation uses.

The amendments provide a basic table showing the quarterly levels of radiation to which all workers may be exposed, and these levels are as follows:

1. A level of $1\frac{1}{4}$ rems per calendar quarter for the whole body; the head and trunk, active blood-forming organs; the lenses of eyes; or the gonads.

2. A level of $18\frac{3}{4}$ rems per calendar quarter for the hands and forearms or for the feet and ankles.

3. A level of $7\frac{1}{2}$ rems per calendar quarter for the skin of the whole body.

The licensee may permit an employee to receive a greater dose than that listed in the basic table [the dose levels from this table are listed above] provided that the quarterly dose to the whole body from radioactive material and other sources of radiation in the employer's possession does not exceed three rems and the dose to the whole body — when added to the employee's accumulated dose of radiation in

---

*Published in the *Federal Register*, 25(97): 4402–4403 (May 18, 1960).

previous jobs — does not exceed that arrived at by a formula based on the individual's age.[*]

To permit exposure above the limits in the basic table, the employer first must make reasonable attempts to obtain reports of the employee's previous occupational exposure to radiation and must take these exposures into account in determining how much additional exposure an employee may receive.

In the absence of exposure records for an employee, the employer is to be guided by a table of assumed occupational exposure for the worker.

. . . . . .

The amendments include a comprehensive revision of the concentrations of radioactive material to which employers may expose persons in areas under their control or which may be released by the employer into the environment without specific approval by the Commission.

With respect to most isotopes listed, the principal changes in the values set forth in the new tables are a reduction to one-third in the concentrations of those radioisotopes having their principal effect upon the gonads or the whole body and the lowering of others to control exposure of the gastrointestinal tract to 15 rems per year.

The reductions in these values do not modify the basic approach of the Commission with respect to levels of radiation and concentrations of radioactive materials in unrestricted areas — that is, areas which are outside the control of the employer. The Commission's regulations are designed to make it unlikely that individuals in unrestricted areas receive exposure in excess of 10 per cent of the limits established for radiation workers.

The above quotations are intended only as a general description of the quantitative changes in the regulations. The *Code of Federal Regulations* itself should, of course, be consulted for the full text, for the tables of radiation levels and permissible concentrations of radioactive isotopes, and for the administrative requirements of the regulations.

*Total accumulated dose = $5(N - 18)$ rems, where N is the individual's age at his last birthday.

Section VIII

FUEL ELEMENTS

Development of Carbide Fuels

Uranium carbides are being studied as reactor fuel materials by several organizations that are conducting research and development programs to determine the basic physical properties of the material, the effect of irradiation on its properties, its compatibility with cladding materials, and economical methods of fabricating carbide fuel pellets.[1–8]

Desirable characteristics for nuclear fuels are high uranium density, low parasitic absorption cross section for neutrons, a high melting temperature with no phase change up to the melting point, high thermal conductivity, compatibility with cladding and coolant, good mechanical stability and thermal-shock resistance, a high degree of irradiation stability, and the ability to retain a high percentage of the gaseous fission products.

The two fuel materials that are now widely used—uranium metal and uranium dioxide—both satisfy most of these criteria, but both also are seriously deficient in at least one respect. The stability of the metal under irradiation at high temperature is so poor that the probability of developing a long-lived high-temperature uranium-metal element appears very doubtful. Uranium dioxide, although excellent in most respects, suffers from very low thermal conductivity. Uranium carbide is expected to have good irradiation stability (references 3, 4, 7, and 8) and is known to have a thermal conductivity several times that of UO_2. Thus the carbide seems to offer the possibility of avoiding the major weaknesses of the two

Table VIII-1 COMPATIBILITY OF URANIUM CARBIDES WITH METALS, LIQUIDS, AND GASES[4]

Compatibility with Metals

Aluminum: Work at Oak Ridge[9] has shown the reaction between aluminum and uranium carbide at 620°C to vary as a function of carbon content, as shown below:

Reaction[9] between aluminum and UC at 620°C

Time at 620°C, hr	Reaction* occurring with alloy shown						
	U–9.2 wt.% C	U–8.24 wt.% C	U–7.98 wt.% C	U–6.96 wt.% C	U–5.75 wt.% C	U–4.86 wt.% C	U–4.46 wt.% C
4	NR	NR	NR	NR	NR	NR	ΔV = 1.2%
10	NR	NR	NR	NR	ΔV = 71%	ΔV = 88%	CD
16	NR	NR	NR	NR			
24	NR	NR	NR	5% UAl_4, ΔV = 4.6%			
48	NR	5% UAl_3	1% UAl_3, 1% UAl_4, ΔV = 0.6%				
74	NR	5% UAl_3					
96	4% UAl_4						

*NR = no reaction; ΔV = change in volume of specimen; CD = complete disintegration.

(Table continues.)

Table VIII-1 (Continued)

Beryllium: Boettcher and Schneider[10] found beryllium to bond to UC at 650°C in 12 hr under a pressure of 15 kg/mm^2. Murray and Williams[11] found reaction between U_2C_3 or UC_2 and beryllium between 600°C and 1000°C.

Bismuth: No reaction between molten bismuth and UC was observed during heating to 950°C and subsequent cooling.[12] At 1100°C, bismuth does not react[4] with either UC_2 or U_2C_3, both of which are considered to be more reactive than the monocarbide.

Lead: Molten lead will not wet UC by dipping.[10]

Molybdenum: Reaction between UC and molybdenum was observed metallographically after sintering[13] at 1200°C.

Nickel: Nickel has been deposited on UC by both vacuum evaporation and electrolytic deposition. Annealing of these specimens for 10 min at 1000°C produced two layers between the UC and the nickel: one was U_6Ni, and the other was of unknown composition.[10]

Nichrome V: A mixture of 30 vol.% UC in Nichrome V showed metallographic evidence of reaction and melting after sintering[13] at 1200°C.

Niobium: Metallographic evidence of reaction between niobium and UC was observed after sintering[13] at 1200°C.

Niobium-titanium: A niobium–40 at.% titanium alloy in contact with UC was found to react, producing a molten phase[13] at 1200°C.

Silicon: Siliconization was found to take place at 1000°C, producing USi_3 on the surface of UC in contact with silicon metal.[10]

Sodium and NaK: Nichols[14] reports satisfactory compatibility of UC with NaK at 800°C after one month's exposure. Price et al.[7] ran tests involving cast uranium–5 wt.% carbon specimens held in molybdenum or type 304 stainless-steel baskets immersed in NaK-filled stainless-steel capsules. After two to six weeks at 1300°F and 12 weeks at 1100°F, the carbide specimens were intact except for minor weight losses.

Steel: Mild steel was found to react with uranium monocarbide[15] at 1000°C in 24 hr.

Stainless steel: Stainless steel could not be bonded to uranium monocarbide at 650°C in 12 hr under a pressure[10] of 15 kg/mm^2. Uranium monocarbide was found to react[15] with stainless steel in 24 hr at 1000°C. Type 304 stainless steel, used to contain UC specimens in a NaK environment, was embrittled[7] by an exposure of 12 weeks at 1100°F. Nichols[14] reports that UC and stainless steel are compatible at 1000°C and that 0.004-in. penetration occurred during six days at 1100°C.

Tantalum: Tantalum will displace uranium from uranium monocarbide. The reaction is slow at 1000°C but becomes rapid near the melting point of uranium monocarbide.[16]

Tin: Molten tin will not wet uranium carbide by dipping.[10]

Titanium: Nichols[14] reports that reaction occurs between UC and titanium at 1100°C, the penetration amounting to 0.005 in. in six days at temperature. Very marked reaction was observed at 1200°C.

Zinc: Molten zinc will wet uranium carbide by dipping.[10]

Zircaloy-2: Zircaloy-2 was found to react with uranium carbide in 1 hr at 1200°C (reference 17) but not at 800°C (reference 18).

Zirconium: Zirconium was bonded to uranium carbide at 650°C in 12 hr under a pressure[10] of 15 kg/mm^2. Considerable reaction was observed between zirconium and uranium carbide[13,15] at 1000°C and 1200°C in 24 hr.

Compatibility with Liquids and Gases

Air, oxygen, and nitrogen: Uranium monocarbide is attacked very slowly by moist air at room temperature, but it can be handled in bulk form if exposure to moisture is minimized, as by storage in a desiccator. It is reported that UC_2 is attacked more rapidly in air than is UC. Thus the presence of UC_2 as a second phase in UC may accentuate this difficulty.[19]

Uranium dicarbide reacts with both oxygen and nitrogen at a rate which is parabolic as a function of temperature. At 300°C, the reaction with oxygen becomes anisothermal. A summary of these data appears below:

Table VIII-1 (Continued)

Corrosion of uranium dicarbide in water vapor, nitrogen, and oxygen

Test medium	Temp., °C	Corrosion rate: Linear, mg/(cm²)(sec)	Corrosion rate: Parabolic, (mg/cm²)²/sec
29 mm H_2O	50	0.04	
(references	150	0.66	
20 and 21)	200	3.2	
H_2O vapor	250		6520
(reference	300		9210
20)	300		6840
Nitrogen	400		16
(reference	600		860
22)	700		3300
Oxygen	150		6.1
(reference	200		75
21)	250		900
	300		Anisothermal

Water: It has been generally noted that UC has very poor compatibility with water at any temperature. Nichols[14] reports that rapid decomposition results from exposure to water at temperatures above 80°C. The gaseous reaction products evolved during hydrolysis of UC at 83 to 400°C were analyzed by Litz.[22] The liberated gas was composed of hydrogen and methane with a hydrogen concentration varying from 12 per cent at 83°C to 100 per cent at 400°C. At all temperatures the solid reaction product was UO_2. Appreciable rates of reaction between water and uranium carbide have been noted at temperatures[23] as low as 40°C. Several investigators have determined the corrosion rate of the dicarbide in water vapor as summarized previously. The results indicate that the rate is linear at 200°C and below but is parabolic above this temperature.

Alkalies and acids: Concentrated acids will react slowly with UC at room temperature, the reaction rate increasing with temperature.[24] Alkalies will readily decompose[25] UC_2.

Organics: Some organic materials react with the carbides of uranium. When UC was exposed in glycerin at 100°C, a weight-loss rate of 50 mg/(cm²)(hr) was measured.[10] Terphenyl (Santowax R) corroded UC at the rate of approximately 5 mg/(cm²)(hr) at 350°C, probably as a result of traces of contained moisture. A weight loss of 0.4 mg/(cm²)(hr) occurred during exposure[26] of UC to ethylene glycol at 150°C.

Halogens: Uranium dicarbide will react with the halogens, usually to form compounds of the UX_4 type. The results are summarized below:[24]

Reaction of UC_2 with the halogens[24]

Reactant	Temp., °C	Product	Comments
Chlorine	350	Volatile chloride	
	600	UCl_4	
Fluorine	30		No reaction
	30		Explosive reaction
Bromine	390		Ignites in bromine vapor
	800–900	UBr_4	
Iodine	500	UI_4	

CO_2: Uranium monocarbide oxidizes at 500°C in a CO_2 atmosphere at an 8-atm gas pressure.[14]

H_2S: Uranium monocarbide ignited in H_2S at 600°C producing a sulfide.[24]

NH_3: Uranium dicarbide was partially decomposed by NH_3 at a red heat.[24]

Hydrogen: UC is compatible with hydrogen, if no second phases are present.[14]

Solvents: Acetone, alcohol, benzene, carbon tetrachloride, kerosene, xylene, and Zyglo solutions did not react with UC during a 5-hr exposure at room temperature.[7]

currently used fuel materials. With regard to the other desirable properties of nuclear fuels, uranium carbide has a significantly higher uranium density than UO_2, has a very low parasitic absorption cross section, and should compare favorably with UO_2 on mechanical stability and thermal-shock resistance. Its melting point is a bit lower than that of UO_2, but not enough lower to counteract seriously the effect of its higher conductivity. The range of materials compatible with uranium carbide differs significantly from that compatible with the oxide. A very serious obstacle to the early widespread use of uranium carbide is its poor compatibility with water. But in some nonaqueous reactors—particularly in the sodium-cooled reactors—uranium carbide looks very promising.

The results of numerous tests of the compatibility of uranium carbide with various materials are summarized in Table VIII-1. Obviously, much of the information is fragmentary, and considerably more investigation would be needed to define the range of applicability of uranium carbide.

Some physical and mechanical properties of uranium carbides are listed in Tables VIII-2 and VIII-3. Figure 14 compares the thermal conductivities of UC, UC_2, and UO_2, and Fig. 15 compares the thermal-expansion coefficients of UC and UO_2.

Although the amount of irradiation testing has been small, it has given encouraging results. Most of it has been done by BMI; the results of this work, to July 1960, are summarized in Table VIII-4, from reference 8. Some of the irradiations were made in the Battelle Research Reactor (BRR), but those giving the higher exposures were made in the MTR. The MTR specimens were 2 in. long and $\frac{3}{8}$ in. in diameter, of melted and cast UC, ground to diameter. Each irradiation capsule contained a stack of two specimens separated by a $\frac{1}{2}$-in.-long UC spacer of the same diameter as the specimens. A small cylinder of UC of the same diameter and $\frac{1}{4}$ in. long was used at each end of the stack to reduce end effects. The stack of bare UC cylinders was supported in a close-fitting cylindrical basket of 304 stainless steel, of expanded-metal construction, which offered negligible restraint to deformation of the samples. The basket was centered in the considerably larger irradiation capsule, and the remaining space was filled with NaK to a level above the top of the specimen stack.

Table VIII-2 PHYSICAL PROPERTIES OF URANIUM, THORIUM, AND PLUTONIUM CARBIDES[4]

	Melting point, °C	Crystal structure	Lattice parameters, A	Theoretical density, g/cm³
UC*	2400	FCC, NaCl type	a = 4.9598 ± 0.0003	13.63
U_2C_3	Decomposes at 1775°C	BCC	a = 8.0885 ± 0.0005	12.88
UC_2	2400	Bct, CaC_2 type	a = 3.509 ± 0.003, c = 5.980 ± 0.005	11.68
PuC	1850	FCC, NaCl type	a = 4.97	13.6
Pu_2C_3	1900	BCC	a = 8.129	12.7
ThC	2625	FCC, NaCl type	a = 5.34	
ThC_2	2655	Monoclinic	a = 6.53, b = 4.24, c = 6.56; β = 104°	

*Specific heat for UC is 0.048 ± 0.003 cal/(g)(°C) at 125°C and is 0.053 ± 0.003 cal/(g)(°C) at 250°C. Electrical resistivity is 100 ± 4 μohm-cm for sintered UC with a density of 10.82 g/cm³ and is 40 μohm-cm for as-cast UC with a density that is 98 per cent of theoretical.

Table VIII-3 SOME MECHANICAL PROPERTIES OF URANIUM-CARBON ALLOYS[4]

Material	Vickers hardness, kg/mm²	Rupture strength, psi		Elastic modulus, 10^6 psi
		Transverse	Compressive	
Cast U–4.6 wt.% C*	900	9,600		
Cast U–5.2 wt.% C†:				
As cast	600		54,500	31.5
Annealed 1 hr at 1000°C	560			
Annealed 1 hr at 1500°C	760			
Cast U–7 wt.% C*	850	13,600		
Sintered UC‡	750–800	40,000–55,000		
Sintered UC§:				
Density, 10.84 g/cm³	700 ± 150		42,500 ± 5,500	
Density, 10.2 g/cm³	550 ± 150			

*Reference 27.
†Reference 28.
‡Reference 29.
§Reference 10.

Table VIII-4 IRRADIATION HISTORY AND POSTIRRADIATION DATA[§] FOR UC SPECIMENS FROM CAPSULES BRR, BMI-23-1, BMI-23-2, BMI-23-3, BMI-23-5, AND BMI-23-6

	BRR			BMI-23-1		BMI-23-2		BMI-23-3		BMI-23-5		BMI-23-6	
				Top	Bottom	Top	Bottom	Top	Bottom	Top	Bottom	Top	Bottom
	12A	15A	25A	3	2	26	37	28	29	42	50B	41	46
Nominal carbon content, wt.%	5.0	5.0	5.0	5.0	5.0	5.0	5.0	5.0	5.0	4.6	4.6	4.8	4.8
Carbon content by determination,* wt.%	5.00	5.4	5.57	5.2	5.2	5.3	5.1	5.0	5.0	4.6	4.7	4.8	4.6
Diameter change, %	0.16	0.28	0.16	0.4	0.3	0.9	0.9		0.8	0.8	1.2	0.48	0.48
Density change, %	0.29	0.45	0.44	0.7–0.9	2.5	0.6–2.0	2.5	1.8	1.8	2.4	1.6	1.2	1.6
Average temperature, °F													
Surface	600	600	600	770	540	915	700	765	623	882	772	850–780	500–700
Core	660	660	660	1,300	880	1,375	1,060	1,178	1,086	1,326	1,248	1,300–1,600	800–1,100
Fission-gas release, cm^3 of Kr^{85}													
Estimated total produced				5.9×10^{-2}		20.9×10^{-2}				20.4×10^{-2}		21.9×10^{-2}	
Estimated released by recoil				2.5×10^{-5}		8.8×10^{-5}				8.7×10^{-5}		9.4×10^{-5}	
Measured release	Negligible			2.4×10^{-5}		9.7×10^{-5}		†	†	8.22×10^{-5}		8.37×10^{-5}	
Burnup, Mwd/ton of uranium‡													
Nominal	700	700	700	1,000		5,000		10,000		5,000		5,000	
Dosimetry	400	400	400	1,420	1,780	5,600	7,800	12,200	12,800	6,500	6,400		
Radiochemical§								15,650		8,600		6,500	
Isotopic¶								13,750		8,100		5,900	
Estimated average heat-generation rates, 10^3 Btu/(sq ft)(hr)													
Based on dosimetry burnup data		170		680	850	880	940		695		710		
Based on isotopic burnup data								750		900		600	

*The estimated composition is based on metallography, density, and a carbon analysis from the top of the cast ingots.

†Fission-gas sample was lost, apparently by leakage from capsule.

‡Based on a 2200-lb ton and a fission energy of 195 Mev.

§Based on an analysis for Cs^{137}.

¶Based on an analysis for U^{236} by mass spectrometry.

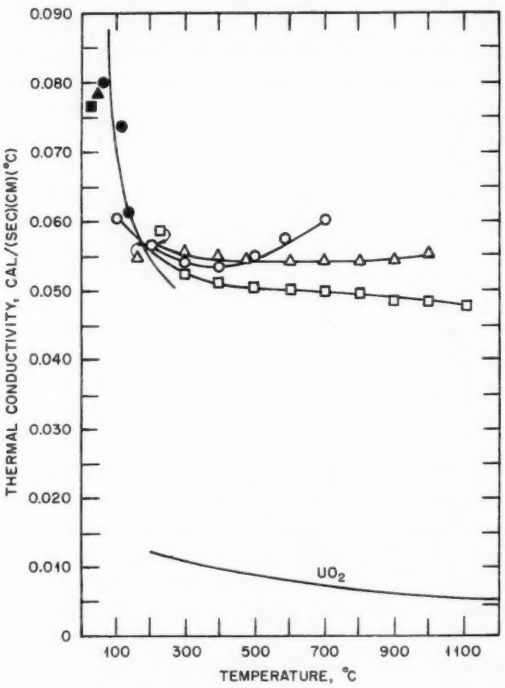

Figure 14—Thermal conductivities of UC, UC_2, and UO_2. ○, U–5.2 wt.% C, arc cast. □, U–4.9 wt.% C, arc cast. △, U–5.3 wt.% C, arc cast. ●, U–4.8 wt.% C, sintered. ■, U–4.8 wt.% C, sintered. ▲, UC_2, sintered. The UC and UC_2 data are from reference 4, which lists additional references. The UO_2 data are Hedge and Fieldhouse values taken from Canadian Report CRL-55 (AECL-754) by O. J. C. Runnalls; this report also lists additional references.

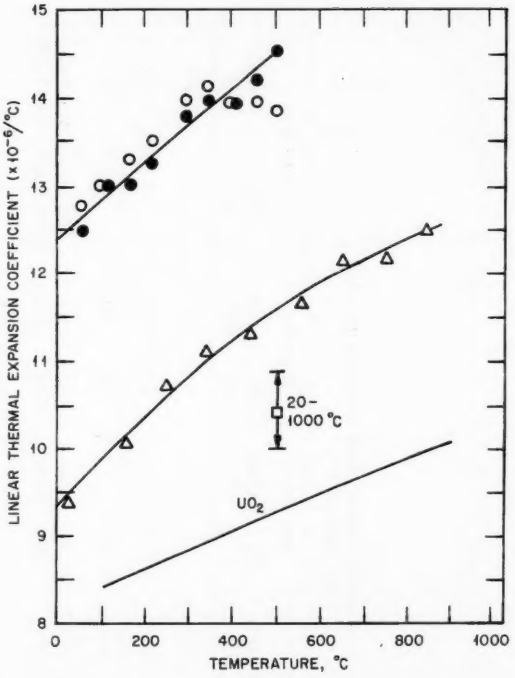

Figure 15—Thermal-expansion coefficients[4] of UC and UO_2. □, U–4.8 wt.% C, heated, density 10.84 g/cm^3, sintered. △, U–4.8 wt.% C, heated, density 13.60 g/cm^3, cast. ○, U–4.6 wt.% C, heated, density 12.87 g/cm^3, sintered. ●, U–4.6 wt.% C, cool, density 12.87 g/cm^3, sintered. The UC data are from reference 4, which lists additional references. The UO_2 curve is from the data of M. D. Burdick and H. S. Parker, *J. Am. Ceram. Soc.*, 39(5): 181–187 (1956).

The results (Table VIII-4) indicate that the radiation-induced dimensional changes are small and that the fission-product release is small, approximately equal to that estimated to result from fission recoil. The reference[8] states that no correlation can be observed between the burnup level and the changes in diameter or density. Some cracking occurred in all the MTR specimens, and the cracking may be responsible for some or all of the observed changes in gross dimensions. Both radial and transverse cracks occurred, and some spalling of the surface occurred in several specimens.

One of the specimens from capsule BMI-23-2 (nominal exposure 5000 Mwd/ton) was heat-treated, after exposure, for 8 hr at 2000°F under vacuum in a quartz tube. The specimen disintegrated into particles. During the heat-treatment the fission-gas release was low; the Kr^{85} release was 2.04×10^{-6} cm^3. This may be compared to a release of 12.0×10^{-5} cm^3 during irradiation and a total estimated production of 8.0×10^{-2} cm^3. An unirradiated specimen subjected to the same heat-treatment experienced no appreciable change. The significance of the behavior of the irradiated specimen is not clear. If it indicates a temperature limitation substantially below the melting point of UC, it may be quite important.

It is probably too early to say which methods show the most promise for making high-density, economical, uranium carbide fuel pellets. Many methods of synthesizing uranium carbide and fabricating pellets are being evaluated.[1] It is not evident, of course, that the irradiation performance of the melted and cast material can be assumed typical for material made and fabricated by other processes.

Some of the methods under investigations are:

1. Heating a mixture of powdered uranium metal in a flowing stream of methane gas to form powdered uranium carbide.
2. Reacting uranium metal with hydrogen to form powdered uranium hydride and heating the resultant powder in a flowing stream of methane to form powdered uranium carbide.
3. Heating a UO_2 powder and carbon mixture.
4. Pressing a mixture of UO_2 powder and carbon into pellets and heating the pellets.
5. Cold pressing a mixture of uranium powder and carbon and sintering the pellets.
6. Hot pressing a mixture of uranium powder and carbon.
7. Arc melting uranium and carbon.

The pellets are formed from the powdered UC by pressing and sintering, by slip casting and sintering, or by arc melting and casting.

Uranium and carbon can be simultaneously synthesized and pelletized by hot pressing or by arc melting and casting.

If pellets of desirable nuclear and mechanical properties can be fabricated by an economical process, it seems probable that their use will be advantageous in those reactor types in which they do not encounter incompatible materials. Uranium carbides seem to be compatible with sodium and NaK and are being considered as fuels for sodium graphite reactors by Atomics International. Uranium monocarbide is the reference fuel for the second core loading of the Hallam Nuclear Power Facility.[6]

Nuclear Development Corporation of America made an analytical evaluation of PuC-UC in existing fast-breeder reactors.[2] Carbide fuel elements were substituted in the core of the Enrico Fermi Fast-Breeder Reactor (EFFBR), and their effects on reactor heat-transfer characteristics, nuclear characteristics, and fuel-cycle costs were calculated. Comparisons were made with fuels of uranium–10 per cent molybdenum and PuO_2-UO_2. The results are summarized in Table VIII-5.

It was concluded that, if certain reasonable performance goals can be achieved, a fuel-cycle cost reduction by a factor of 2 to 3 (relative to metal fuel) is possible. This reduction would be due to the increased burnup and power-generation capabilities of PuC-UC compared to presently available metallic fuels. A factor of 2 increase in fuel pin diameter and a factor of 4 decrease in the number of fuel pins required appeared to be possible with UC-PuC compared to uranium–10 per cent molybdenum at maximum carbide temperatures well below the melting point. With PuO_2-UO_2 fuel, the low thermal conductivity requires a reduction in fuel pin size below that of uranium–10 per cent molybdenum, and a large increase in the number of fuel pins is needed.

Uranium carbide yields a smaller critical mass in the fast reactor than does uranium–10 per cent molybdenum. The PuC-UC core critical mass is larger than the PuO_2-UO_2 core because of greater amounts of U^{238} present. The lower fuel density and softer neutron spectrum caused by the introduction of carbon in UC yields a lower breeding ratio than uranium–10 per cent molybdenum. PuC-UC, however, has a higher breeding ratio than uranium–10 per cent molyb-

Table VIII-5 SUMMARY OF CONCEPTUAL DESIGN RESULTS[2]

Reactor	EFFBR U–10% Mo core	EFFBR UC core	EFFBR PuC-UC core	EFFBR PuO_2-UO_2 core
Heat-transfer characteristics:				
No. of fuel pins per subassembly	144	36	36	225
Fuel pin diameter, in.	0.148	0.289	0.289	0.104
Corresponding maximum fuel temp., °F	1135	2900	2900	3900
Nuclear characteristics:				
Calculated breeding ratio	1.12	1.09	1.57	1.48
Critical mass, kg U^{235} or Pu^{239}	433	397	279	253
Estimated fuel costs:				
Fuel fabrication cost, $/kg (U + Pu)	540	←— 340* —→	←— 550* —→	2200*
Assumed burnup, at.% of U + Pu	1.25	1.25 2.0 5.0	2.0 5.0	2.0
Fuel cost, mills/kw-hr (Pu at $30/g)	8.8	7.3 4.7 2.1	6.4 2.9	18.1
Fuel cost, mills/kw-hr (Pu at $12/g)	11.7	10.0 7.4 4.9	5.9 3.4	16.4

*Based on pressing, sintering, and grinding pellets. Relaxation of tolerances to eliminate grinding will reduce fuel-cycle costs more on plutonium cores than on the others.

denum due to the presence of plutonium as a fissile material, and a higher breeding ratio than PuO_2-UO_2 due to its higher fuel density.

The reduction in cost of the UC core as compared with the uranium–10 per cent molybdenum core is due to fabrication savings resulting from the use of fewer pins and to the higher burnup. The relative cost of UC or PuC-UC fuel is dependent on the plutonium cost as shown, with a $30 per gram cost favoring UC fuel and the $12 per gram cost favoring PuC-UC fuel. Fuel costs were predicted to be much higher for PuO_2-UO_2 fuel than for PuC-UC fuel because of the large number of small pins required.

In summarizing the present status of carbide fuels, it can be said that their use offers a promising means of reducing fuel-cycle costs for some reactors, but more information about their irradiation behavior and their compatibility with cladding and coolant materials is needed to prove their practicability. Very little irradiation information has been obtained to date. Numerous irradiation tests were scheduled to be started in 1960, and these results will probably be available some time in 1961. Some short-term tests have shown carbide fuels to be compatible with sodium and NaK, and they are therefore being considered most seriously as fuels for sodium-cooled reactors. They react with water to a degree that causes uranium monocarbide to disintegrate in a short time, and they react to a lesser degree with many other coolants and cladding materials. Some doubt, however, has been expressed as to the value of some of the past compatibility tests that were conducted with uranium carbide of questionable composition.[1] Efforts are being made to develop carbide fuels which are compatible with water. A solid solution of ZrC and UC which was evaluated by Combustion Engineering appeared to have a considerable resistance to water and steam[1] at 100°C.

Fission-Product Release

A series of tests with ThO_2-UO_2 fuel specimens having intentional defects was conducted over a six-month period of operation in the EBWR to obtain information on irradiation behavior of thoria-urania fuel.[10] There is an acute need for such data because of the increasing use of oxide fuels and because of the scarcity of quantitative information on the effects of failures.

The objectives of the tests reported in reference 10 were:

1. To study the rate of release of fission products from a defective thoria-urania fuel element
2. To study the distribution of the fission products throughout the reactor system
3. To attempt to assess the hazards involved in operating a boiling-water reactor fueled with a ceramic fuel which contains defects in the cladding

Two specimens were used, one in Test 1 and the other in Test 2. The specimen used in Test 1 was small and was tested primarily to determine the order of magnitude of activity levels; the specimen used in Test 2 was much larger. The fuel pellets used in the specimens were prepared by cold pressing a ThO_2-U_3O_8 mixture and then firing in air at 1750°C. The final composition was 90 wt.% ThO_2–10 wt.% $U^{235}O_2$. The pellets were then encased in a stainless-steel tube. Physical details of the specimens are listed in Table VIII-6. To ensure sensitivity to control-rod motion, each specimen was fitted into a coolant channel of an EBWR natural-uranium fuel element adjacent to a control rod.

Table VIII-6 FUEL TEST SPECIMENS[30]

	Test 1	Test 2
Composition, wt.%:		
$UO_{2.1}$	10	10
ThO_2	90	90
Density:		
g/cm³	9.7	9.1
% of theoretical	95	90
U^{235} enrichment, wt.% U	93	93
Wt. U^{235}, g	2.73	43.5
Pellet diameter, in.	0.300 ± 0.001	0.312 ± 0.002
Fuel length, in.	3.1	48
Fuel sheath clearances (cold), in.:		
Diametral	0.004	0.010
Axial	0.125	0.125
Sheath material	Stainless steel	Stainless steel
Sheath thickness, in.	0.035	0.025
Sheath defect:		
Location	Center of fuel	Top of fuel
Diameter, in.	0.010	0.020

The rate of release of fission-product gases was studied by taking samples of air ejector gases during reactor operation. These samples were analyzed by chemical means and by the use of a 200-channel gamma-ray spectrum analyzer

for the four nuclides Xe^{138}, Kr^{88}, Xe^{135}, and Xe^{133}.

The distribution of fission products in the steam system was studied by placing material specimens, representative of turbine construction materials, in the steam line before the steam dryer and by placing other specimens, representative of condenser construction materials, along the top row of condenser tubes. These samples were counted in a 256-channel gamma-ray pulse-height analyzer. Also, samples of reactor water and effluent from the ion-exchange resins were taken throughout the test, and the gross beta-gamma count rate was determined with a gas flow proportional beta counter. Samples of reactor water were also withdrawn through four stainless-steel tubes which were located close to, in the vicinity of, and far removed from, the defective element.

The tests were conducted over a power range from 5 Mw(t) to 26 Mw(t). Operating characteristics of the two fuel specimens at 20 Mw(t) are listed in Table VIII-7. Central temperatures were calculated from thermal conductivity values of ThO_2, on the assumption that the UO_2 content was small enough to neglect. Surface temperatures used for the calculation of central temperatures were determined by assuming an average gap width (see Table VIII-6) between the fuel and cladding and by assuming that this gap was filled with steam. The cladding surface temperature was assumed to be 3°C higher than the EBWR bulk water temperature (T_w) which was taken at 254°C (490°F).

Table VIII-7 OPERATING CHARACTERISTICS[30] OF FUEL SPECIMENS; REACTOR POWER 20 Mw(t)

	Test 1	Test 2	
		Maximum	Average
Reactor operation, Mwd	787	2016.7	
nvt, neutrons/cm^2	2.7×10^{19}	7.0×10^{19}	4.0×10^{19}
Burnup, at.% U^{235}	1.2	3.2	1.9
Thermal-neutron flux, neutrons/(cm^2)(sec)	8×10^{12}	8×10^{12}	4.6×10^{12}
Fissions/sec	3.25×10^{13}	4.83×10^{14}	2.81×10^{14}
Surface heat flux (fuel):			
watts/cm^2	52	48	28
Btu/(hr)(sq ft)	1.65×10^5	1.52×10^5	0.89×10^5
$\int k(T)\,dT$, watts/cm	10	9.6	5.6
Temperatures, °C:			
Central	900	1300	1000
Surface (fuel)	650	1000	800

One of the most significant observations during the tests was made at the air ejector monitor while control rods were being moved. At constant power, withdrawal of the control rod adjacent to the specimen caused a peaking in the count rate. This phenomenon was probably due to the temperature increase in the fuel; this increase would cause (1) an expansion of the fission gases in the space between fuel and cladding and (2) an ejection of a burst of fission-product gases through the cladding defect. Lowering of the same control rod had no effect on count rate. A method of detecting and locating fuel cladding defects in operating reactors might be based on this burst effect.

When reactor power was increased, release rates of all fission gases increased. Immediately after power was decreased, all release rates fell sharply. Release rates of short-lived gases then returned to a new steady level. The longer-lived gases continued to increase for a period of a few days, after which they fell to a new low steady rate. The initial reduction in release rates was expected since the temperature decrease within the gap caused the fission-gas pressure to drop below reactor pressure. The behavior of the longer-lived gases might be attributed to fuel cracking during the transient, releasing the longer-lived gases from pores that previously had been closed.

Observed fission-gas release rates were corrected by subtracting the release rate that was observed when no defect was present. This background rate was probably due to recoils from uranium oxide contamination on the surface of the EBWR elements. From these observed release rates, it was determined that the ratio R/Y was proportional to $1/\sqrt{\lambda}$, where R is the rate at which gas was escaping from the defect (atoms/sec), Y is the fission yield, and λ is the decay constant of the gas (sec^{-1}). Fission-gas release from an unclad fuel pellet under irradiation was shown to follow the relation

$$\frac{R}{Y} = 3F\sqrt{D'}\,\frac{1}{\sqrt{\lambda}}$$

where F is the number of fissions per second and D' is the special diffusion constant for the fuel as defined by Booth and Rymer.[31] In a defective fuel element, however, an additional diffusion process takes place in the space between

the fuel pellet surface and the cladding. The reference suggests that this additional process has more effect on the release rate of the short-lived nuclides, whereas diffusion through the oxide is probably rate controlling for the long-lived nuclides.

Release rates obtained were compared to published data on the VBWR at Vallecitos and on the PWR at Shippingport. It was shown that radioiodines are released at a higher rate from a VBWR (UO_2) or PWR (UO_2) defect than from the EBWR defect. This was also verified in the BORAX-IV (ThO_2-UO_2) experiment.[32] VBWR and PWR radioiodine release rates due to defects were nearly equal to those of fission-product xenon and krypton, whereas in the EBWR the release was not appreciable. It was concluded that possibly ThO_2 retains iodine in the crystal lattice to a greater extent than UO_2 does.

In the EBWR tests, iodine release rates were obtained from reactor water samples. No iodine activity was reported at the stack, probably because of a high decontamination factor afforded by the water in the reactor and the main condenser. Despite the additional release rates of xenon and krypton from the defect, stack activities were still well below maximum permissible concentrations for release to the atmosphere.

Examinations of the metal specimens in the steam line and in the condenser were conducted after each test. Gamma-ray spectra indicated the presence of Co^{58} and Co^{60}, but no characteristic fission-product activities could be observed. It was concluded that any deposited fission-product activity was very small compared to Co^{58} activity. This would indicate that the main radioactive nuclides that escape from the defect are fission-product gases and that the main activities throughout the system are due to these gases or their decay products.

Both tests showed that, with one defect present in EBWR, the activities throughout the system were about the same as with no defect (and a slight amount of uranium contamination) present. In the reactor circulating water and in the condenser, N^{16} activities predominated; whereas in the reactor water, fission-product activities were orders of magnitude lower than those from activation products such as Na^{24}, Mn^{56}, or Co^{58}.

Reference 33 is a recent study of fission-product release from UO_2, in which all information available up to the fall of 1959 is considered and correlated. It indicates that a large increase in fission-gas release occurs above the sintering or grain-growth temperature. On inspection of the fuel irradiated in the EBWR tests, no signs of melting or recrystallization of the thoria-urania were detectable. This grain-growth effect would be important to evaluate if the ThO_2-UO_2 fuel were considered for use in a reactor in which portions of the fuel operated at these higher temperatures, as is usually the case. Useful information for determining maximum activity levels throughout the reactor system could also be obtained from a test designed to simulate fission-gas release following a cladding defect which occurred after a buildup of fission gas had occurred in the fuel-cladding gap.

A review of the literature describing inert fission-gas release from natural-uranium specimens is given in reference 34. All but one of the papers reviewed conducted the gas-release portion of the tests during postirradiation heating. Quantitative correlation of the various test results was not possible; however, it was shown that postirradiation temperatures and surface conditions of the specimens were two controlling factors in the rate of gas release. Diffusion coefficients were assigned to xenon and krypton, but discrepancies of several orders of magnitude in these values led to the conclusion that the process of gas release in natural uranium is not diffusion in the classical sense.

Specimens with polished surfaces released xenon at a slower rate than those with sand-blasted surfaces, suggesting that surface area is a significant parameter. Oxidation of the uranium surface further enhanced the release rate, as indicated by sweeping the specimen, during postirradiation heating, with various oxidizing atmospheres. Heating in a vacuum, in gettered (high-purity) argon or in ungettered argon atmospheres, illustrated this dependence.

The temperature used in postirradiation heating had the greatest effect on gas-release rates. Below about 900°C, the gas release was about 1 per cent of the total present in the specimens. In the vicinity of 1000°C, as high as 64 per cent release of the total gases present was measured. This region of transition was marked by gross swelling of the uranium. Diffusion constants calculated for the lower gas-release region were generally lower for krypton than for xenon, although the actual time dependence of the release was not obvious. It should be noted that more rapid diffusion of the heavier atom, xenon,

is contrary to the classical diffusion mechanism. In the region around 1000°C, when gross swelling occurred, gas release was so erratic that the data could not be evaluated; however, thermal cycling from room temperature to about 1000°C was shown to increase the gas release in this region.

One paper was reviewed which described the release of xenon from uranium during irradiation. The diffusion constants calculated for this case were higher than expected, on the basis of postirradiation release data, but the differences might be attributed to the method of measurement.

Future study areas were proposed for determining the mobility of inert gases in uranium. It was suggested that unirradiated uranium, containing inert gases introduced into the metal by nonirradiation techniques, be used in these studies. Studies conducted in reactor environments, however, should yield more meaningful results for application to fuel-element design.

References

1. Battelle Memorial Institute, Progress in Carbide Fuels, Notes from the Second AEC Uranium Carbide Meeting Held at Battelle Memorial Institute March 22 and 23, 1960, USAEC Report TID-7589, Apr. 20, 1960.
2. R. Bolomey et al., Carbide Fuel Development, Phase I Report, Period of May 15 to September 15, 1959, USAEC Report NDA-2140-2, Nuclear Development Corp. of America and The Carborundum Co., Oct. 15, 1959.
3. C. A. Smith and F. A. Rough, Properties of Uranium Monocarbide, USAEC Report NAA-SR-3625, Atomics International, June 1, 1959.
4. F. A. Rough and Walston Chubb, An Evaluation of Data on Nuclear Carbides, USAEC Report BMI-1441, Battelle Memorial Institute, May 31, 1960.
5. N. R. Koenig and B. A. Webb, Properties of Ceramic and Cermet Fuels for Sodium Graphite Reactors, USAEC Report NAA-SR-3880, Atomics International, June 30, 1960.
6. D. H. Turner, Process Development of Uranium Monocarbide Fuel Slags, USAEC Report NAA-SR-4904, Atomics International, Mar. 15, 1960.
7. R. B. Price et al., Irradiation-Capsule Study of Uranium Monocarbide, USAEC Report BMI-1425, Battelle Memorial Institute, Mar. 2, 1960.
8. A. W. Hare and F. A. Rough, Irradiation Effects on Massive Uranium Monocarbide, USAEC Report BMI-1452, Battelle Memorial Institute, July 21, 1960.
9. W. C. Thurber and R. J. Beaver, Dispersions of Uranium Carbides in Aluminum Plate Type Research Reactor Fuel Elements, USAEC Report ORNL-2618, Oak Ridge National Laboratory, Nov. 19, 1959.
10. A. Boettcher and G. Schneider, Some Properties of Uranium Monocarbide, *Proceedings of the Second United Nations International Conference on the Peaceful Uses of Atomic Energy, Geneva, 1958*, Vol. 6, pp. 561–563, United Nations, New York, 1958.
11. P. Murray and J. Williams, Ceramic and Cermet Fuels, *Proceedings of the Second United Nations International Conference on the Peaceful Uses of Atomic Energy, Geneva, 1958*, Vol. 6, pp. 538–550, United Nations, New York, 1958.
12. Chicago University Metallurgical Laboratory, Technological Research, Section II, Report for Month Ending January 15, 1943, USAEC Report CT-423.
13. Sylvania-Corning Nuclear Corp., Quarterly Technical Progress Report for the Period Ending June 30, 1958, USAEC Report SCNC-279, September 1958. (Classified)
14. R. W. Nichols, Ceramic Fuels, *Nuclear Eng.*, 3: 327–333 (August 1958).
15. R. W. Dayton and C. R. Tipton, Jr., Progress Relating to Civilian Applications During September 1959, USAEC Report BMI-1381, p. 58, Battelle Memorial Institute, Oct. 1, 1959.
16. M. G. Bowman, Bonding Uranium Carbide to Tantalum, USAEC Report AECU-4304, Los Alamos Scientific Laboratory, May 19, 1959.
17. Armour Research Foundation, Illinois Institute of Technology, Development and Properties of Uranium Monocarbide Cermets, USAEC Report AECD-4289, Sept. 17, 1956.
18. S. J. Paprocki et al., Fabrication of Dispersed Uranium Fuel Elements Using Powder-Metallurgy Techniques, USAEC Report BMI-1184, Battelle Memorial Institute, May 6, 1957.
19. E. Barnes et al., The Preparation, Fabrication, and Properties of Uranium Carbide and Uranium-Uranium Carbide Cermets, in *Progress in Nuclear Energy, Series V, Metallurgy and Fuels*, pp. 435–447, edited by H. M. Finniston and J. P. Howe, Pergamon Press, New York, 1956.
20. R. W. Dayton and C. R. Tipton, Jr., Progress Relating to Civilian Applications During November 1957, USAEC Report BMI-1238, p. 48, Battelle Memorial Institute, Dec. 1, 1957.
21. W. M. Albrecht and B. G. Koehl, Reactivity of Uranium Compounds in Several Gaseous Media, *Proceedings of the Second United Nations International Conference on the Peaceful Uses of Atomic Energy, Geneva, 1958*, Vol. 6, pp. 116–121, United Nations, New York, 1958.
22. L. M. Litz, Uranium Carbides—Their Properties, Structure, and Hydrolysis, Report NP-1453, Ohio State University, 1948.
23. W. M. Phillips, Battelle Memorial Institute. (Unpublished)

24. J. E. Baker, Report on the Carbides of Uranium: UC, UC_2, and U_2C_3, USAEC Report NEPA-273, Fairchild Engine and Airplane Corp., Aug. 7, 1947.
25. J. E. Baker, Uranium Carbide, Technical Report, USAEC Report NEPA-138, Fairchild Engine and Airplane Corp., Dec. 31, 1946.
26. R. W. Dayton and C. R. Tipton, Jr., Progress Relating to Civilian Applications During October 1959, USAEC Report BMI-1391(Rev.), p. 61, Battelle Memorial Institute, Nov. 1, 1959.
27. W. M. Phillips, Battelle Memorial Institute. (Unpublished)
28. A. C. Secrest et al., Preparation and Properties of Uranium Monocarbide Castings, USAEC Report BMI-1309, Battelle Memorial Institute, Jan. 2, 1959.
29. R. Keiffer et al., The Preparation of Uranium Monocarbide and Its Behavior Compared with Other High-Melting Carbides, *Planseeber. Pulvermet.*, 5: 33–35 (1957); see British Translation IGRL-T/C-52.
30. R. F. S. Robertson, Tests of Defected Thoria-Urania Fuel Specimens in EBWR, USAEC Report ANL-6022, Argonne National Laboratory, May 1960.
31. A. H. Booth and G. T. Rymer, Determination of the Diffusion Constant of Fission Xenon in UO_2 Crystals and Sintered Compacts, Canadian Report CRDC-720(AECL-692), August 1958.
32. R. F. S. Robertson and V. C. Hall, Jr., Fuel Defect Test. BORAX-IV, USAEC Report ANL-5862, Argonne National Laboratory, October 1959.
33. W. B. Cottrell et al., Fission-Product Release from UO_2, USAEC Report ORNL-2935, Oak Ridge National Laboratory, Sept. 13, 1960.
34. D. L. Gray, Release of Inert Gases from Irradiated Uranium (A Review of the Literature), USAEC Report HW-62639, Hanford Atomic Products Operation, January 1960.

Section IX

POWER DEMONSTRATION REACTORS

A bibliography[1] has been published which lists the reports issued on 10 reactors of the Power Reactor Demonstration Program. The 310 reports listed cover the following reactors: Elk River, Enrico Fermi, Florida, Hallam, Parr Shoals, Pathfinder, Piqua, Puerto Rico, Saxton, and Yankee.

Reference

1. J. M. Jacobs, comp., Selected Reactors of the Power Reactor Demonstration Program, a Literature Search, USAEC Report TID-3556, June 1960.

Section X

ORGANIC-MODERATED REACTORS

Several reports relating to organic-moderated reactors have been published this year. Reference 1 is an account of the reactor physics calculation methods used in the design of the Organic-Moderated Reactor Experiment (OMRE) and gives the results of the calculations. The report is useful for an understanding of the reactor, although certain changes were made in the design after the calculations described in the reference.

Reference 2 is a physics analysis of the use of plutonium in an organic-moderated reactor. The study treats plutonium of an isotopic composition considered to be typical of that recovered from slightly enriched uranium fuel irradiated to 10,000 Mwd/ton. Three modes of loading the plutonium are considered: (1) a uniform mixture of uranium and plutonium in all fuel elements; (2) separate elements of uranium and plutonium-aluminum alloy, uniformly distributed in different proportions throughout the core; and (3) separate uranium and plutonium-aluminum elements segregated into zones in the core. U^{235} enrichments from 0.72 to 2.5 per cent are considered, with plutonium admixtures from zero to 2 per cent relative to the total uranium. The effects of the plutonium concentration on reactivity, reactivity lifetime, conversion ratio, and intracell power distributions are considered. The results are of considerable interest for the specific reactor lattice considered. Basically this lattice consisted of an array of square fuel assemblies made of uranium–3.5 wt.% molybdenum alloy plates clad with finned aluminum and contained in a square stainless-steel box. When separate plutonium-fueled elements were used, it was assumed that the plutonium would be contained in plutonium-aluminum alloy plates of thickness equal to that of the uranium-molybdenum plates. The metal-to-organic volume ratio was held constant for all cases.

Reference 3 is a summary of reactor physics and heat-removal calculations which were made to arrive at a choice between square plate type fuel assemblies and round double-annular assemblies for the Piqua organic-moderated reactor. The two assembly types are shown in cross section in Fig. 16. Both assemblies employ aluminum-clad uranium alloy fuel elements with fins on the aluminum cladding. The fins on the plate type elements are longitudinal, whereas those on the annular elements are spiraled. The annular elements were arranged in the reactor core in an equilateral triangular pattern, whereas the plate type assemblies were considered in two different square arrays: a close-packed array and a spaced array.

Of the three arrangements considered, the square, spaced lattice was found to be least attractive, primarily because of high flux peaking near the organic channels at the edges of the assemblies. In most respects, the annular element was found to be most attractive. In particular, the flux peaking within the element was quite low because of the symmetrical distribution of the fuel and because the flux peaking in the moderator-filled central hole approximately balanced the effect of the flux peak due to the moderator surrounding the assembly. Relative performances of the three types of elements in the Piqua core, and comments on their relative advantages and disadvantages, are listed in Table X-1. The main potential disadvantage of the annular element is that growth of the uranium fuel may have a greater effect on the coolant channel thickness.

Reference 4 summarizes the fuel-element development work for the Piqua reactor. It covers both the fabrication process and testing. During

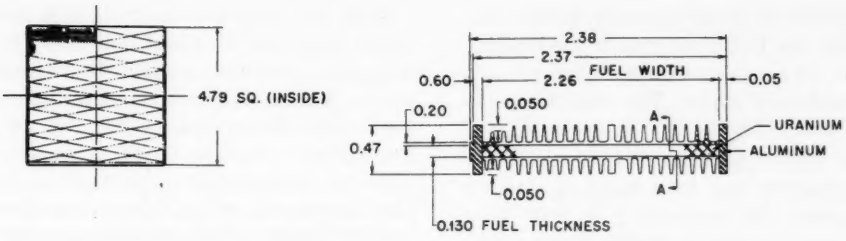

(a)

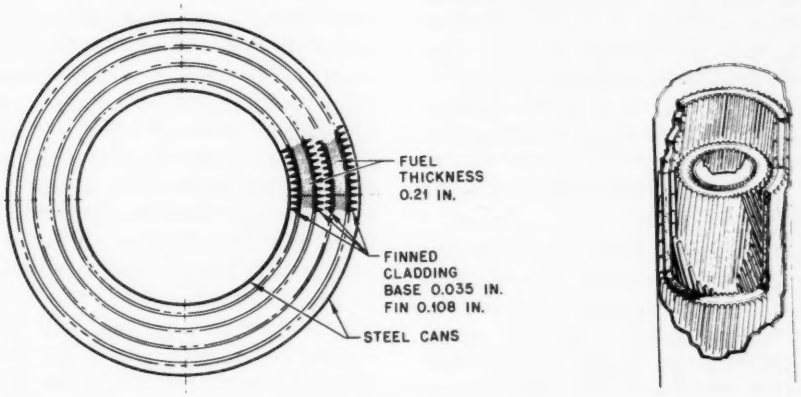

(b)

Figure 16 — OMR fuel assemblies.[3] (*a*) Plate type assembly. (*b*) Double-annular assembly.

Table X-1 RELATIVE PERFORMANCE OF THREE TYPES OF FUEL ELEMENTS[3]

	Square fuel element		Circular fuel element
	Spaced	Close packed	
Total flow rate	1.37	1.79	1.0
Core pressure drop	1.08	0.73	1.0
Core pumping power	1.48	1.31	1.0
Reactor diameter and length	0.99	0.79	1.0
Fuel-cycle costs	1.41	1.42	1.0
Enrichment, %	2.0	3.4	2.0
Element flux peaking	1.63	1.30	1.05
Advantages:	Low enrichment; upper grid plate can readily be used	Low flux peaking in the element; smaller core; moderate flow rate	Low enrichment; upper grid plate can readily be used; low flux peaking in the element; low flow rates
Disadvantages:	High flux peaking in the element; high flow rate	Difficult to use upper grid plate; high enrichment	Fuel cylinder growth due to burnup

the development, the fuel-element design was changed from the flat plate type to the double-annular type as a result of considerations such as those mentioned above. The report covers the work on both types.

The basic objective of the fuel-element development program was to develop an element with a maximum life expectancy of 5000 Mwd per metric ton of uranium (3000 Mwd/metric ton for the average life), which would require a fuel enrichment of less than 2 wt.% U^{235}. Metallurgically, the reference fuel element to meet these objectives consists of a fuel alloy of uranium–3.5 wt.% molybdenum–0.1 per cent aluminum, bonded metallurgically through a nickel diffusion barrier to a finned cladding of 2S aluminum. The uranium-molybdenum-aluminum alloy has been chosen over uranium-molybdenum and uranium-molybdenum-silicon for its high creep strength.

The steps in the manufacture of a tubular fuel element are briefly described. The uranium derby and the other alloying metals are vacuum-induction-melted and cast into graphite molds which have been outgassed by vacuum and coated with magnesium zirconate. The cast tubular section, approximately 13 in. long, is machined on inside and outside diameters to obtain the required tolerance of ±0.003 in. on wall thickness and to meet the ovality specification. The tubular sections are then degreased, degassed in vacuum for a minimum of 12 hr, grit-blasted, washed in methyl alcohol, and electroplated with nickel. The cleaned inner and outer cladding tubes of finned aluminum are slipped onto the plated uranium tube, and aluminum rings which serve as end plugs are slipped in between the two cladding layers at each end. The inner and outer clad tubes are Heliarc welded to the end plugs, with water-cooled chill blocks used on the inside and outside diameters of the cladding. The assembly is then helium leak-tested and evacuated, at room temperature and then at 1000°F, through an evacuation tube which is subsequently closed by hot knifing. The cladding is then bonded to the uranium by isostatically pressing the assembly by argon pressure at a temperature of approximately 1000°F and a pressure of 4 to 5 tsi.

Testing of the fuel elements for metallurgical bond between the uranium and the cladding presents a problem. A satisfactory nondestructive test has not yet been developed.

After the clad fuel sections have been fabricated, they must be assembled into a full-length assembly; then the annular stainless-steel can, which defines the inner and outer boundaries of the coolant flow passages (see Fig. 16), and the end fittings must be added. This assembly is done by a straightforward welding procedure. The completed fuel assembly consists of two coaxial stacks of the tubular segments inside the annular steel flow can, each stack containing eight segments.

Three of the plate type fuel assemblies have been tested in-pile, and one additional plate type assembly and one tubular assembly are currently under irradiation in the OMRE. The first two assemblies tested contained some plates of uranium-molybdenum alloy and some plates of uranium-molybdenum-silicon alloy rather than the uranium-molybdenum-aluminum alloy which is the present reference material. The assemblies were irradiated in the OMRE to approximately 2300 Mwd/ton and were removed because of damage which resulted from blocking of the coolant passages by deposited materials (reviewed in the September 1960 issue of *Power Reactor Technology*, Vol. 3, No. 3). It was concluded from examination that the damage did not result from a deficiency in the fuel assemblies, and the performance of the assemblies was considered satisfactory during their residence in the reactor. The third plate type assembly, containing plates of the uranium-molybdenum-aluminum alloy, was irradiated for 4000 Mwd per metric ton of uranium before it was removed for examination. Preliminary examination showed no evidence of any failure, and only one plate, that subjected to the highest burnup, showed a change after exposure. This change amounted to a dishing in one area, a decrease of thickness, and an increase of length.

The conclusions of the report are as follows:[4]

> The development program for the Piqua fuel element is essentially complete. Through this work, it has been determined that ternary alloys, based on U–3.5 Mo, can be cast into thick sections and are stable under the operating conditions for the Piqua reactor. Aluminum is a suitable cladding material for such alloys, for use at temperatures of 750°F in organic media. A process has been developed and tested for the fabrication of an extended-surface tubular fuel element, which is an advanced element design. Hot isostatic pressing has proved successful for the metallurgical bonding of the components for such elements, and the use of infrared tech-

niques has shown the greatest promise for the nondestructive testing of these bonds.

The goal of 3000 Mwd/ton for the average life of the uranium-metal fuel elements is a relatively low one, but the chance of exceeding it by a large margin seems to depend on the use of a higher percentage of alloying material. The economic attractiveness of this approach would depend on how much additional alloying material would be required and would involve a balance between the advantages of longer fuel life and the disadvantages of increased parasitic absorption of neutrons. The major economic advantages of long fuel life are reductions in the fuel cost components due to fuel fabrication costs and chemical processing costs. Of these, the latter are nearly inversely proportional to the fuel life, as measured in megawatt days per ton, for large-volume processing of slightly enriched fuels. For a given type of fuel element, the fabrication cost is also inversely proportional to the megawatt days per ton, but the proportionality factor may be quite different for fuels of different types. For example, there is no reason to presume that the cost of fabricating a pound of uranium-metal fuel would be the same as the cost of fabricating a pound of uranium oxide fuel because not only are the densities of the materials quite different but the degree of subdivision of the fuel and the manufacturing processes differ widely also. These rough generalizations do not specify a minimum acceptable life for fuel of a given type, but it is evident that the problem of fuel life is sufficiently important to stimulate the search for other fuel materials as alternates for uranium-metal alloys. Reference 5 is a survey of possible dispersion type fuels for this application.

Although a number of dispersions appear to be of interest, present information does not seem to single out one as the outstanding candidate. Those presently considered to be most promising are listed, with some comments, in Table X-2. They have been arranged in four groups, and the characteristics of the groups are well summarized by the following quotation from the reference:[5]

> Group I: Aluminum and magnesium matrix elements are listed under Group 1 of Table X.[*] Such fuel elements would be characterized by a ductile but structurally weak diluent and a strong brittle dispersed phase. The primary disadvantages of these elements are the low melting point and low strength of the matrix materials. Fortunately, both aluminum and magnesium have high thermal conductivities, and this in part offsets the two disadvantages mentioned.
>
> Group II: Zirconium and columbium matrix elements are listed under Group II of Table X.[*] Dispersions of this type are characterized by a moderately strong and ductile matrix and a strong brittle dispersed phase. The good high-temperature

Table X-2 COMPARISON OF MOST PROMISING DISPERSIONS*[5]

Diluent	Dispersant	Fuel,† g of U per cm^3	Remarks
		Group I	
Al or APM	UC	3.24	ΔF favors reduction of UC
Al or APM	UN	3.48	ΔF favors UN slightly
Al or APM	U_3Si_2	2.83	No Al-Si compound for Si
Mg or Mg alloy	UAl_2	1.66	No ΔF data available
Mg or Mg alloy	UC	3.24	ΔF favors UC strongly
Mg or Mg alloy	UN	3.48	ΔF favors UN
		Group II	
Zr or Zr alloy	UC	3.24	ΔF favors reduction of UC
Zr or Zr alloy	UO_2	2.40	ΔF favors reduction of UO_2
Zr or Zr alloy	U_3Si_2	2.83	No ΔF data available
Cb	UC	3.24	ΔF favors reduction of UC
Cb	UO_2	2.40	
		Group III	
Be	UAl_2	1.66	No Be-Al compound for Al
Be	UC	3.24	Be-UC reaction of 600°C
Be	UN	3.48	ΔF favors reduction of UN
Be	UO_2	2.40	Be-UO_2 reaction at 600°C
Be	U_3Si_2	2.83	No Be-Si compound for Si
		Group IV	
Graphite	UC_2	2.65	Compatible
Graphite	UO_2	2.40	UO_2 reduction at 1200°C

*See W. C. Hayes, Review of the Proposed Matrix Fuel-Element Development for AOMR, Report TDR-4664, Nov. 17, 1959.

†25 vol.% dispersant, 75 vol.% matrix.

*Table X-2 in this Review.

strength and the small likelihood of catastrophic melting are two major advantages of such systems. Columbium does not have an exceptionally low absorption cross section, and this fact alone may rule the material out as a matrix material.

Zirconium will require a completely reliable cladding material because of its poor corrosion resistance to the organic coolant (see Table II).[*] The use of zirconium cladding over a zirconium matrix element will be dependent upon the development of a zirconium alloy or diffusion coating which will be compatible with the coolant.

Thus far, compatibility studies of columbium with organics have not been made. Use of stainless-steel cladding on either columbium or zirconium would present bonding problems.

Group III: Beryllium matrix fuel elements are included in Group III of Table X.[†] Fuel elements of this type would be composed of a moderately strong brittle matrix and a strong brittle dispersed phase. The high strength and melting point of beryllium make it attractive for AOMR operations. The fact that it is so brittle may be detrimental.

Beryllium shows very good compatibility with organics. Claddings for beryllium elements have not been definitely established. Roll-cladding of several different materials on beryllium has formed hard brittle diffusion products at the beryllium interface, resulting in bond weakening [Report BMI-728].

Group IV: Graphite matrix fuel elements are listed in Group IV of Table X.[†] Such systems are characterized by a relatively brittle nonmetallic matrix and a strong brittle dispersed phase. Graphite is attractive because of its good high-temperature strength and good thermal-conductivity properties. Unfortunately, the material is brittle and does not retain fission products. Corrosion resistance in organic coolants will probably be good [Report HW-55516].

By cladding the graphite element, the effects of both brittleness and poor fission-product retention will be minimized. The choice of cladding materials, of course, will be dictated by such factors as internal pressure to be sustained and compatibility with organics. Cladding studies have been made for gas-cooled-reactor applications and should be no problem in AOMR work.

The uranium density in the dispersion (grams of uranium per cubic centimeter of fuel), listed in Table X-2, is an important quantity because it determines the enrichment requirement of the fuel. In an appendix, reference 5 lists the required enrichments for most of the dispersants, on the assumption that the volume density of U^{235} in the fuel element is the same as that in 2 per cent enriched uranium–3.5 wt.% molybdenum metal. The required enrichments range from about 7 per cent to about 21 per cent. This evaluation is, of course, a very rough one because many other factors enter to determine the required enrichment. It does, however, point up the fact that the attainment of sufficiently high uranium density for good neutron economy may be a serious problem with dispersion fuels.

*This table is not included in this Review.
†Table X-2 in this Review.

References

1. R. O. Williams, Jr., and R. F. Wilson, A Summary of Nuclear Calculations for the Organic-Moderated Reactor Experiment (OMRE), USAEC Report NAA-SR-4066, Atomics International, May 15, 1960.
2. T. J. Connolly, Plutonium-Enriched OMR Cores, USAEC Report NAA-SR-4812, Atomics International, May 1, 1960.
3. E. B. Baumeister and J. D. Wilde, Selection of the Piqua OMR Fuel Element, USAEC Report NAA-SR-4239, Atomics International, Mar. 15, 1960.
4. M. H. Binstock, Fuel-Element Development for Piqua OMR, USAEC Report NAA-SR-5119, Atomics International, June 30, 1960.
5. J. Kroehler, Jr., Dispersion Fuels for Advanced Organic-Moderated Reactor, USAEC Report NAA-SR-5018, Atomics International, June 30, 1960.

Section XI

GAS-COOLED REACTORS

The Experimental Gas-Cooled Reactor

The EGCR is an experimental reactor which will produce 22 Mw of electric power for the local grid and which contains several experimental through loops for in-pile testing of reactor fuels and structural materials.[1]

The reactor core is a vertical, cylindrical, graphite structure, with vertical channels for the fuel, control rods, and experimental loops, and with other miscellaneous channels. Each active fuel channel is filled with six 29-in.-long fuel assemblies, each of which consists of a cluster of seven stainless-steel-clad fuel rods containing slightly enriched UO_2 pellets.

The reactor coolant is helium gas at a nominal pressure of 300 psi. It enters the bottom of the reactor at 510°F and leaves the top at 1050°F. The coolant then flows to two separate loops, each of which contains its own heat exchanger and blower. In the heat exchangers, steam is generated and superheated to 900°F at 1300 psi. The steam plant is of conventional design, including a single-pressure, nonreheat steam turbine and a 3600-rpm generator which generates gross power of 29.5 Mw(e).

The design of the EGCR plant and the associated research and development program are being performed under the combined efforts of Kaiser Engineers Division of the Henry J. Kaiser Company, the Nuclear Power Department of the Allis-Chalmers Manufacturing Company, and the Oak Ridge National Laboratory (ORNL).

The design of the EGCR prototype plant is nearly complete, and construction is in the early stages. Ground was broken in August 1959 on the Gallaher Bend site, which is located within the Oak Ridge, Tenn., AEC area. The electric power generated will be distributed through the local TVA power system. Construction of the EGCR plant as of Oct. 1, 1960, was about 13 per cent complete and was on schedule. The first stage of the containment shell has been erected, and foundation concrete within the shell was being poured. Initial criticality is scheduled for December 1962, and full-power operation is scheduled for March 1963.

The EGCR type reactor draws heavily on the technological background developed by the British and French in their gas-cooled-reactor programs. Specific aims of the EGCR project are to advance this technology to include the use of UC_2 fuel and to increase operating temperatures so as to enable the use of modern steam-plant equipment. The research and development programs associated with the EGCR project are intended not only to solve the immediate problems of the prototype design but also to try to improve the performance of future similar reactors.

A major portion of the research and development effort under the EGCR project is being performed by ORNL and is reported in references 2 and 3. The development of a satisfactory fuel assembly and related research and development are receiving particular attention by ORNL. In the course of developing a suitable fuel assembly, experiments on heat transfer, coolant-gas flow, structural integrity, materials compatibility, and fission-gas release have been and are being performed. The first EGCR fuel will probably be clad in stainless steel, but experimental programs are under way to determine the suitability of other cladding materials, such as ceramics and beryllium, which may have improved operating characteristics. The Title-II design of the EGCR fuel assembly has been completed; an assembly drawing is shown in Fig. 17.

Several alternate designs for the top and bottom spiders and the intermediate spacers for

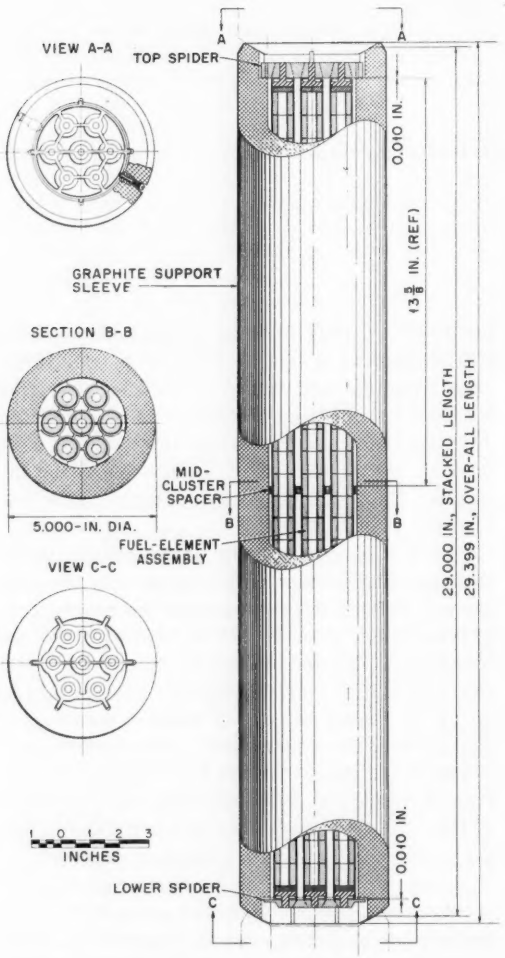

Figure 17—EGCR Title-II fuel-element assembly.[3]

the EGCR seven-rod cluster fuel assembly have been considered. The original H-shaped top and bottom spiders were found to cause serious maldistribution of coolant flow. The current Title-II design of the EGCR fuel assembly utilizes more symmetric end spider designs which, experiments have shown, give more uniform coolant-gas distribution.

The EGCR reactor core and fuel assembly design does not provide for rotational alignment between adjacent fuel clusters in a process tube. The relative location of the fuel rods in adjacent clusters is, rather, completely random. The effect of relative orientation of adjacent clusters on coolant-gas flow and heat transfer has been studied by means of mass-removal experiments with naphthalene-coated rods.

The ORNL fuel development program includes quite an extensive in-pile capsule test program. Fission-gas release data obtained from this program indicate that the fraction of fission gas released from the UO_2 increases substantially at temperatures above 2900°F, thereby verifying the previously reported Canadian fission-gas release data which indicate that almost 100 per cent release will occur at temperatures above the UO_2 grain-growth temperature. This UO_2 grain-growth temperature is in the range 2900 to 3100°F, much below the 5000°F UO_2 melting temperature previously thought to define the onset of rapid fission-gas release.

The in-pile capsule tests are also being used to investigate the dimensional stability and mechanical behavior, under operating conditions, of 95 per cent dense UO_2 pellets having an annular cross section. Important questions are whether a core of inert material must be included to prevent the thermally cracked UO_2 pellets from breaking up and falling into the core space and, if such a filler material must be provided, what material will be compatible with the UO_2 at the very high temperatures of operation. Tests have indicated that, although the UO_2 pellets will probably crack when subjected to thermal gradients, they remain in relatively large sections. Furthermore, the powder and the fines created during cracking are insignificant, and there is no shifting of material into the core of the pellet stack. It may therefore be possible to leave the pellet core as a void and thereby provide a relatively large volume within the fuel cladding for any fission gas that is released.

The fuel development program for the EGCR is looking ahead toward developing more advanced reactor core materials than those which will be utilized in the first EGCR core. This includes some work on UC, siliconized silicon carbide coatings, and other ceramic fuels, but a major amount of effort is being placed on the development of another metallic cladding, beryllium.

Beryllium tubing has been purchased from several vendors, both domestic and foreign, and is currently being evaluated. Other testing with beryllium includes corrosion testing, compatibility tests, development of brazing and welding techniques, and the investigation of irradiation properties. The fusion welding of beryllium

using an edge weld is currently favored by ORNL for the cladding tube to end-cap closure.

A high-temperature beryllium irradiation experiment in the Oak Ridge Research Reactor (ORR) was terminated after a fast-neutron exposure of 7×10^{19} neutrons/cm^2. The planned exposure was 10^{21} neutrons/cm^2, but the experiment had to be terminated early because of the failure of furnace heating circuits. The purpose of this experiment was to investigate the irradiation properties of beryllium in general but particularly to determine whether the helium atoms produced by the reactions of beryllium with gamma rays and fast neutrons would cause the beryllium to swell. Density measurements made on the irradiated beryllium specimens in this test showed that swelling of from 1.5 to 5 per cent occurred. The apparatus was modified, and a second test is currently under way to check these results.

Because the EGCR will also be an experimental reactor, a great variety of combinations of experiments, in which each of the eight experimental loops can add or subtract a varying amount of reactivity, must be considered. ORNL is conducting a series of two-group two-dimensional computer calculations to determine the nuclear physics characteristics that will be associated with the loadings in these experimental loops. The effect on the reactor flux and power distributions is of particular concern.

Design and Testing of Large Gas Ducts

The gas-cooled commercial power reactors designed in Great Britain all have essentially the same features of station layout, namely, a central pressure vessel, containing the core, connected by large gas ducts to the several smaller heat exchangers used in the production of steam. This ductwork must be designed to meet stringent requirements of safety, flexibility, leaktightness, and pressure drop. Reference 4 reviews the various methods of obtaining flexibility and evaluates each with regard to the above requirements. A partial summary of the reference is given below.

There seem to be four practical solutions to the problem of providing large ducts with flexibility. They are:

1. Short-radius mitered ("lobster back") bends on single large-diameter ducts.
2. Mitered bends on two or more smaller diameter ducts in parallel for each heat-exchanger circuit.
3. Corrugated ducts.
4. Single large-diameter ducts with three tied expansion bellows in each line of ducting.

In the case of large ducts, the most common provision for differential expansion is the use of a number of short-radius mitered bends in the line. However, even though a large amount of theoretical and experimental work has been carried out on pipe bend flexibility and stress distribution, most of the work was performed on small-diameter pipes with large thickness-to-diameter ratios rather than on large-diameter ducts. Further experiments are needed to validate an extrapolation of this information to ducts with a thickness-to-diameter ratio in the range of 1 : 100 to 1 : 150.

A design with short-radius flexible bends is attractive because of its simplicity and because of the low initial cost of the ducting. A technically feasible design for gas-cooled-reactor ductwork is thought to be possible within the limits of knowledge of the behavior of short-radius pipe bends. At the same time, however, this approach requires a complicated duct layout with a large number of pipe bends which would increase other components of the plant cost and which would lead to other economic losses because of the higher coolant pressure drop.

Multiple small-diameter ducts are attractive because their increased flexibility means that they will exert much smaller thrusts upon reactor components than will single large-diameter ducts, whereas the pressure drop may be about the same in the two cases. The main disadvantage of this scheme is the increased cost that results from duplication of equipment.

Corrugated ducts offer another solution to the flexibility problem. However, even though flexibility on large ducts can be increased 20-fold by corrugations, many serious disadvantages exist in this design. Internal gas pressure tends to stretch the corrugations, thus increasing the total movement which must be absorbed in the duct system. Significant bending stresses also occur which give rise to a creep problem. Pressure drop over a given length of corrugated duct is 8 to 10 times greater than that in a smooth pipe of the same diameter.

A fourth design possibility is the use of large-diameter ducts with tied expansion bellows. This design requires the least space and has the smallest pressure drop. The reduced costs of construction and of blower power are considered to easily outweigh the cost of the expansion bellows. The surplus flexibility which usually accompanies bellows design gives extra protection to the reactor vessel against unforeseen thrusts which result from errors in erection of ductwork, differential settlement of the plant foundations, and maloperation of the plant. However, because bellows become so highly stressed during operation, they can be a serious source of weakness in a pressure circuit unless they are designed with extreme care. Expansion bellows are used in the ducts of all British gas-cooled reactors in service or presently under construction.

The reference[4] points out that the majority of manufacturers of thin-walled commercial bellows recommend their products as being suitable for service under conditions so severe that their materials are subject to stresses which bring them well into the plastic range. Although these bellows normally perform well, it is questionable whether such high design stresses should be used in reactor work, where the consequences of failure may be quite serious. The reference recommends that for this service the total stress in the convolution wall should not exceed the 0.5 per cent proof strength or the yield point of the material. The value of the applied stress must be obtained by calculation, using formulas with empirical constants derived from strain-gauge tests on the particular type of convolution under consideration.

During the design of the Bradwell plant, a full-size prototype bellows joint was built and subjected to the following proof tests:

1. Standard hydrostatic test (1.5 × design pressure + 50 psi).
2. Tilting test to determine the moment of resistance of the bellows unit.
3. Cold tilt test under design pressure. Strain measurements were made on the internal and external surfaces of the convolutions and at many places on the adjacent ductwork.
4. Fatigue test to 10,000 cycles at the design pressure and temperature, with a tilt per convolution of ±0.0015 radian.
5. Pressurization to four times design pressure, with strain measurements being taken at the bellows convolution and at other highly stressed points.
6. A simulated brittle failure of the tongue, under design gas pressure, with measurement of transient strains in tie bars and their brackets.*

The valve requirements in gas-cooled-reactor systems are also reviewed in the reference.[4] Specifications of the Bradwell design for 60-in.-diameter valves include the following:

1. Valves are to be fabricated of mild-steel plate.
2. Materials which are incompatible with the fuel cladding material or which become highly radioactive are not to be used in the valves.
3. Valves must give trouble-free service without maintenance for 20 years.
4. No lubricants are to be used on bearings that are in contact with the gas stream.
5. Valves must be capable of giving absolute closure against a pressure difference equal to the design pressure both in the cold condition and in the hot condition at the design temperature. (This requirement was later relaxed to permit a small amount of leakage.)
6. Leakage rate of gas from valve glands to the atmosphere must not exceed 15 standard cu ft/day during the life of the plant.
7. Pressure drop across a valve in the fully open position is not to exceed one-third of a duct velocity head.
8. Valves must be capable of being closed in less than 10 sec against a pressure difference of 1 atm.

The butterfly valve chosen for this service is closed by means of two independent motions. The valve disk is first turned into the closed position, and it is then translated onto the valve seat by means of a pair of eccentric bushes in the valve trunnions. When tested, the valves gave leakage rates ranging from 0.4 to 0.7 standard cu ft/hr when at 400°C with a pressure difference of 10 atm across the disk. The combined leakage to the atmosphere from the three glands on the valve is less than 4 standard cu ft/day.

*The tongue is the flexible member, inside the bellows, which ties the two ends of the ductwork together mechanically through the bellows. It takes the axial thrust due to gas pressure, while allowing angular flexure. The tie rods are not normally under substantial tension but must take over if the tongue should fail.

The reference contains further discussion of duct design, installation, and testing, in considerable detail, with the design of the Bradwell station as the focal point.

References

1. Kaiser Engineers Div. of Henry J. Kaiser Co. and Nuclear Power Dept., Allis-Chalmers Mfg. Co., Experimental Gas-Cooled Reactor: Preliminary Proposal, USAEC Report AECU-4701, August 1959.
2. Oak Ridge National Laboratory, Gas-Cooled Reactor Project Quarterly Progress Report for the Period Ending March 31, 1960, USAEC Report ORNL-2929, June 30, 1960.
3. Oak Ridge National Laboratory, Gas-Cooled Reactor Project Quarterly Progress Report for the Period Ending June 30, 1960, USAEC Report ORNL-2964, Aug. 22, 1960.
4. A. T. Bowden and J. C. Drumm, Design and Testing of Large Gas Ducts, *J. Brit. Nuclear Energy Conf.*, 5(2): 49–63 (April 1960).

Section XII

BOILING-WATER REACTORS: SL-1

The Stationary Low-Power Plant No. 1 (SL-1), formerly called the Argonne Low-Power Reactor (ALPR), was designed and constructed by Argonne National Laboratory (ANL) under the auspices of the Military Reactors Branch of the USAEC and the U. S. Army. Reference 1 is an account of the equipment installation, reactor assembly, reactor zero-power experiments, plant startup, and plant performance tests for this installation. Included are descriptions of selected items of equipment and the techniques and procedures used in their assembly and test, resumés of the malfunctions encountered, their causes and the corrective measures taken, and some test results and operating data.

The SL-1 facility is a prototype of a plant for use in remote arctic locations for military applications. The reactor is a direct-cycle light-water-moderated and -cooled boiling-water type rated at 3 Mw(t).

The reactor core is contained in a steel pressure vessel (about 4 ft 8 in. in inside diameter) and is designed to operate at 300 psig. The core is approximately 20 in. in diameter and is composed of 531 aluminum-uranium metallic fuel plates arranged in 59 assemblies. Control is achieved by the vertical motion of a maximum of five cruciform-shaped rods and four T-shaped rods. Each rod is equipped with a rack-and-pinion type drive mechanism mounted on the upper head of the pressure vessel.

The pressure vessel is insulated and mounted within a steel shield tank that is enclosed by a boral and lead thermal-neutron shield. The vessel and shield tank are, in turn, mounted on concrete piers that penetrate the floor of a steel building about 60 ft in diameter and 85 ft high. The top of the vessel and tank terminate at the operating floor, located about 25 ft above the base of the building. Radial biological shielding is provided by filling that portion of the building which lies below the operating floor with gravel after installation of the shield tank. The top biological shield consists of a concrete, steel, and masonite top hat mounted on the operating floor immediately above the shield tank.

The power-generation equipment is housed within the reactor building and is designed to produce a maximum of 360 kw(e). In addition, 400 kw(t) is provided for space heating. The turbine exhausts to air-cooled condenser banks mounted on the exterior surface of the building.

The reactor- and power-generating equipment are provided with the usual auxiliary systems, instrumentation, and controls. The entire facility, including the auxiliaries, is operated from a central control room located adjacent to the reactor building.

The plant was released to the designer (ANL) on July 3, 1958, for installation of all remaining components, systems testing, initial startup and power operation experiments, and plant performance tests. These tasks were accomplished, and the plant was released to the operating contractor, Combustion Engineering Nuclear Division, on Feb. 5, 1959.

The major equipment components installed were the reactor core structure, control rods and the control-rod drives, reactor top shielding, and some reactor instrumentation. Installation of these consumed about five weeks and was accomplished without incident. Concurrently, preliminary tests were conducted on all plant systems. These included flow investigations, cleanup, and some equipment performance tests. The major difficulties encountered during the systems tests were associated with the primary-purification-system resin removal, the turbine, and the oil leakage from the deep-well pump.

The difficulty experienced during resin removal resulted from excessive pressure build-

up in a flexible hose connecting the resin columns to the waste system. Replacement of the flexible hose with steel pipe corrected the malfunction.

A number of problems were encountered in the turbine. First, a minor misalignment, probably caused by shield placement subsequent to setting of the turbine-generator set, necessitated realignment of the turbine and generator. Second, the main reduction gear thrust-bearing faces were found to be out-of-tolerance and required remachining. Third, the turbine steam drains were improperly installed and were not provided with individual isolating valves. These defects permitted steam to bypass the governor valve and resulted in overspeeding of the turbine. Modification of the drain piping corrected the malfunction. Fourth, the main and auxiliary pump check valves were found to have been interchanged during installation at the factory, causing the auxiliary oil pump to idle in reverse. Also, the air-cooled turbine oil cooler was found to have been installed in the inverted position, thereby entrapping air in the cooler and reducing cooler efficiency. These deficiencies were corrected, and a successful turbine test was accomplished.

During the plant performance test, the life of the second charge of primary-purification-system resins was drastically reduced. Upon examination, the resins were found to be badly fouled with oil. This oil was traced to the oil-lubricated bearings of the deep-well pump. The resins were subsequently changed, the reactor water was cleaned up, and a recommendation was made to replace the original deep-well pump with one using water-lubricated bearings.*

The zero-power experiments were conducted in the SL-1 facility from Aug. 11 to Oct. 9, 1958, following the preliminary systems tests. The experiments consisted of the initial criticality and of both the hot and cold critical experiments for the expected operating loading. The initial criticality was obtained with 10 fuel assemblies in the central core lattice positions. Two operating loadings were investigated, one with 40 assemblies and the other with 59 assemblies. Relative control-rod worths were evaluated for all loadings. Experiments were also conducted to determine the relative worth of the burnable poison strips (boron) attached to some of the fuel assemblies. Flux maps, using gold wires, were obtained for both the 40- and 59-assembly cores. Although a complete list of the experiments performed is contained in reference 1, neither the techniques used nor the specific measurements made are given. These details will be found in reference 2.

The power operation experiments were accomplished during the period Oct. 11 to Dec. 11, 1958. Full power was achieved on Oct. 28, 1958. During these experiments, the following items were investigated:

1. A complete checkout of the steam and feedwater system, including all the required instrumentation calibrations.
2. The operation of all safeties was tested, including safety valves, high- and low-pressure trips, temperature trips, water-level trips, and over-power trips.
3. The calibration of control rods as a function of temperature and steam flow was determined.
4. The effects of feed-water and steam-flow transients upon reactor power were investigated.
5. The calibration of both steam bypass valves was accomplished.
6. The automatic power-demand control system was operated, and the optimum travel ratio and dead band width were determined.
7. The turbine-generator was tested for voltage and frequency regulation under load change.
8. The effectiveness of the biological shielding was determined by plant radiation surveys made at various reactor and steam-plant power levels.
9. The performance of the plant was demonstrated under simulated operating conditions during the period Nov. 19 to Dec. 11, 1958.

The techniques and results of all measurements are not given in reference 1. However, sufficient information is presented, in the form of plant operating records, to make the data useful for those interested in the details of the plant characteristics. The data consist of reproductions of selected plant operating logs, recorder charts for both the reactor and steam plant, tabulated results of radiation surveys, and the results of water chemistry investigations. Included in the latter information is the effect of hydrogen addition both on dissociated

*Editor's Note: After the operation contractor assumed operation of the plant, extensive oil contamination of the fuel-element heat-transfer surfaces and primary system was discovered. Thorough cleaning of these components and systems was required before reactor operations were resumed.

oxygen levels within the primary system and on the radiation levels exhibited by this system.

References

1. E. E. Hamer, ed., Initial Testing and Operation of the Argonne Low-Power Reactor (ALPR), USAEC Report ANL-6084, Argonne National Laboratory, December 1959.

2. D. H. Shaftman, Argonne National Laboratory. (Unpublished)

Section XIII

NUCLEAR SUPERHEATER: BORAX-V

Brief descriptions of the experimental reactor BORAX-V have been given in the Argonne National Laboratory annual report[1] for 1959 and in papers at the Chicago meeting of the American Nuclear Society.[2,3] A preliminary design and hazards report has been issued.[4] BORAX-V is a modification of and an addition to the BORAX-IV plant. It will have a nominal design thermal capacity of 20 Mw and an operating pressure of 600 psig; the nuclear superheater section will yield steam at a temperature of 850°F. The reactor is scheduled for criticality in early 1961 and for operation as an integral superheater by mid-1961. A cutaway drawing of the reactor is given in Fig. 18.

Three separate core configurations are to be possible in the reactor: a pure boiler core without superheater, a boiler-superheater core with the superheater section at the center, and a boiler-superheater core with the superheater at the periphery. Operation will be possible with both natural and forced circulation of the water. The fuel assemblies are all square in cross section, the boiler assemblies being made up of rods composed of slightly enriched UO_2 in steel jackets and the superheater assemblies being composed of thin UO_2–stainless steel cermet plates. Each superheater assembly contains 20 fuel plates which are grouped into five subassemblies, each containing four fuel plates and each separated from its neighbors by a water-filled moderator channel. A 30-mil static steam space is provided as thermal insulation between the plate subassembly and the surrounding water moderator. The steam is superheated in two passes through superheater assemblies. Each superheater assembly is provided with a steam pipe which leads up to the steam space near the top of the reactor vessel. The pipes to half of

Table XIII-1 DESIGN CHARACTERISTICS OF BORAX-V

Operating pressure, psig	600
Maximum steam temperature, superheated, °F	850
Maximum steam temperature, saturated, °F	489
Nominal design full power, Mw(t)	20
Maximum plant capacity, Mw(t)	40
Percentage of heat to steam production	83
Percentage of heat to superheating	17
Core height, in.	24
Core effective diameter, in.	39
Total number of fuel assemblies	60
No. of superheater fuel assemblies:	
If superheater is centrally located	12
If superheater is peripherally located	16
Dimensions of fuel assembly active region, in.	4 × 4 × 24
No. of cruciform control rods	5
No. of T-shaped control rods	4
Design maximum temperature, superheat fuel plate, °F	1200
Design maximum temperature, boiler fuel rod center, °F	3800
Water recirculation	Forced or natural
Steam flow through superheater	Two pass
Forced-circulation system flow, gal/min	10,000
Average power density at 20 Mw, kw/liter of core:	
Boiler zone	95
Central superheater zone	80
Boiler fuel:	Rods, UO_2 in 15-mil, 304 stainless-steel jackets
Rod diameter, in.	0.375
No. of rods per assembly	49
Superheater fuel:	Plates, highly enriched UO_2 in 304 stainless-steel cermet
Plate thickness, in.	0.030
Plate spacing (coolant channel), in.	0.062
No. of plates per assembly	20

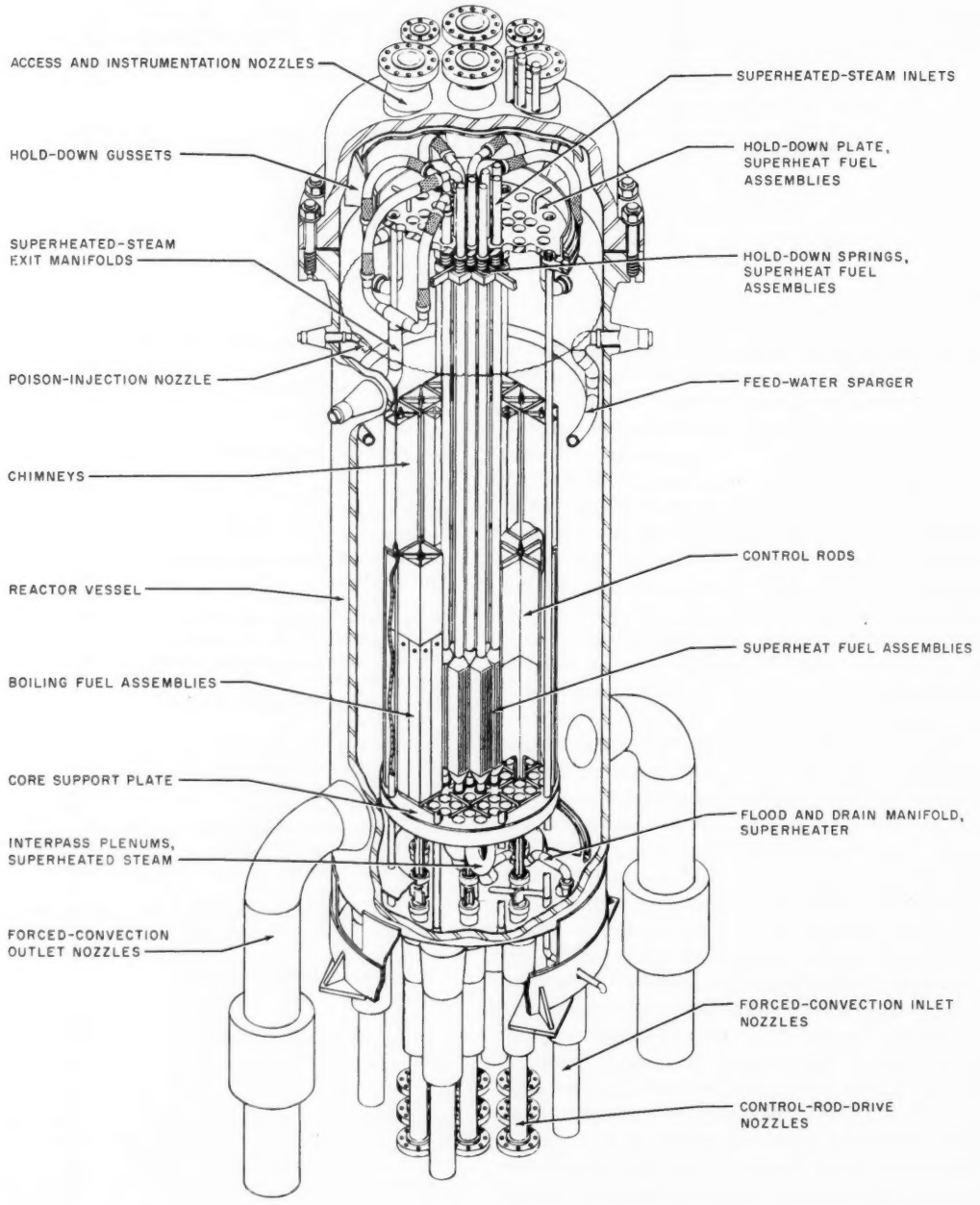

Figure 18 — Reactor with central superheater: BORAX-V.[4]

the assemblies are left open as inlets for the saturated steam. This steam flows downward through half of the assemblies into a plenum at the bottom of the reactor vessel where it is distributed to the remainder of the superheater assemblies and passes upward through them to an exit manifold at the top of the vessel.

The reactor is controlled by nine bottom-driven control rods made of boral clad with X-8001 aluminum. Five of the rods are cruci-

form, and four, located near the core boundary, are T-shaped.

The main design characteristics of the reactor are summarized in Table XIII-1.

References

1. Argonne National Laboratory, Annual Report 1959, USAEC Report ANL-6125.
2. R. E. Rice, BORAX V, An Integral Boiling-Superheating Reactor, *Trans. Am. Nuclear Soc.*, 3(1): Paper 4-6 (June 1960).
3. R. A. Cushman, Thermal Design of an Integral Nuclear Superheater Core for BORAX V, *Trans. Am. Nuclear Soc.*, 3(1): Paper 4-7 (June 1960).
4. Argonne National Laboratory, Preliminary Design and Hazards Report. Boiling Reactor Experiment V (BORAX V), USAEC Report ANL-6120, February 1960.

Section XIV

NEW REACTOR TYPES

The Spray-Cooled Reactor

Spray evaporation of water is a method being considered for reactor cooling in which a mixture of water and steam is injected into fuel channels. This system is therefore different from other systems wherein only water or steam is injected into fuel channels. Two groups are studying spray-cooled reactor systems. In Italy, the CISE Laboratories, in conjunction with Ansaldo (an Italian engineering firm) and Nuclear Development Corporation of America, are studying and conducting tests to determine the feasibility of the concept for a power reactor, under a contract within the framework of the U. S.–Euratom agreement.[1] In the United Kingdom, a UKAEA group at Risley has conducted a limited study of a small reactor, and another UKAEA group at Harwell is conducting tests on the heat-transfer and fluid dynamic characteristics of the system.

In the reactor core the spray-cooled system utilizes a thin film of water on all fuel-element heating surfaces together with wet steam flow through coolant channels between fuel-element heating surfaces. The water film thickness is maintained at about 0.005 in. by steam-entrained water droplets which are deposited at about the same rate as water is removed from the film by evaporation and disruption of the film into spray. Steam quality, defined as the ratio of steam flow to total mass flow, is maintained at about 20 wt.% at the coolant channel entrance by injecting water and steam into the coolant channel. Quality at the exit of the coolant channel is about 60 wt.% steam. Fuel cladding temperatures are maintained very close to the saturated-steam temperature.

The spray-cooled system was originally proposed as a means for avoiding the characteristic power fluctuations which were thought to limit the power density of boiling-water reactors.[2] In the spray-cooled reactor concept, there is no power coefficient of reactivity which results from steam voids as there is in boiling-water reactors. Since the amount of coolant water in the core is small, normal variations in water flow should have only a small effect on reactivity. Further, because of the small amount of coolant water within the core, the opportunity exists for achieving a low-enrichment reactor, provided that low-absorption materials can be used for moderator and structure. Heavy water is being considered for the moderator, with light water for the spray coolant. The use of H_2O coolant with a low-absorption moderator poses the usual problem of a reactivity increase in case of loss of the H_2O coolant. Reference 1 cites an estimated case for a reactor 15 ft in diameter operating at 1500 psi with a mean coolant density of 30 wt.%. Complete loss of coolant was estimated to increase reactivity approximately 1 per cent. It is stated that, although a reactivity increase of this amount might be safely accommodated by control-rod action plus the fuel temperature coefficient of reactivity, the problem can be reduced by undermoderating the reactor. This, in general, would mean a fuel-moderator ratio lower than that giving maximum reactivity, a consequent increase in the enrichment requirement, and probably an increase in neutron economy.

The concept of spray cooling, at least at its present stage, requires the injection, separately, of steam and water into the inlet of each coolant channel and the production of saturated steam. A number of the reactor concepts, however, consider the superheating of this steam in other fuel-coolant channels which are essentially gas-cooled channels. In any case a basic decision that must be made in the design of the spray-cooled system is how to provide the steam

for injection at the required inlet pressure. The pressure can, of course, be supplied by a blower, but in those designs which provide for a substantial degree of superheating, a more attractive solution may be to use a small portion of the superheated steam as the heat source for a separate steam generator which produces saturated steam at a higher pressure for injection purposes. The quantity of steam required for injection can be reduced by the use of a multipass design.

As reported in reference 1, the Italian design concept is embodied in a natural-uranium-metal-fueled reactor with the D_2O moderator. The reactor is of the pressure-tube type with the moderator contained in a calandria tank and with thermal insulation between pressure tube and moderator provided by an air gap between the pressure tube and the calandria tube. The design is for a thermal output of 714 Mw. The fuel, uranium–2 per cent zirconium alloy clad with Zircaloy, is annular in shape. Two configurations are considered: a cluster of seven small annuli within the pressure tube, with each annulus surrounded by a Zircaloy guide tube to form a coolant passage (see part *a* of Fig. 19) and a coaxial arrangement of two larger fuel annuli about a central Zircaloy rod (see part *b* of Fig. 19). The operating pressure is 800 psi; the steam quality is 20 per cent at the coolant-channel inlet and 60 per cent at the exit. Steam circulation is accomplished by a blower. No superheater section is provided; the outlet steam-water mixture is separated in a steam drum, and the saturated steam is fed directly to the turbine.

The British design study is for a small power reactor or reactor experiment with outputs of 30 Mw(e) and 85 Mw(t) developed from 64 fuel channels. Multipass steam flow is used, and a superheater section is provided. The steam makes three passes through the spray-cooled elements and one pass through the superheated elements. Steam conditions at the turbine are 615 psi and 850°F. The fuel is uranium dioxide. One of the fuel-element designs considered is of the "heat-exchanger" type. The fuel assembly consists of a Zircaloy calandria can containing 19 calandria tubes in a hexagonal pattern. Each tube runs through the center of a stack of hollow hexagonal UO_2 pellets. The spaces between the pellet cluster and the outer wall of the can are filled with graphite powder (see part *c* of Fig. 19). The reactor is of the pressure-tube type with the D_2O moderator contained in a calandria tank. Stainless-steel-jacketed elements are used in the superheater section.

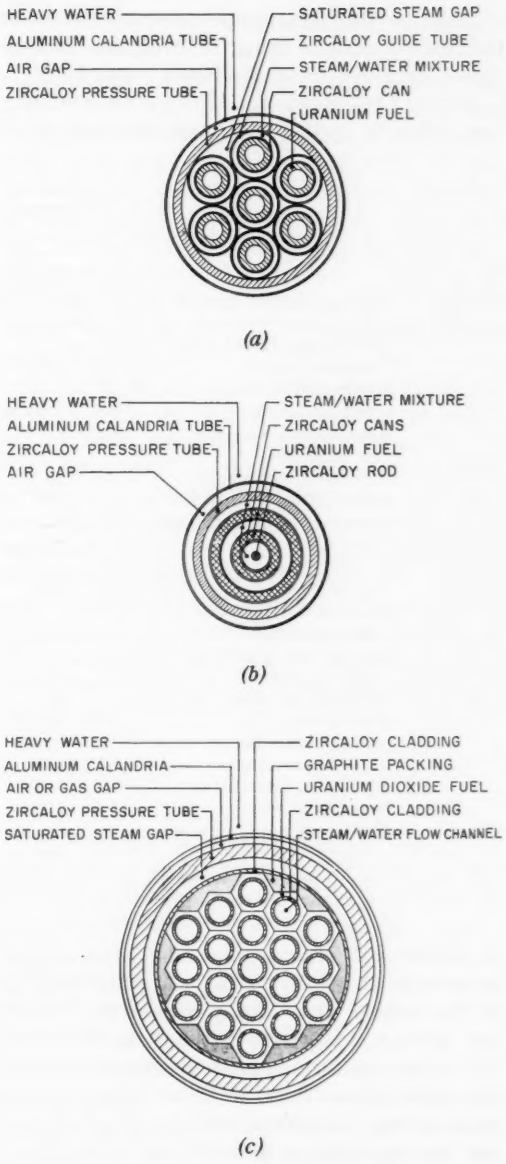

Figure 19—Spray-cooled fuel elements.[1] (*a*) CISE fuel element, design A. (*b*) CISE fuel element, design B. (*c*) UKAEA fuel-element design. (Reprinted by permission from *Nuclear Power*, Rowse Muir Publications, Ltd., London.)

Some of the informative characteristics of the reactor designs using the three fuel-element types described above are listed in Table XIV-1.

Although the spray-cooled reactor has in common with the boiling-water reactor the feature of steam production within the reactor and the consequent possibility of feeding steam directly to the turbine, it is hardly reasonable to make any further comparison between the two types. The spray-cooling concept is being considered for applications that are quite different from those of the conventional boiling-water reactor and for applications in which the conventional boiling-water principle might not be suitable. Hence the observation that the spray-cooling system introduces a number of new complexities and new problems is hardly pertinent as a comparative criticism.

Table XIV-1 CHARACTERISTICS OF SPRAY-COOLED-REACTOR DESIGNS[1]

Fuel-element Details	CISE Design A (part *a* of Fig. 19)	CISE Design B (part *b* of Fig. 19)	UKAEA Design (part *c* of Fig. 19)
Power output from center channel, Mw	1.36	1.67	2.5
Maximum heat flux, Btu/(hr)(sq ft)	363,000	469,000	370,000
Mass velocity of coolant, lb/(hr)(sq ft)	0.7×10^6	$1.0-1.3 \times 10^6$	1.1×10^6
Inlet quality, wt.% steam	20	20	15
Outlet quality, wt.% steam	60	60	50
Pressure drop along channel, psi	7.65	14.7	13% pass
Pumping power as percentage of thermal output	0.67	1.3	2.75
Rating of fuel (maximum), Mw/metric ton	25	25	30
Fuel lifetime (expected), Mwd/metric ton	6800		6000
Maximum fuel temp., °C	400	400	2100
Core diameter, ft	20	18	9.5
Fuel channel pitch, in.	8	8.3	9.3
No. of fuel channels	660	481	64
Axial form factor	1.302	1.249	~1.5
Radial form factor	1.263	1.159	1.88
Reactor operating pressure, psi	800	800	700

The concept appears to involve several possible problems or uncertainties. The first is the problem of actually maintaining the desired heat flow and steam-water flow characteristics, and maintaining them with sufficient reliability to make possible the desired heat fluxes, which are in the same range as those in conventional boiling-water reactors. Reference 1 states that the characteristics of the spray-cooling process are sufficiently well known to give confidence in the performance of coolant passages which have relatively simple shapes. It is the desire to retain such shapes (e.g., circular and annular) which leads to fuel-element configurations that may require considerable research and development. Thus, although some of the designs presently being considered might involve what appear to be difficult fuel-element problems, these difficulties are not necessarily inherent in the spray-cooling concept.

A second uncertainty is the degree to which solids may be deposited on the walls of the coolant channels. Reference 1 expresses considerable confidence that this problem will not be significantly different from that occurring in boiling-water reactors. The water film is expected to be maintained on the heat-transfer surfaces, and evaporation is expected to take place only from the free surface of this film. The reference cites the results of Russian work pertinent to this problem:[3]

It was remarked above that in the experiments of N. G. Patsukov and Yu. O. Novi[*] at $p = 35$ to 43 atm., the appearance of deposition over the whole circumference of the pipe was observed only at high steam contents ($x > 0.7$), when the flow rates were very high, reaching 30 m/sec, and a thin film of liquid remaining on the pipe wall could be partly detached, and the remainder be evaporated, leaving the wall bare. Naturally, at such high flow rates and steam contents, the position in space of the pipe has no particular significance, and the same phenomenon would be observed in a vertical pipe also. However, at steam contents below 0.7, uniform deposits over the whole circumference, indicating evaporation of a liquid film on the pipe wall, were not observed[3] even at heat flow above 800,000 kcal/m^2 hr.

A related question is whether there will be a problem of radioactivity carry-over in the steam. Depositions on the heat-transfer surfaces which might have insignificant effects on heat transfer could still lead to carry-over problems if they remained attached long enough to become activated and then were entrained with the steam. In the conventional boiling-water reactor, the evaporation process provides a relatively high decontamination factor which reduces the effects of any nonvolatile or soluble active materials, including fission products from defective fuel elements, that may exist in the water. Presumably the spray-cooled reactor would have a similar, but not necessarily equal, decontamination factor for the steam. This would not hold for radioactive material picked up in any superheater sections of the reactor; the same uncertainty holds for other types of direct-cycle superheater reactors.

In reference 1 it is stated that Zircaloy-2 and Zircaloy-3 appear to be suitable for use as fuel-element jackets in the spray-cooled system. If it should be found that zirconium alloys are not satisfactory for use in the system (where steam velocities apparently are much higher than in conventional boiling-water reactors, although the water film is described as a relatively slow-moving one), much of the attractiveness of the concept might be lost. It appears quite probable that Zircaloy will be satisfactory, but apparently long-term proof tests have not been made.

In addition to the reactivity effects of coolant loss, the thermal effects must, of course, also be considered. Reference 1 states that, in the event of failure of the water flow to any coolant channel, the steam flow alone will keep the temperature down to the region of 450 to 600°C and that Zircaloy may be expected to withstand this temperature for a short time. The results of stoppage of the steam injection, either with or without a concurrent loss of water flow, are not discussed.

Again it should be said that the concepts of spray cooling which have been put forward are not so much attempts to modify the concept of the boiling-water reactor as they are attempts to achieve a reactor which will give high neutron economy and high specific power and which will at least constitute a step in the production of high-temperature steam. This goal is not an easy one to attain, and, although the concept of spray cooling may involve complexities and, at the moment, uncertainties, the attainment of its objectives are certainly worth a considerable effort.

The Variable-Moderator Reactor

The Variable-Moderator Reactor concept is being investigated for the AEC by the Advanced Technology Laboratories, a division of American-Standard. A recent hazards summary report,[4] covering proposed critical experiments for the study at Battelle Memorial Institute, is of general interest because of the information it gives on the reactor concept.

The principle of this reactor concept is to arrange the fuel rods in clusters that are separated from one another by relatively wide moderator channels. The coolant water within the clusters is separated from the moderator water outside the clusters by a suitable calandria design of the core structure so that the level of the moderator water can be adjusted, independently of the coolant-water flow system, to regulate and control reactivity.

The particular embodiment of the principle described in reference 4 employs rod type fuel elements containing UO_2 of about 2.2 per cent enrichment, jacketed in zirconium tubes about 0.5 in. in diameter. The hexagonal fuel assemblies consist of 37 such fuel rods, and the as-

*N. G. Patsukov and Yu. O. Novi, Investigation of the Conditions Determining the Possibility of Deposition of Easily Soluble Salts on the Steam-Forming Part of Horizontal Pipes, in the symposium on Physico-Chemical Processes in Boilers and the Water System in High-Pressure Boilers, Gosenergoizdat, 1951.

semblies are arranged in a spaced hexagonal lattice to form a core about 6 ft in diameter. The operating pressure of the reactor would be about 600 psig, and it is stated that the concept is applicable in power ranges from 20 to 200 Mw(e).

The core structure is like a shell-and-tube heat exchanger, with the hexagonal fuel-element channels representing the tubes, and the vessel immediately surrounding the core representing the shell. This core assembly is contained within a second vessel (the reactor pressure vessel). The region between the vessels is filled with water and serves as a reflector and as a downcomer for the recirculating water. Steam condensate and makeup enter at the top of the moderator region (the region around the fuel-assembly channels) through a variable-speed water pump. The water level in the moderator region is controlled by this pump in combination with a control valve. The moderator water passes downward through the moderator space, and at the bottom it passes into a coolant inlet plenum where it mixes with water from the reflector. The water then passes upward within the fuel-element channels and boils as it cools the fuel rods. Steam is separated from the water in an upper plenum, and the water is recirculated downward through the reflector to the coolant inlet plenum.

Of course, the effect on reactivity of voiding the moderator channels will depend on, among other things, the fuel-to-water ratio in the reactor and the relative volumes of the moderator spaces and the coolant-water spaces. Theoretically, a large amount of reactivity control should be possible, but rather careful design studies and analyses are no doubt required to evaluate what the practical limits will be. The proposed critical experiments will, of course, contribute information for these analyses.

References

1. J. G. Collier and P. M. C. Lacey, The Spray-Cooled Reactor, *Nuclear Power*, 5(52): 68–73 (August 1960).
2. H. R. C. Pratt and J. D. Thornton, Spray Evaporation: A New Method of Steam Generation and Its Possible Application to Boiling Reactors, *Proceedings of the Second United Nations International Conference on the Peaceful Uses of Atomic Energy, Geneva, 1958*, Vol. 7, p. 813, United Nations, New York, 1958.
3. M. A. Styrikovich et al., On the Interrelation Between the Hydrodynamics of Steam-Water Mixtures, the Temperature Distribution in a Metal, and the Deposition of Easily Soluble Salts in Horizontal Steam-Generating Pipes, *Izvest. Akad. Nauk S.S.S.R., Otdel. Tekh. Nauk*, No. 3: 432–440 (1953); see translation by J. B. Sykes, British Translation AERE-Lib/Trans-499.
4. R. A. Egen et al., Hazards Summary Report for the VMR Critical-Assembly Experiments, USAEC Report BMI-1445, Battelle Memorial Institute, June 10, 1960.

NUCLEAR SCIENCE ABSTRACTS

The U. S. Atomic Energy Commission, Office of Technical Information, publishes *Nuclear Science Abstracts (NSA)*, a semimonthly journal containing abstracts of the literature of nuclear science and engineering.

NSA covers (1) research reports of the U. S. Atomic Energy Commission and its contractors; (2) research reports of government agencies, universities, and industrial research organizations on a world-wide basis; and (3) translations, patents, books, and articles appearing in technical and scientific journals.

Complete indexes covering subject, author, source, and report number are included in each issue. These are cumulated quarterly, semiannually, and annually providing a detailed and convenient key to the literature.

Availability of *NSA*

SALE *NSA* is available on subscription from the Superintendent of Documents, U. S. Government Printing Office, Washington 25, D. C., at $18.00 per year for the semimonthly abstract issues and $15.00 per year for the four cumulated-index issues. Subscriptions are postpaid within the United States, Canada, Mexico, and all Central and South American countries, except Argentina, Brazil, British and French Guiana, Surinam, and British Honduras. Subscribers in these Central and South American countries, and in all other countries throughout the world, should remit $22.50 per year for subscriptions to semimonthly abstract issues and $17.50 per year for the four cumulated-index issues.

EXCHANGE *NSA* is also available on an exchange basis to universities, research institutions, industrial firms, and publishers of scientific information. Inquiries should be directed to the Office of Technical Information Extension, U. S. Atomic Energy Commission, P. O. Box 62, Oak Ridge, Tennessee.